KING FAHD UNIVERSITY OF PETROLEUM & MINERALS

Dhahran, Saudi Arabia

Basic Properties of Reservoir Rocks

By

Dr. Sidqi A. Abu-Khamsin

Professor, Department of Petroleum Engineering

Contents

1. INTRODUCTION

1.1: The nature of petroleum

All chemical compounds found in nature are classified as either organic or inorganic. Organic compounds are those that contain carbon; and one condition in this classification is that the carbon atoms must be covalently bonded to some of the other atoms in the molecule. An important group within the organic family of compounds is the hydrocarbons, which are compounds composed of carbon and hydrogen only. Hydrocarbon molecules range in size and complexity from simple methane (CH_4) to asphaltenes containing hundreds of carbon atoms.

Like coal, petroleum constitutes a prime source of hydrocarbons in nature. It is a mixture of hundreds of thousands of compounds and is found in many forms: in the gaseous state as natural gas, in the liquid state as crude oil, or in the solid state as tar and bitumen. Petroleum is mostly found trapped within sedimentary rocks at various depths below the surface of the earth where it has accumulated over millions of years.

1.2: The petroleum reservoir

A petroleum trap is a geological structure where petroleum accumulates within a layer (formation) of sedimentary rock and cannot move out of it. The obstacle to the movement of petroleum is caused by the geometry of the layer or its properties, the properties of adjacent layers, or all of these factors combined. A typical trap is the *anticline*, formed when several sedimentary layers become folded as shown in Fig. 1.1. Here in this example, petroleum migrates from where it is generated deep under the surface into the limestone layer. By doing so, petroleum displaces water that originally fills the layer. Because petroleum is lighter than water, it accumulates at the top of the structure. However, the anhydrite layer above the limestone is too impervious to allow petroleum to continue its movement upwards, which causes the petroleum to remain trapped in the limestone.

Discovering a petroleum trap does not necessarily mean that petroleum can be produced (recovered) economically from it. This depends on two key factors: (1) the quantity of petroleum within the trap and (2) the rate at which it can be produced. If these two parameters justify the cost of production then the trap is considered a petroleum reservoir.

1.3: Significance of rock properties

The quantity of recoverable petroleum in a trap and the rate at which it can be produced depend primarily on the properties of the trap rock and the fluids it contains. Some properties determine the total volume of petroleum in the trap; others limit the fraction of

this volume that can be recovered. The rate of flow is dictated by other rock properties and in conjunction with some fluid properties. In this book, basic rock properties that aid in determining the reservoir quality of a trap will be presented. Moreover, fluid properties that control, alone or with other rock properties, the rate of flow will be presented as well.
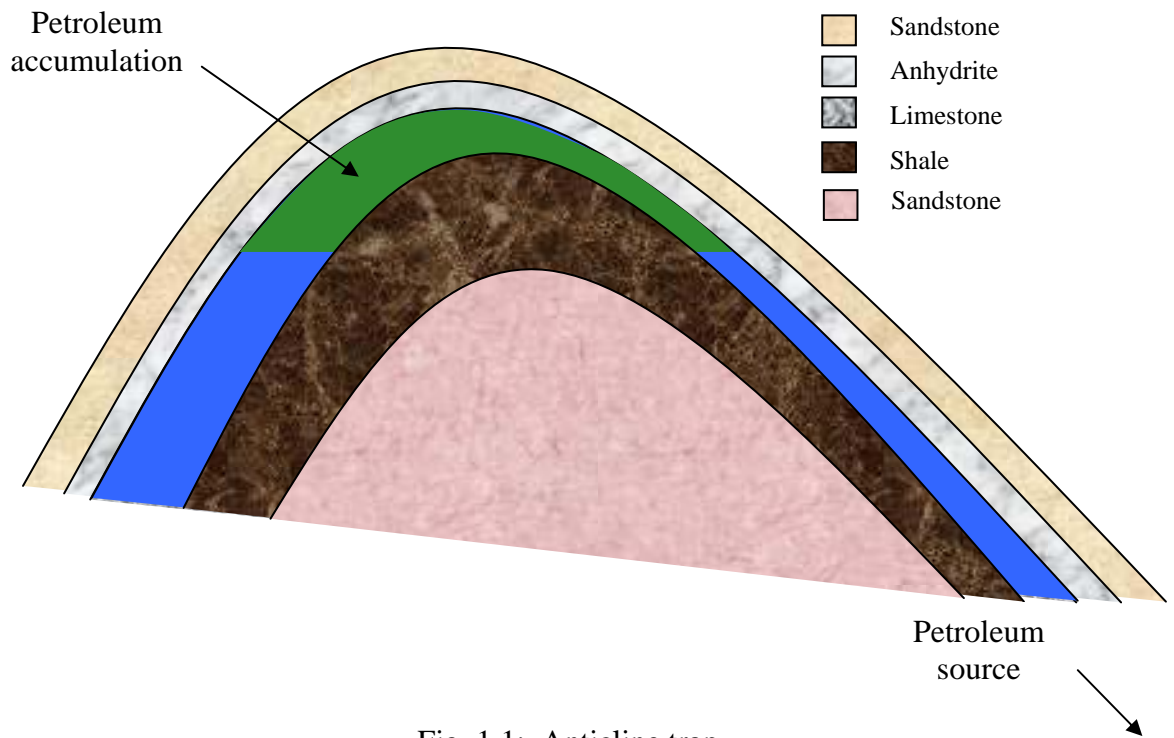

Fig. 1.1: Anticline trap

1.4: Sources of rock samples

Most rock properties are estimated from rock samples obtained from the reservoir.

2. POROSITY

2.1: Definition

Sedimentary rocks are invariably made up of grains of various sizes that are held together by fusion forces or other cementing material. The grains are composed of fragments of crystals of one or more rock minerals, all fused together. In sandstone, the predominant mineral is quartz (SiO_2); in limestone, the mineral is calcite ($CaCO_3$). The cementing material is crystals of minerals that are deposited between the grains during or after the sedimentation process. These minerals could be similar to the ones that make up the grains or others such as anhydrite, dolomite, and clay minerals.

If the grains have regular shapes with plain surfaces, e.g., cubes, then they could fit together in an orderly manner during sedimentation (Fig. 2.1-a). This way, no spaces are left between the grains and the whole body of the rock is solid material. However, rock grains are never regular in shape, which results in many spaces (pores) left between them (Fig. 2.1-b). Even if the grains are perfect spheres, they could not be packed together perfectly - like the cubes - no matter how we try. Therefore, the body of the rock is not entirely solid, rather a fraction of it is actually space. The spaces between the grains are called *pores* and the total volume of pores in a sample of rock is called its *pore volume*. The net volume of the grains is called the *grain volume*.
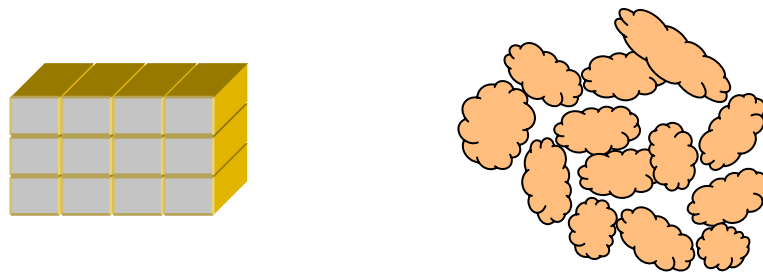
(a) Ordered packing of cubes   (b) Random packing of irregular shapes

Fig. 2.1: Packing of two different sorts of grains

Obviously, the total volume of a sample − termed the *bulk volume* − is the sum of both the grain volume, V_g, and the pore volume, V_p.

$$V_b = V_p + V_g \qquad (2.1)$$

where

V_b :   bulk volume, cm^3

This leads to a basic rock property called the *porosity,* which is defined as the fraction of the bulk volume of a sample that is pore space. In mathematical terms,

$$\varphi \quad = \quad V_p / V_b \tag{2.2}$$

where

$\quad\quad \varphi \quad : \quad$ absolute porosity, fraction

Knowledge of the porosity of a sample of rock enables us to estimate its pore volume since its bulk volume can be easily determined. If this sample is representative of the reservoir, i.e., the reservoir rock is the same everywhere, then the pore volume of the entire reservoir can be estimated by Equ. 2.2 using the sample's porosity. The bulk volume of the reservoir is computed by simple arithmetic from its area and average thickness. Since the maximum volume of fluids a reservoir can contain is equal to its pore volume, porosity becomes a primary property that must be determined most accurately.

Example 2.1

Suppose a rectangular reservoir is 10 miles long, 3 miles wide and 100 feet thick; and suppose the porosity of a rock sample obtained from the reservoir is 22%. The bulk volume of the reservoir is then

$$V_b \quad = \quad 10 \text{ x } 5280 \text{ x } 3 \text{ x } 5280 \text{ x } 100$$

$$= \quad 8.364 \text{ x } 10^{10} \quad\quad\quad\quad\quad ft^3$$

and its pore volume is

$$V_p \quad = \quad 8.364 \text{ x } 10^{10} \text{ x } 0.22$$

$$= \quad 1.840 \text{ x } 10^{8} \quad\quad\quad\quad\quad ft^3$$

$$= \quad 3.277 \text{ x } 10^{7} \quad\quad\quad\quad\quad bbl$$

Note: Units most commonly used in the petroleum industry and their conversion factors are listed in Appendix A.

Porosity is seldom constant within a reservoir; it varies with location and depth. To compute the average porosity, a simple weighted-mean formula is applied:

$$\overline{\varphi} \quad = \quad (\Sigma \overline{\varphi}_i V_{bi}) / V_b$$

where

$\quad\quad \overline{\varphi} \quad : \quad$ average porosity of whole reservoir

$\quad\quad \overline{\varphi}_i \quad : \quad$ average porosity of a given section (*i*) in the reservoir

$\quad\quad V_{bi} \quad : \quad$ bulk volume of section (*i*)

The summation should include all sections of the reservoir.

Example 2.2

The contour map below depicts porosity variation within a reservoir. The lines connect points of equal porosity. If the reservoir is 10 miles long, 3 miles wide, and 100 feet thick, its average porosity is estimated as follows:

There are 4 sections within the reservoir, the area and average porosity of each are computed to be:

Section	Area (ft^2)	Avg. Porosity (%)
1	155,399,147	12.5
2	277,261,208	17.5
3	122,322,723	22.5
4	14,303,684	25.0
Total	569,286,762	

Since the reservoir thickness is uniform, section areas only are used in the computation.

$$\overline{\varphi} \; = \; (\Sigma \overline{\varphi}_i A_i) / A$$
$$= \; 9{,}904{,}413{,}847 \, / \, 569{,}286{,}762$$
$$= \; 17.4$$
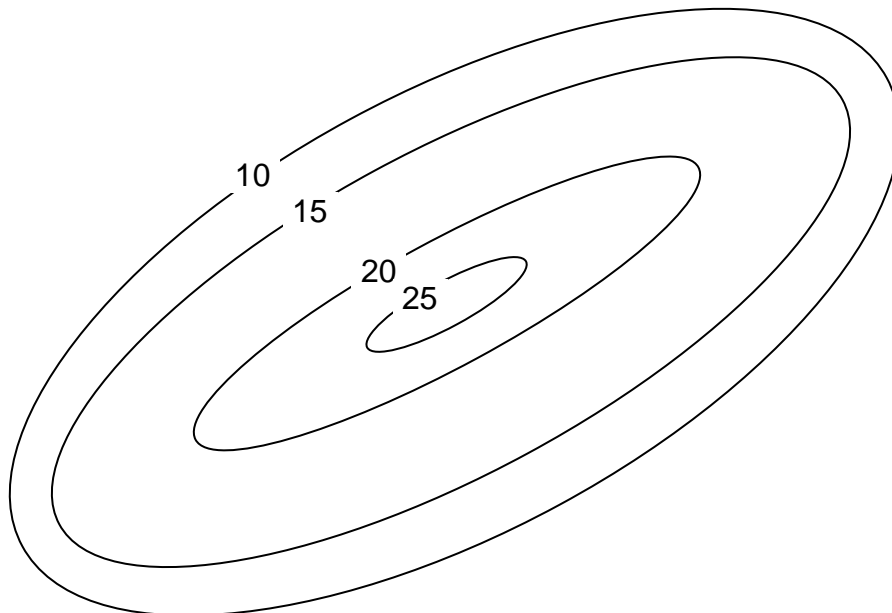
2.2: Types of porosity

Because of the variety and complexity of sedimentation processes, several types of porosity could be created. Usually, the porosity that arises after initial sedimentation is simple. All grains are loosely packed and pores within the sediments are connected. Fluids can later on move through and fill the entire pore space. Invariably, however, secondary processes alter the pore space by several ways. As the weight of the sediments increase, compaction presses grains closer to each other causing some pores to be closed and isolated from the rest of the pore space (Fig. 2.2). Although compaction reduces the pore volume a little, more importantly, it makes some of the pore space inaccessible to fluid flow. Therefore, part of the fluids within the reservoir cannot be produced as it is trapped within the isolated pores. The *effective porosity* is defined, hence, as the fraction of the bulk volume of a sample that is *connected* pore space.
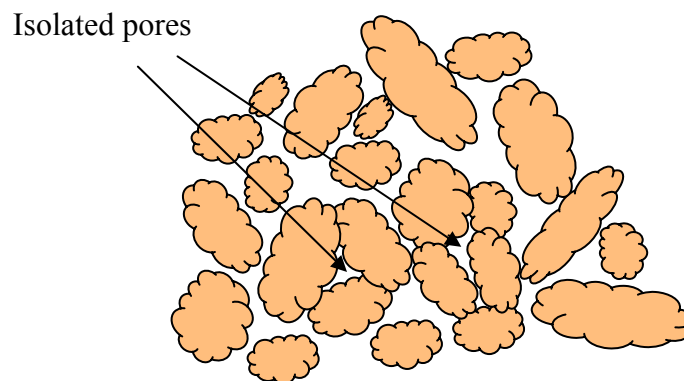
Isolated pores

Fig. 2.2: Isolated pores in a compacted bed

Reduction of pore volume and isolation of pores can also be a result of secondary deposition. Brines that flow through the rock could deposit minerals of various types between the grains, usually at the grain-to-grain contacts. Such deposits cement grains together, but could also plug pore throats or even fill entire pores. In other instances, brine can dissolve some of the grain material causing pore enlargement, which creates extra porosity (Fig. 2.3-a). For this reason, the initial porosity is referred to as the *primary*, *intergranular* or *matrix porosity* while the added porosity is referred to as the *secondary porosity*. Secondary porosity can also be created by cation exchange between the water and the rock. For example, some of the calcium ions in a calcite crystal may be replaced by magnesium ions from the brine, which forms the mineral dolomite ($MgCa(CO_3)_2$). Since dolomite has a smaller molar volume than calcite, this causes shrinkage of the grains and, thus, secondary porosity (Fig. 2.3-b). Fractures created within the rock also contribute to secondary porosity (Fig. 2.3-c).
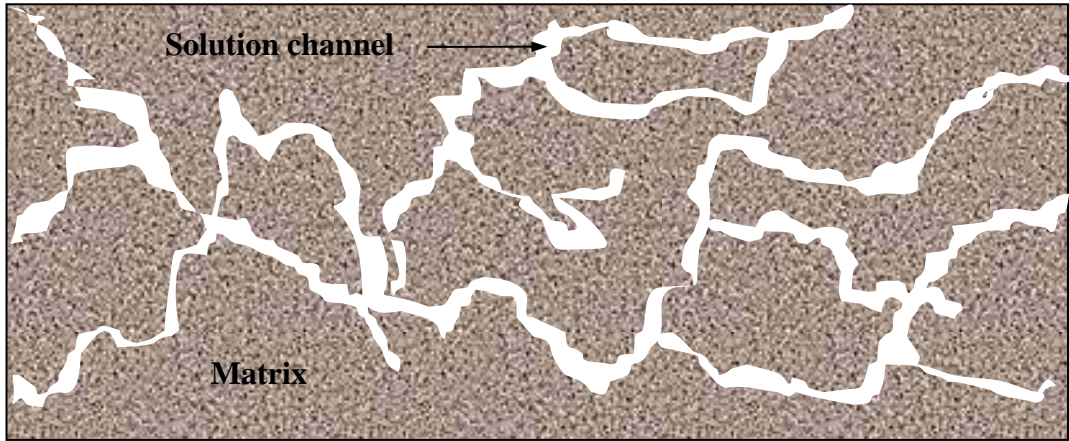
(a) Secondary porosity by solution
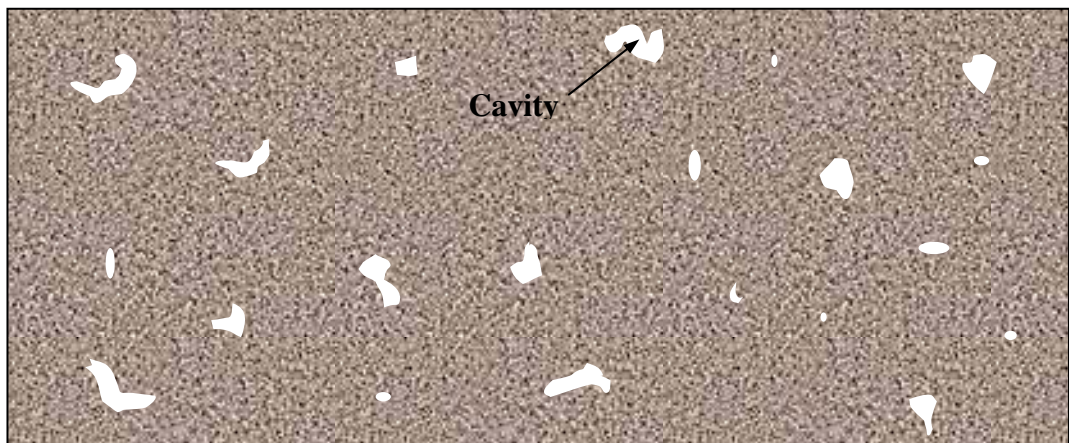
(b) Secondary porosity by dolomitization of calcite
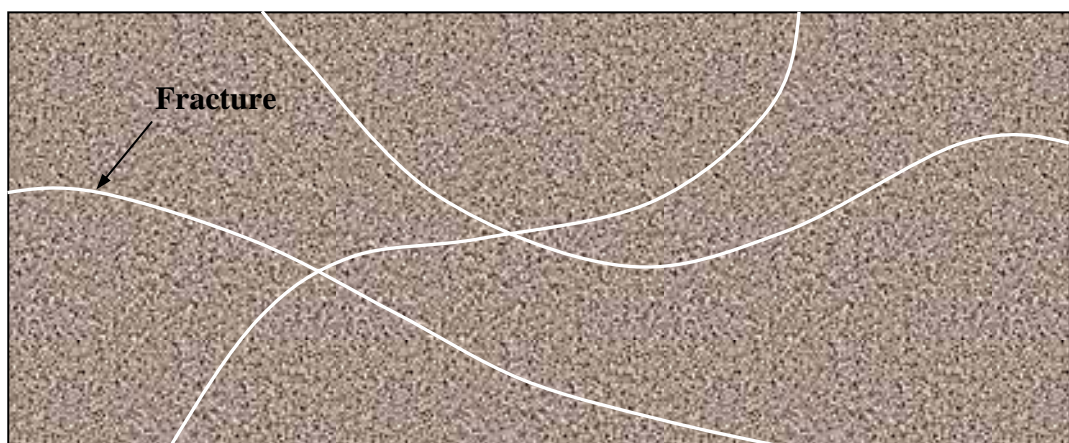
(c) Secondary porosity by fractures

Fig. 2.3: Examples of secondary porosity

2.3: Measurement of porosity

Estimates of reservoir porosity can be obtained from several sources both direct and indirect.

2.3.1: Direct methods

Direct measurements are conducted on samples of the reservoir rock recovered during drilling of wells. These samples could be rock fragments (cuttings) that are brought up to the surface by the drilling mud or samples cut during coring operations, which are called *cores*. Core samples are more desirable since they are relatively larger and more uniform, and their depth is known precisely. Small pieces, called core plugs, are usually cut from the cores for use in various tests. The plugs or cuttings are first cleaned with solvents to remove their fluid content of oil and water and then dried.

To determine porosity of a sample, all that is needed is to estimate two of the three parameters in Equ. 2.1. We will start with the bulk volume since it is usually the easiest to determine.

Bulk volume estimation

If the sample is regular in shape, e.g., a cylindrical core plug, then V_b is computed from its length and cross-sectional area.

$$V_b = A_c L \tag{2.3}$$

where A_c is the core plug cross-sectional area in cm^2 and L is the core plug length in cm. If the sample is irregular in shape, e.g., a cutting, then V_b is estimated by submerging it in water and measuring the volume of water it displaces (Fig. 2.4-a). To prevent water from entering the sample's pores, the sample is first coated with a thin layer of wax or varnish. The volume of the coating must obviously be subtracted later; this volume is determined from the mass of the coating and the density of the coating material. Mass of the coating is obtained from the difference in the mass of the sample before and after coating.

Grain volume estimation

If the rock is predominantly composed of one mineral, e.g., quartz, then the mass of the clean and dry sample, m_s, divided by the density of the mineral, ρ_g, equals the total volume of the grains

$$V_g = m_s / \rho_g \tag{2.4}$$

If the rock is composed of many minerals whose types and volume fractions are known, an average grain density, $\bar{\rho}_g$ must then be estimated as follows:

$$\overline{\rho}_g \;=\; \sum v_i\,\rho_{gi} \tag{2.5}$$

where

v_i :   volume fraction of mineral i

ρ_{gi} :   density of mineral i, g/cm^3

(a) Bulk volume   (b) Grain volume
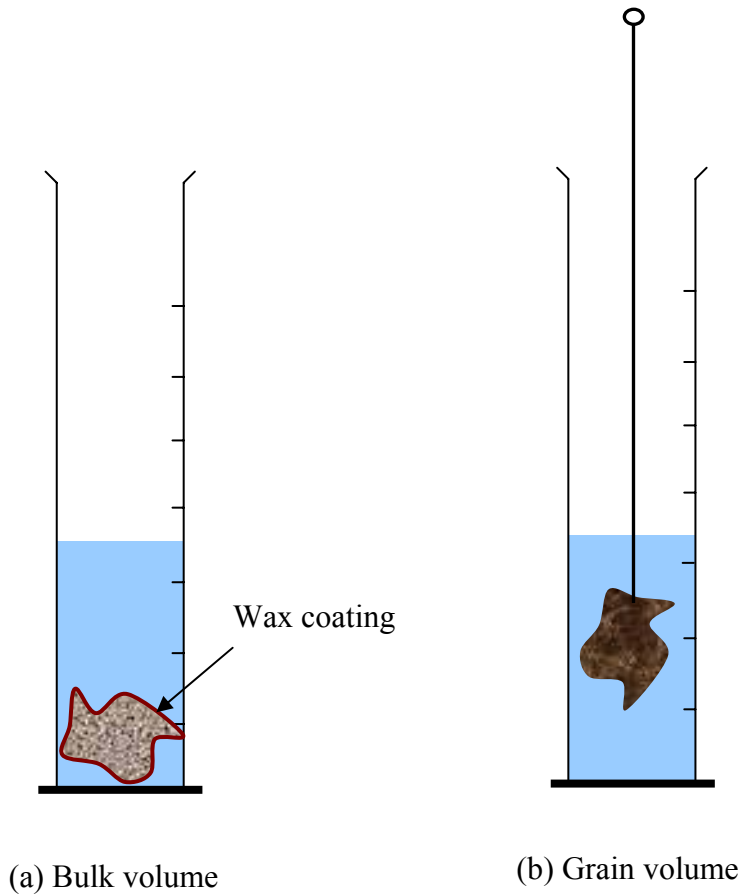
Fig. 2.4: Measurement of volume by submerging in water

Example 2.3

An irregular piece of sandstone is 35.25 grams in mass. When coated with varnish, its mass increased to 36.55 grams. Compute the rock porosity if the coated sample displaces 15.7 ml of water when fully submerged. $\rho_g = 2.65$ g/cm^3, $\rho_w = 1.00$ g/cm^3, $\rho_v = 1.80$ g/cm^3.

V_g = 35.25 / 2.65

    = 13.30   cm^3

V_v = (36.55 − 35.25) / 1.80

    = 0.72   cm^3

$$V_b = 15.70 - 0.72$$

$$= 14.98 \qquad\qquad cm^3$$

$$\varphi = (14.98 - 13.3) / 14.98$$

$$= 0.112 = 11.2\%$$

Note: This value is the absolute porosity.

Sometimes the rock's mineral composition is unknown. We can still determine V_g by liquid displacement. An uncoated sample is submerged in water or another suitable liquid and left for a sufficient time to ensure that all the pore space has been filled. Then, while suspended in the liquid by a string, the sample is weighed (Fig. 2.4-b). The difference in the sample's weight before and after submerging is equal to the weight of liquid displaced, whose volume must be equal to the grain volume. For this procedure to be effective, all the air present within the sample must be displaced by the liquid, which is rather impossible as some air will be trapped within the smaller pores. And even if complete air displacement is achieved, only the connected pore space will be filled leading to a V_g value larger than the true one. It should be noted, then, that while Equ. 2.4 results in computing the absolute porosity, the liquid displacement procedure results in the effective porosity.

Example 2.4

The varnish coating on the sample of Example 2.3 was removed and the sample was submerged in water. When air bubbling stopped, the sample was weighed while suspended in water. It weighed 21300 dynes. Assuming that you don't know the rock composition, compute the rock porosity.

Weight of sample in air = 35.25 x 980 = 34,545 dynes

Weight of sample in water = 21,300 dynes

Weight of displaced water = 34545 – 21300 = 13,245 dynes

Volume of displaced water = 13245 / (980 x 1) = 13.52 cm^3

$$V_g = 13.52 \qquad\qquad cm^3$$

$$\varphi = (14.98 - 13.52) / 14.98$$

$$= 0.097 = 9.7\%$$

Note: This value is the effective porosity.

Pore volume estimation

Estimating V_g requires simple procedures and, usually, available equipment. On the other hand, direct measurement of the pore volume provides a more accurate porosity value. However, this requires some additional instruments. A simple method starts with weighing the sample in air followed by placing the sample in a vacuum flask (Fig. 2.5-a) for a few hours. Water is then introduced into the flask gradually until the sample is completely submerged (Fig. 2.5-b). The sample is then removed from the flask, shaken to remove excess water and then weighed quickly. The increase in the mass of the sample is equal to the mass of water introduced into the sample, and the volume of the water is equal to the *connected* pore volume. Care must be taken to minimize water evaporation; and if the rock contains clay minerals that absorb water, another liquid – oil, mercury, or KCl brine – must be used instead.

liquid reservoir

Vacuum gauge

Vacuum valve

(a) under vacuum
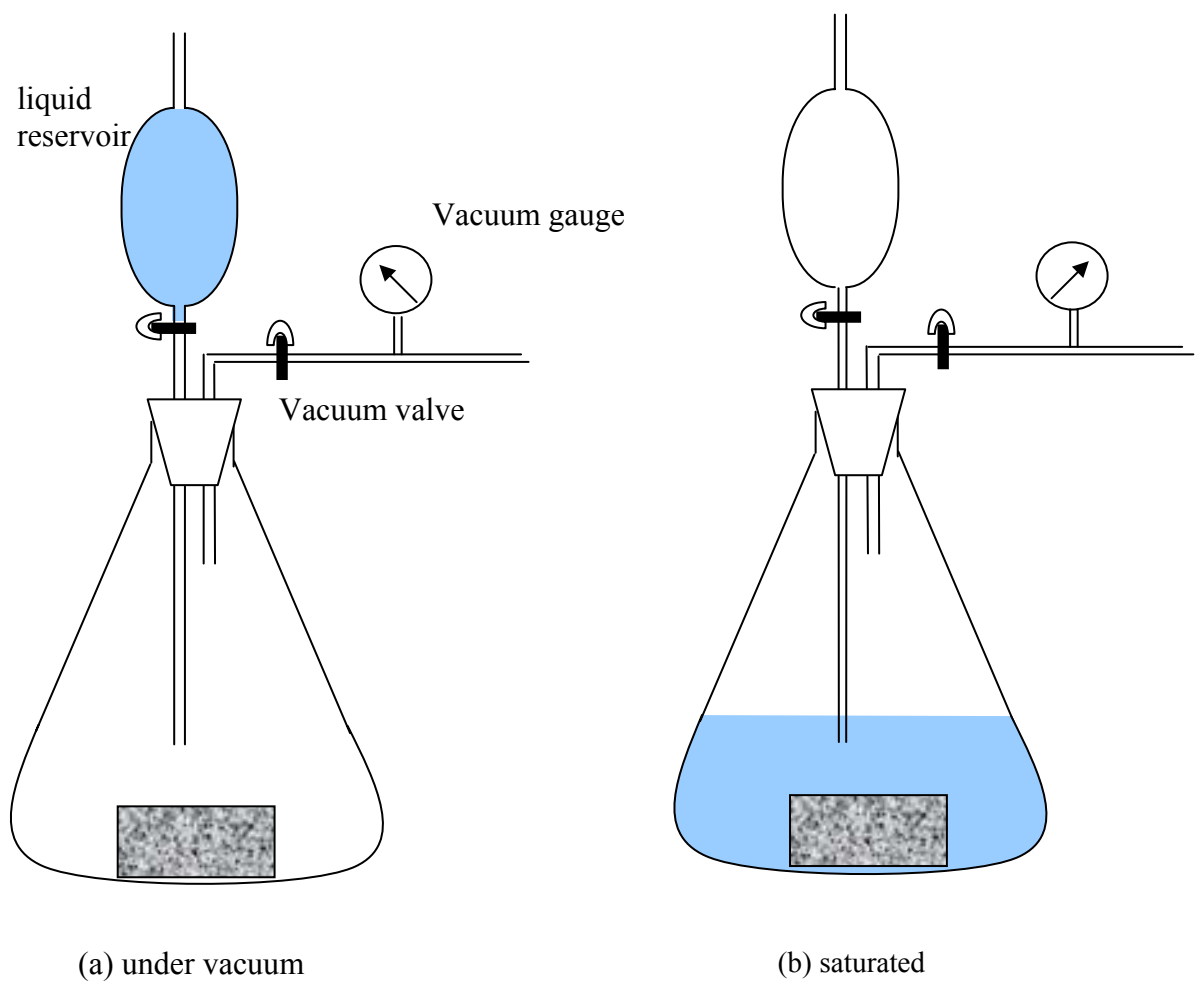
(b) saturated

Fig. 2.5: Pore volume measurement by the liquid saturation method

Example 2.5

A sandstone core plug is 1 inch in diameter, 2 inches long, and has a mass of 56.6 grams. When completely saturated with water, its mass increases to 60.9 grams. Compute the rock porosity.

Mass of water in sample = 60.9 – 56.6		=	4.3 grams
Volume of water = 4.3 / 1		=	4.3 cm^3
V_b =	π (0.5 x 2.54)^2 x 2 x 2.54	=	25.74 cm^3
φ =	4.3 / 25.74	=	16.7%

Note: The absolute porosity of the sample computed from its estimated grain volume is 17%.

Another method utilizes gas expansion to fill the pore space of the sample, and it requires a special instrument called a *porosimeter* (Fig. 2.6). In this method, the sample is first placed in a chamber and placed under vacuum to remove all air within it. Then gas, usually helium, is allowed to expand from a container of known volume and initial pressure into the chamber. By application of Boyle's law, the final volume of the gas is computed from its final pressure. The increase in the gas volume is equal to the connected pore volume of the sample plus the dead volume in the chamber and tubing.
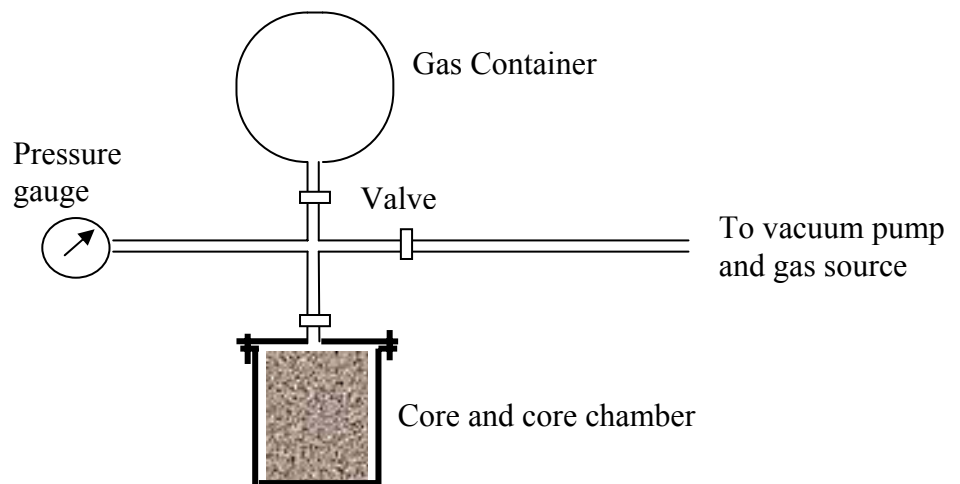
Fig. 2.6: Gas expansion porosimeter

2.3.2: Indirect methods

Indirect methods of estimating porosity rely on measurement of other rock and fluid properties. These measurements are carried out in the well employing special instruments as part of well logging operations. Therefore, no core samples are needed and the porosity is estimated for the rock as it exists in the reservoir. Two of the most common well logs are discussed below.

The sonic (acoustic) log

In this log, the instrument - the sonde - generates sound waves, which travel through the reservoir - in the vicinity of the well bore - and are detected by the sonde upon their return. The time lapse between generation and detection – travel time - is recorded continuously versus the depth of the instrument. Since travel time is related to porosity by

$$\Delta t_{log} = \varphi \, \Delta t_f + (1 - \varphi)\Delta t_{ma} \tag{2.6}$$

where

Δt_{log} : sound travel time in the reservoir as measured by the log, µs

Δt_{ma} : sound travel time in the grain material of the reservoir, µs

Δt_f : sound travel time in the fluids of the reservoir, µs

and since Δt_{ma} and Δt_f are usually known for the reservoir, the porosity can be estimated at all depths.

The formation density log

Another logging sonde emits gamma rays, which mostly pass through the reservoir rock and fluids, but some are scattered back into the well bore and are detected by the sonde. The fraction of scattered gamma rays is used to compute the bulk density - rock and fluids - of the reservoir, which is related to porosity by

$$\rho_{log} = \varphi \, \rho_f + (1 - \varphi)\rho_{ma} \tag{2.7}$$

where

ρ_{log} : bulk density of the reservoir as measured by the log, g/cm^3

ρ_{ma} : density of the grain material of the reservoir, g/cm^3

ρ_f : density of the fluids of the reservoir, g/cm^3

Since laboratory values of the porosity are more reliable, these are used to correct log-estimated values at the same depth(s) of the core sample(s), and then the same correction is applied to the entire thickness of the reservoir. It should be noted that both logs provide estimates of the absolute porosity.

Example 2.6

A sonic log measured travel time of 58 μs for a formation. If the formation is primarily limestone (46 μs) and contains oil only (190 μs), compute the rock porosity.

Rearrange Equ. 2.6

$$\varphi = \frac{\Delta t_{log} - \Delta t_{ma}}{\Delta t_f - \Delta t_{ma}}$$

$$= \frac{58 - 46}{190 - 46}$$

$$= 8.3\%$$

Note: This value is the average absolute porosity of the formation.

Exercises

1. Suppose we pack spherical balls, all of the same size, in a cubic packing arrangement. What will the porosity of the medium be?

2. Suppose the balls of Exercise 1 have 1 mm diameter. How big are the largest balls that we can fit in between them? What will the new porosity be?

3. A core plug 1 inch in diameter and 2 inches long is placed in the chamber of a gas expansion porosimeter whose container is 20 cm³ large. The initial and final pressure readings are 25 and 21 psi, respectively. Ignoring the dead volume of the apparatus, what is the porosity of the sample?

4. A dry and clean core sample 1 inch in diameter and 4 inches long weighs 120 grams. Mineral analysis shows that the grains are 80% (by volume) calcite and 20% anhydrite. Estimate the sample's porosity. ($\rho_{ca} = 2.71$ g/cm³, $\rho_{an} = 2.98$ g/cm³)

5. Suppose the core sample of Problem 4 was obtained from a formation which contains only water ($\rho_w = 1$ g/cm³). In one location of the formation, the density log measured a bulk density of 2.48 g/cm³, what is the formation's porosity at that location?

3. ROCK COMPRESSIBILITY

3.1: Definition

The compressibility of a substance is defined as the shrinkage of a unit volume of the substance per unit increase in pressure. In equation form:

$$c = -\frac{1}{V}\left(\frac{\partial V}{\partial P}\right)_T \qquad (3.1)$$

where

c : compressibility, psi^{-1}

V : volume, ft^3

P : pressure, psi

T : temperature, °F

Since volume always decreases with increase in pressure, the partial derivative in Equ. 3.1 is negative. Therefore, the minus sign is added to give a positive compressibility value. Note that compressibility varies slightly with temperature, which explains why the derivative is fixed at a given T. All minerals found in sedimentary rocks are elastic, i.e., they show compressibilities of various magnitudes. Quartz, for example, has a compressibility of about 2×10^{-8} psi^{-1} at 68 °F.

3.2: Significance

Buried deep under the surface, reservoir rock is exposed to a large *overburden* pressure, P_{ob}, created by the weight of all rock strata above it. This pressure is transmitted from grain to grain at the points of contact. Another pressure that is exerted on the grains of the rock is the pressure of the fluids within the pore space. This *pore* pressure, P_p, is usually equal to the hydrostatic pressure at the depth of the reservoir and is mostly independent of P_{ob}. One can imagine a wall built with hollow bricks. The P_{ob} felt by the bottom bricks corresponds to the weight of the wall while P_p within the cavities of the bricks is the atmospheric pressure of air that can move freely through them.

Reservoir engineers are interested in rock compressibility because of its effect on porosity, both in laboratory measurement and during the life of the reservoir. Let us first look into laboratory measurement. Suppose a core sample is cut from a sandstone reservoir 6000 feet deep, where a reasonable P_{ob} would be 6000 psia. If a quartz grain within the sample has a reservoir volume of 1 mm^3, its volume in the laboratory where P_{ob} is atmospheric, would increase by

$$\Delta V = -c\,V\,\Delta P$$

$$= -2 \times 10^{-8} \times 1 \times (14.7 - 6000) = 0.00012 \quad mm^3$$

Remember, this is the expansion of one grain only; millions of other grains would expand as well. Since an increase in the grain volume causes an equal decrease in the pore volume of the core sample, an error, though very insignificant, would be inherent in the laboratory-determined porosity. However, a more significant error is introduced because of another effect. As P_{ob} increases, the grains are also brought closer together because of compaction. Taking the core sample to the surface reverses this process and causes significant increases in both bulk and pore volumes. Both increases, though, are difficult to relate to the *matrix* (grain material) compressibility.

Similarly, P_p in the laboratory is very low compared to its value in the reservoir, which causes further expansion of the grains and some collapse in the bulk volume. This phenomenon is similar to deflating a piece of sponge. Thus, an added error is introduced in porosity.

The resultant effect of reduction in P_{ob} and P_p on porosity is difficult to quantify analytically. Many workers in the field have proposed empirical correlations that predict variation of porosity with pressure. An example is the one presented by Fatt[1] and shown in Fig. 3.1. In his correlation, Fatt defined the net overburden pressure, $P_{ob,net}$, as

$$P_{ob,net} = P_{ob} - 0.85 \, P_p \tag{3.2}$$

and the pore volume compressibility as

$$c_p = -\frac{1}{V_p}\left(\frac{\partial V_p}{\partial P_p}\right)_T \tag{3.3}$$

Assuming that changes in V_b are small compared with changes in V_p, Equ. 3.3 can be rewritten as

$$c_p = -\frac{1}{\varphi}\left(\frac{\partial \varphi}{\partial P_{ob,net}}\right)_T \tag{3.4}$$

Therefore, once c_p is estimated from Fig. 3.1 Equ. 3.4 can be used to estimate reduction in porosity from lab to reservoir as follows

$$\Delta\varphi = -c_p \, \varphi_{lab} \, \Delta P_{ob,net} \tag{3.5}$$

_____

Example 3.1

A core plug was obtained from a reservoir where the overburden pressure is 5000 psi and the pore pressure is 2200 psi. If the plug shows a porosity of 18% in the laboratory, what is its

porosity under reservoir conditions? Assume the pore compressibility follows curve E in Fig. 3.1.

$$P_{ob,net} = P_{ob} - 0.85\ P_p$$
$$= 5000 - 0.85 \times 2200 \qquad = 3130\ psi$$

From Fig. 3.1, $c_p = 10 \times 10^{-6}\ psi^{-1}$

$$\Delta\varphi = -c_p\ \varphi_{lab}\ \Delta P_{ob,net}$$
$$= -10 \times 10^{-6} \times 0.18 \times 3130 \qquad = 0.0056$$

Therefore, porosity under reservoir conditions is

$$\varphi = 0.18 - 0.0056$$
$$= 0.1744\ \ or\ 17.44\%$$

Note: Under laboratory conditions, net overburden pressure is usually negligible.
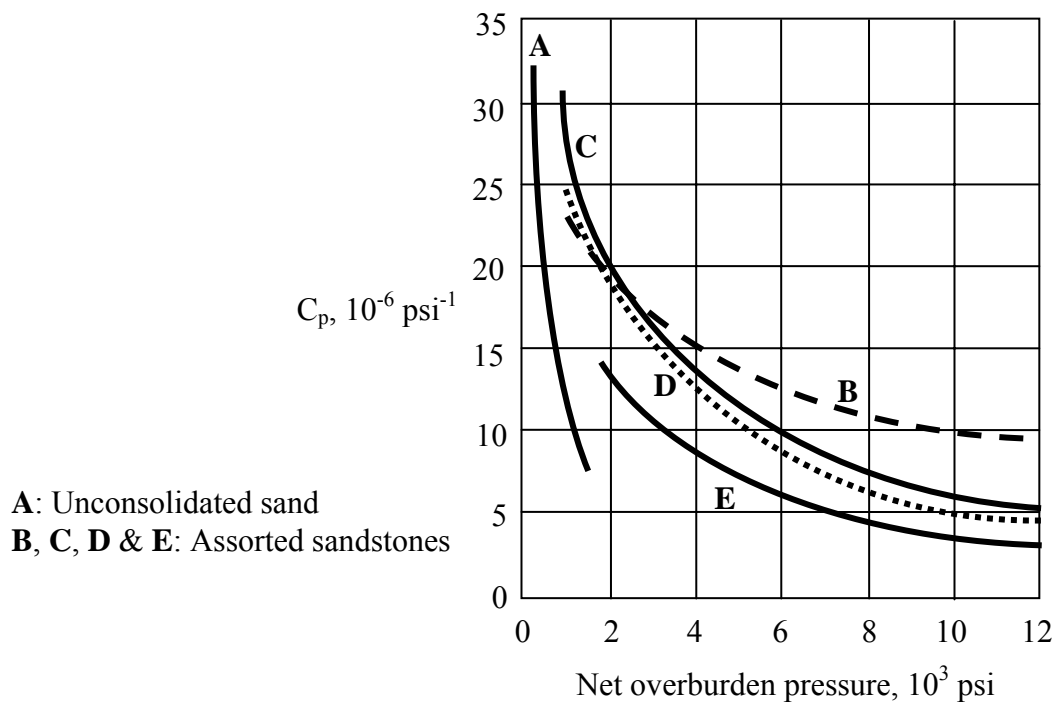
Fig. 3.1: Variation of pore-volume compressibility with net overburden pressure
(*from Fatt[1]*)

3.3: Measurement of compressibility

Pore-volume compressibility can be measured in the laboratory by measuring the variation in the pore volume of a core sample at different conditions of P_{ob} and P_p. The pore volume of the sample is first measured at atmospheric pressure and the reservoir temperature following the procedures of Chapter 2. The saturated sample is then loaded into a core holder

17

(Fig. 3.2), which is a device that allows application of different combinations of overburden and pore pressures independently. At each set of P_{ob} and P_p, the liquid that is squeezed out of the sample is collected, and its volume is used to compute the current porosity. A plot of φ versus $P_{ob,net}$ would yield the pore volume compressibility as depicted in Fig. 3.3.
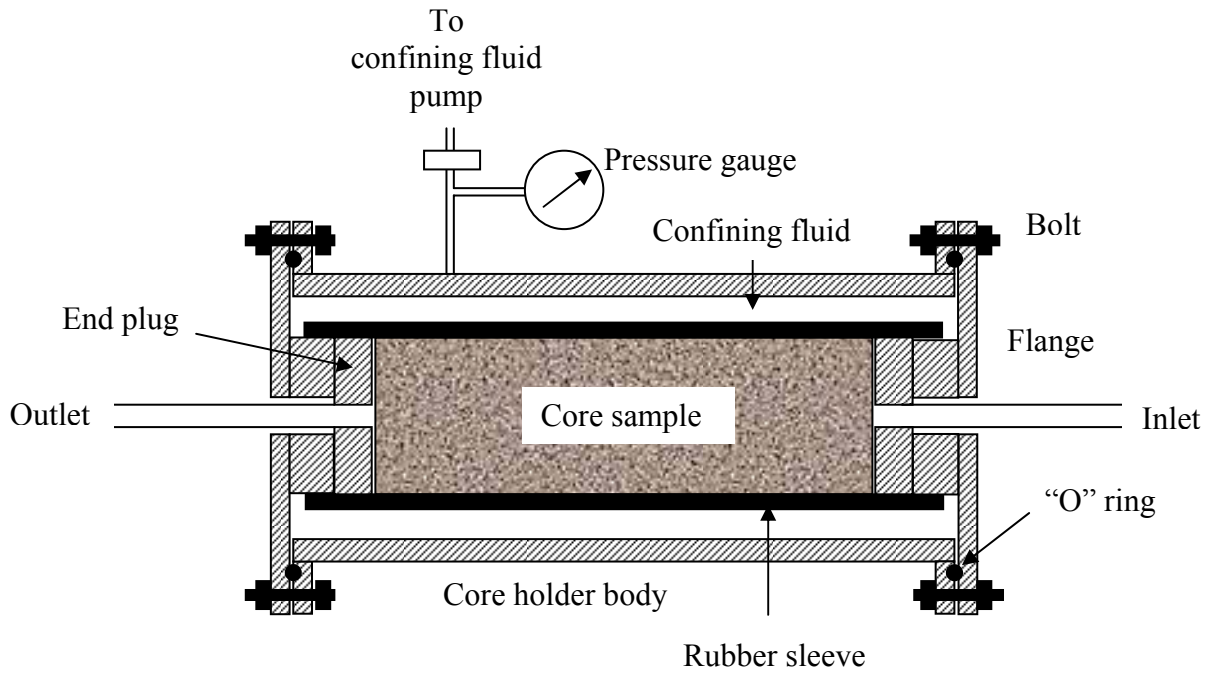
Fig. 3.2: Schematic of a core holder
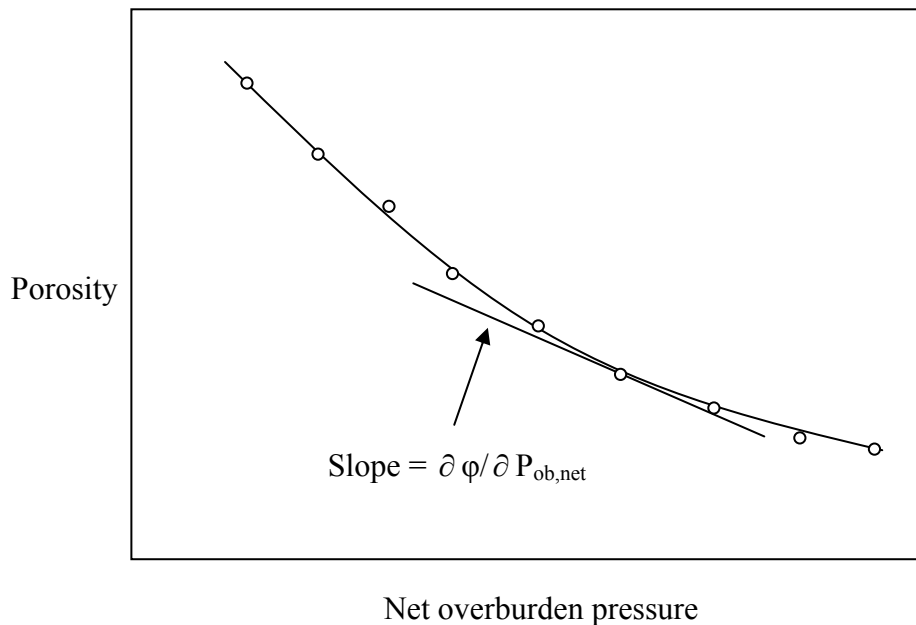
Fig. 3.3: Computation of pore-volume compressibility

3.4: Applications

Rock compressibility – matrix, bulk or pore – is useful in correcting laboratory-measured porosity as discussed above. However, other reservoir calculations also require compressibility.

In some well testing techniques, the production rate of an oil well is changed suddenly while its pressure is monitored over a period of time. The transient pressure response of the well is influenced by fluid as well as rock compressibilities, and these values are needed for an accurate interpretation of the test results.

Some reservoir engineering calculations require reservoir pore pressure and total production data for the estimation of reserves. But since the pore volume of the reservoir changes as P_p decreases with production, c_p is needed to correct the pore volume from its initial value.

Exercises

1. With the bulk, pore and grain compressibilities defined as

$$ c_b = - \frac{1}{V_b}\left(\frac{\partial V_b}{\partial P}\right) \qquad c_p = - \frac{1}{V_p}\left(\frac{\partial V_p}{\partial P}\right) \qquad c_g = - \frac{1}{V_g}\left(\frac{\partial V_g}{\partial P}\right) $$

   respectively, show that the definition of porosity implies

   $$ c_b = (1 - \varphi)\, c_g + \varphi\, c_p $$

2. The data below was obtained from a compressibility experiment on a core sample whose bulk volume is 52.0 cm^3 and initial pore volume is 8.82 cm^3. The sample's pore space is initially filled with water. Estimate the sample's pore-volume compressibility at 1000 and 2000-psi net overburden pressures.

P_p (psi)	14.7	50	50	100	100	500	500	1000	1000
P_{ob} (psi)	500	750	1000	1500	2000	2500	3000	3500	4000
V_{wp} (cm^3)	0.222	0.328	0.361	0.452	0.470	0.481	0.487	0.494	0.506

   V_{wp} is total water squeezed out of sample at each step.

3. For a reservoir whose pore-volume compressibility is 17×10^{-6} psi^{-1}, and where overburden pressure and pore pressure increase by 1 psi and 0.5 psi, respectively, per foot of depth, show that the porosity decreases by 1% ($\varphi_2/\varphi_1 = 0.99$) for every 1000 feet increase in depth.

4. FLUID SATURATION

4.1: Definition

The pore space of a petroleum reservoir is never filled completely with hydrocarbons; water is always present in the liquid state, and the hydrocarbons can exist in one or more states − gas, solid or liquid. The saturation of a given fluid is defined as the fraction of the pore space occupied by that fluid. In equation form:

$$S_f \quad = \quad V_f / V_p \tag{4.1}$$

where

S_f :   saturation of the fluid, fraction or percent

V_f :   total volume of fluid in reservoir or core sample, cm^3

V_p :   total pore volume of reservoir or core sample, cm^3

The sum of all fluid saturations in a reservoir is obviously equal to unity

$$1 \quad = \quad S_w + S_o + S_g \tag{4.2}$$

Knowledge of the average saturation of a fluid, say oil, in a reservoir allows the reservoir engineer to estimate the total volume of the fluid in the reservoir simply through application of Equ. 4.1. This is the prime utility of saturation. Another, equally important utility, is how some fluid-dependent rock properties vary with saturation as will be seen in the following chapters.

The saturation of a fluid in a reservoir seldom remains constant. Water can enter the reservoir either naturally - from an adjacent aquifer - or artificially by water injection. Oil saturation decreases with oil production and the replacement of oil by another fluid such as water. Gas saturation could increase with gas injection into the reservoir or as gas evolves naturally from the oil when the pressure drops. The saturations of the different fluids in a reservoir are, therefore, measured periodically employing direct and indirect methods.

4.2: Measurement of saturation

4.2.1: Direct methods

Direct measurement methods rely simply on the removal of all liquids − by evaporation or extraction - from a core sample and determining their individual volumes. Dividing each fluid volume by the pore volume of the sample yields the saturation of that fluid. One device used commonly for this purpose is the Modified ASTM Extraction Unit (Fig. 4.1). The procedure starts with placing the core sample in a paper thimble and weighing them together. The thimble is then placed in the flask, the heater is turned on, and water flow through the condenser is started. As the toluene in the flask boils, its vapors rise and exit the

flask, condense in the condenser and accumulate in the condenser's graduated tube. Once the tube is full, excess toluene refluxes back into the flask flowing through the thimble. Oil present in the core sample is extracted by the refluxing toluene and ends up dissolved in the bulk toluene mass.
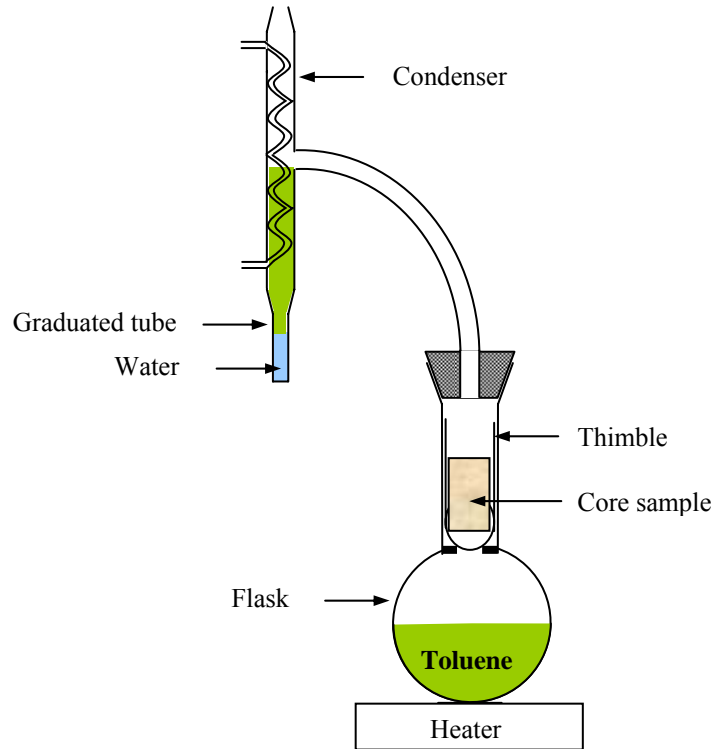
Fig. 4.1: ASTM extraction unit

The water present in the sample evaporates and condenses back into the graduated tube. Since water is heavier than toluene, it sinks to the bottom of the tube rather than returning to the flask. Extraction is continued until no more water accumulates in the tube at which point heating is stopped and the volume of water is read. When the unit cools down, the sample and thimble are removed and placed in a vacuum oven to dry, after which they are both weighed again. The mass of the oil is computed by a mass balance on the core sample before and after extraction as follows

$$m_o = \Delta m_c - V_w \, \rho_w \tag{4.3}$$

and

$$V_o = m_o / \rho_o$$

where

m_o :   mass of oil extracted, g

Δm_c :   reduction in mass of core sample, g

V_o :   volume of oil extracted, cm^3

V_w :   volume of water extracted, cm^3

The pore volume of the sample is determined by one of the methods described in chapter 2 and the liquid saturations are then computed. It should be noted that if oil and water saturations do not add up to 100%, gas must have been present in the sample.

Example 4.1

A sandstone core sample 4" long, 1" in diameter with an absolute porosity of 23% was cleaned in an extraction unit. The reduction in the sample's mass was 7.4 g, and 3.2 ml of water were collected. If the oil and water densities are 0.88 and 1.02 g/cm^3, respectively, compute the fluid saturations.

$$m_w \; = \; 3.2 \times 1.02 \; = \; 3.26 \text{ g}$$

$$m_o \; = \; 7.4 - 3.26 \; = \; 4.14 \text{ g}$$

$$V_o \; = \; 4.14 / 0.88 \; = \; 4.7 \text{ cm}^3$$

$$V_p \; = \; \frac{\pi}{4}(1)^2 \times 4 \times 0.23 \; = \; 0.723 \text{ in}^3 \; = \; 11.84 \text{ cm}^3$$

$$S_w \; = \; 3.2 / 11.84 \; = \; 0.27 \; = \; 27\%$$

$$S_o \; = \; 4.7 / 11.84 \; = \; 0.397 \; = \; 39.7\%$$

$$S_g \; = \; 100 - 27 - 39.7 \; = \; 33.3\%$$

4.2.2: Indirect methods

Fluid saturations can also be estimated through indirect methods such as measurement of rock resistivity and well logging. Both of these techniques will be presented in the next chapter.

Exercises

1. Suppose the oil in a core sample contains material which cannot be dissolved by toluene, e.g. wax. How would the oil and water saturations determined by the extraction method be affected?

2. A sandstone core sample (V_b = 49 cm^3, V_p = 8.8 cm^3, total mass = 115.2 g) contains both oil and water (ρo = 0.82 g/cm^3, ρw = 1 g/cm^3). Compute the fluid saturations. What are the uncertainties in your answer?

5. ROCK RESISTIVITY

5.1: Definition

Resistivity is a measure of the resistance of a substance to the flow of electrical current. It is equal to the resistance of a sample of the substance having a volume of unity. For samples with regular geometric shapes, the resistivity can be computed as follows

$$\mathcal{R} = r A / L \tag{5.1}$$

where

$\mathcal{R}$: resistivity of sample, Ωm

r : resistance of sample, Ω

A : cross-sectional area of sample, m^2

L : length of sample, m

The resistance is measured by a simple electric circuit (Fig. 5.1) where

$$r = V / I \tag{5.2}$$
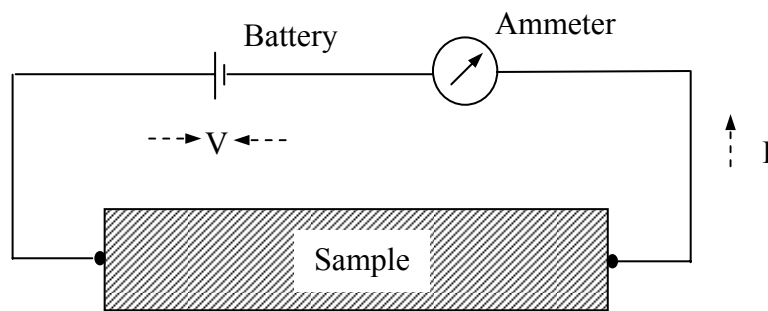
Fig. 5.1: Measurement of electrical resistance

5.2: Significance

Most rock minerals have very high resistivities; so do all crude oils and natural gas. However, water, especially salt water, is an excellent conductor and, thus, shows low resistivity. It is this resistivity contrast that is utilized by reservoir engineers to look for oil and estimate its saturation within reservoir rock. To illustrate this principle, let us follow a simple experiment. Suppose we have an empty rubber tube fitted with a circuit to measure resistivity (Fig. 5.2). The copper plates are only to ensure good electrical contact with whatever substance that fills the tube's cavity. With only air filling the tube, the resistivity would be near infinite as air is an excellent insulator. If sweet water fills the tube, the resistivity would drop to 30 Ωm, since water is a better conductor. Replacing sweet water with brine - salt water - the resistivity would drop to about 1 Ωm. Again brine is a good

conductor. Now suppose we insert in the tube a sandstone core sample saturated completely with the brine. The resistivity would increase to 95 Ωm. The reason is that only part of the cross-sectional area of the core sample, namely the brine-saturated pores, is available for current flow since the sand grains are nonconductors. Another reason is that the current has to travel a longer distance between the terminals, having to follow a tortuous path between the grains. Finally, suppose we reduce the water (brine) saturation in the sample by replacing some of it with crude oil. The resistivity would jump to 300 Ωm, as oil is a poorer conductor than brine. If we repeat the last step with different water saturations, we can construct a graph of resistivity versus water saturation, which can be used to estimate other water saturations in the core sample by simply measuring its resistivity. However, such a graph would be limited to that particular sample. To generalize this technique to other core samples or the reservoir as a whole we need to develop a basic theory of rock resistivity.
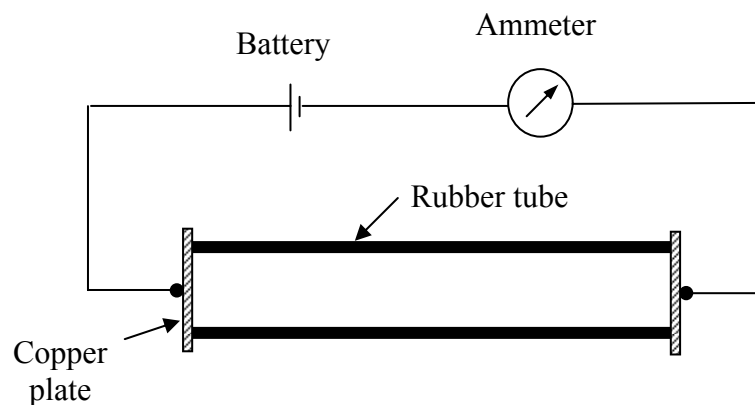
Fig. 5.2: Measurement of resistivity

5.3: Mathematical formulations

Let us begin with some definitions:

$\mathcal{R}_w$:   resistivity of reservoir water, Ωm

$\mathcal{R}_o$:   resistivity of reservoir rock saturated with reservoir water, Ωm

$\mathcal{R}_t$:   resistivity of reservoir rock saturated with both oil and water, Ωm

Define the *formation factor, $\mathcal{F}$*, as

$$\mathcal{F} \;\; = \;\; \mathcal{R}_o \, / \, \mathcal{R}_w \tag{5.3}$$

Obviously, the formation factor is always greater than unity since the only difference between the two resistivities is the presence of the rock matrix. The more tortuous the path of current flow, the larger $\mathcal{R}_o$ becomes. Also, the smaller the fraction of pore area, relative to

the total area of the rock, the larger $\mathcal{R}_o$ becomes. One can, therefore, conclude that the porosity of the rock has a considerable influence on $\mathcal{F}$, and indeed it does. The two parameters have been found by Archie[2] to relate to each other according to the following general correlation:

$$\mathcal{F} = C \varphi^{-m} \tag{5.4}$$

where

C : tortuousity constant

m : cementation factor

The two parameters, C and m, vary with the type of rock. For clean sandstone, a widely used form of Archie's correlation is the Humble equation:

$$\mathcal{F} = 0.62 \varphi^{-2.15} \tag{5.5}$$

To introduce the effect of other fluids within the rock, let us define the *resistivity index, I*, as

$$I = \mathcal{R}_t / \mathcal{R}_o \tag{5.6}$$

Again, the resistivity index is always greater than unity since the only difference between the two resistivities is the presence of oil within the rock matrix. Therefore, it must be related to S_w. Archie was able to correlate this effect by his second equation:

$$I = 1 / S_w^n \tag{5.7}$$

where n is called the saturation exponent and varies with the type of rock; a common value used is 2. Combining Equs. 5.3 and 5.6, the following relationship is derived:

$$1/I = \mathcal{F} \mathcal{R}_w / \mathcal{R}_t \tag{5.8}$$

Substituting for I and $\mathcal{F}$, Equs. 5.3 and 5.7, in Equ. 5.8 yields

$$S_w^n = C \varphi^{-m} \mathcal{R}_w / \mathcal{R}_t \tag{5.9}$$

Equation 5.9 is the basic tool of the theory of rock resistivity. All that is needed is the values of the three constants, C, m and n, which are usually fixed for a given reservoir and can be determined from simple laboratory experiments. Equation 5.9 is the basis of the laboratory resistivity test and the resistivity log, which is described below.

5.4: Resistivity log

The basic resistivity sonde sends current into the reservoir and measures its resistivity, $\mathcal{R}_t$, versus depth. A graph of a typical resistivity log is shown in Fig. 5.3. High

oil-saturation zones display large resistivity while water-saturated zones display the lowest resistivity. The logging engineer utilizes this information to identify oil zones within the reservoir as well as the aquifer, where $S_w = 1$ and $\mathcal{R}_t = \mathcal{R}_o$. If values of C, m and n are not available from laboratory tests on core samples, the engineer selects a few points within the aquifer and computes the values of C and m according to Equ. 5.4. Note that a porosity profile for the formation should be available from a porosity log. The computed values are assumed to apply for the reservoir as well since both aquifer and reservoir exist within the same rock formation. Finally, the engineer constructs a water saturation profile of the reservoir with Equ. 5.9. The value of n can be assumed.
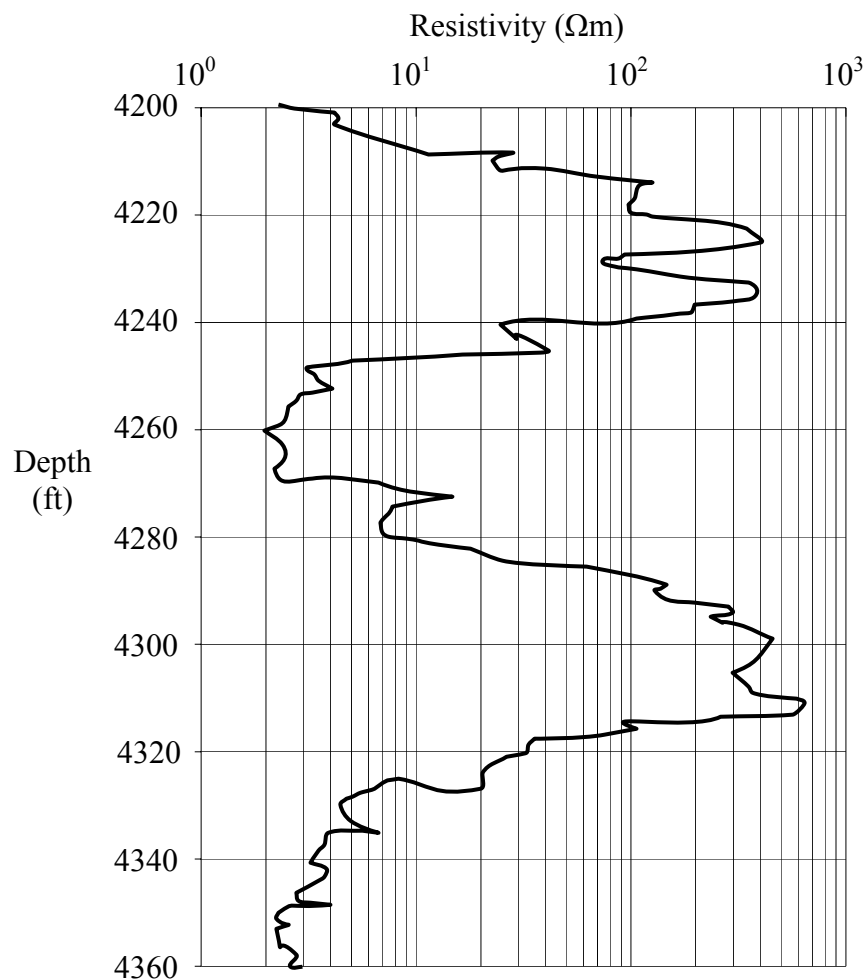
Fig. 5.3: Resistivity log

Example 5.1

Consider the reservoir whose resistivity log is shown in Fig. 5.3. The reservoir water resistivity is 1.2 Ωm. If the Humble equation applies to this reservoir, and the saturation exponent is 2.2, estimate the oil saturation at 4226 ft where the porosity is 24%.

At 4226 ft, the resistivity is approximately 400 Ωm. Applying Equ. 5.9 to this depth

$$S_w^n = C \varphi^{-m} R_w / R_t$$

$$S_w^{2.2} = 0.62 (0.24)^{-2.15} \times 1.2 / 400$$

$$= 0.04$$

$$S_w = 0.232 = 23.2\,\%$$

$$S_o = 76.8\,\%$$

Exercises

1. Estimate the electrical resistance of a round bar of copper (L = 50 cm, D = 1.27 cm) if copper has a resistivity of 1.59×10^{-8} Ωm.

2. Sonic and resistivity logs on a sandstone aquifer (R_w = 1.1 Ωm) yielded the following data:

R_o (Ωm)	40.1	28.2	19.1	55.0	17.9	33.8
φ	0.16	0.19	0.22	0.14	0.23	0.17

Estimate the tortuousity constant and cementation factor for this formation.

3. An oil accumulation exists in another part of the formation of Exercise 2. Resistivity and porosity data on this part is listed below. Plot the oil saturation profile vs. depth assuming a saturation exponent of 2.

Depth (ft)	4700	4800	4900	5000	5100	5200	5300	5400	5500	5600	5700	5800	5900	6000
R_t (Ωm)	365	622	731	906	863	872	775	740	948	811	629	568	589	767
φ	0.11	0.12	0.14	0.11	0.16	0.17	0.15	0.14	0.11	0.13	0.17	0.22	0.21	0.16

6. ROCK PERMEABILITY

All rock properties discussed in the previous chapters facilitate estimation of the quantity of various fluids within a reservoir. They do not provide, however, any information on the rate at which such fluids could flow through the reservoir rock, which is another basic requirement for reservoir engineering calculations. Such information is provided by rock permeability.

6.1: Definition

Permeability is defined as the ability of a porous medium, e.g., sedimentary rock, to conduct fluids. The larger the permeability, the more fluid flow can be achieved through the medium for a given set of conditions. The earliest attempt at quantifying permeability was the work of Henry Darcy in 1856. Conducting many experiments on beds of packed sand and using different liquids, Darcy observed the following relationships:

$$q \propto \Delta P$$
$$q \propto A$$
$$q \propto 1 / L$$

where

q : volumetric flow rate of the fluid through the medium, cm^3/s

ΔP : difference in pressure between inlet and outlet of medium, atm

A : cross-sectional area of medium that is open to flow, cm^2

L : length of medium, cm

Combining the three relationships, the following equation was obtained

$$q = c A \Delta P / L \tag{6.1}$$

The proportionality constant, c, was found to be inversely proportional to the viscosity of the fluid used. Therefore, it was replaced with k / μ and Equ. 6.1 became

$$q = k \frac{A}{\mu} \frac{\Delta P}{L} \tag{6.2}$$

The new constant, k, was found to be the same for a given porous medium regardless of its dimensions, the type of fluid used or the pressure drop applied. It was an inherent property of the medium that controlled its ability to conduct fluids. Darcy termed this property the coefficient of permeability, which was later called simply the permeability, and Equ. 6.2 became known as Darcy's law. It should be noted that implicit in the definition of permeability is the requirement that the fluid saturates the porous medium completely.

The units of permeability are a little confusing. If we substitute consistent units for all the variables in Equ. 6.2 – such as $g/cm.s^2$ for pressure and $g/cm.s$ for viscosity, we find that the unit of permeability is cm^2 and this is indeed one of the units employed in the metric system of units. However, one cm^2 is a very large permeability that is not encountered in natural rock. Therefore, reservoir engineers have adopted another, more practical, unit defined as follows:

If 1 atmosphere of pressure drop is required to flow a liquid of 1 cp viscosity through a porous medium of 1 cm length and 1 cm^2 cross-sectional area at a rate of 1 cm^3 per second, then the medium has a permeability of 1 darcy.

Thus, 1 darcy = 9.869 x 10^{-9} cm^2. A more common unit of reservoir rock permeability is the millidarcy (md), which is one thousandth of a darcy. Since the petroleum industry still uses the system of field units, a conversion factor is introduced in Darcy's law as follows

$$q \quad = \quad 1.127 \, k \, \frac{A}{\mu} \frac{\Delta P}{L} \qquad\qquad (6.3)$$

where q, k, A, ΔP, μ and L are in bbl/day, darcy, ft^2, psi, cp and ft, respectively.

6.2: Differential form of Darcy's law

Equation 6.2 can be used in situations where the flow is linear and at steady state, i.e., the flow streamlines are parallel and all variables are constant with time at any given location. These conditions are highly idealized and are seldom encountered in real situations. The differential form of Darcy's law, which is more general and can be the starting step in the solution of any flow problem, is expressed by Equ. 6.4.

$$q_s \quad = \quad - k_s \, \frac{A_s}{\mu} \frac{\partial P}{\partial s} \qquad\qquad (6.4)$$

where s is the coordinate along which flow is calculated and subscript s denotes the value of the variable in the s-direction. Since flow always takes place in the direction of decreasing pressure, which means the pressure gradient – the partial derivative in Equ. 6.4 - is always negative, the negative sign is added in Equ. 6.4 to make the flow positive in the s-direction. Equation 6.4 applies to any flow system, and it can be used to compute the flow in the s-direction at any given point in the system.

To complete the differential form of Darcy's law, one more detail has to be addressed. It is well known from fluid statics that the pressure increases with depth within any static body of fluid. This hydrostatic pressure, P_h, is the result of the weight of the fluid column above the depth of interest, and is given by

$$P_h \quad = \quad \rho \, g \, d \qquad\qquad (6.5)$$

where

ρ :   density of the fluid, g/cm^3

g   :   gravitational acceleration (980 cm/s^2)

d   :   depth measured from a reference horizon, cm

Equation 6.5 provides P$_h$ in dyne/cm^2. In field units where ρ is in lb/ft^3, depth is in ft and g = 32.17 ft/s^2, Equ. 6.5 becomes

$$P_h \quad = \quad \rho\, d\, /\, 144 \qquad\qquad\qquad\qquad\qquad\qquad (6.6)$$

where P$_h$ is in psi.

However, the pressure at a point within the body of fluid may be greater than the hydrostatic pressure at that point. This could be caused by an external force applied to the fluid such as pump action. Suppose a flow system has its inlet and outlet at two different elevations – or depths. If the difference in fluid pressure between the inlet and outlet is equal to the difference in hydrostatic pressure at these two points, we intuitively know that no flow would take place. Therefore, the hydrostatic component of the pressure at any depth must be subtracted to yield the net pressure. This dynamic pressure component, which is the true driving force of flow, is called the *flow potential* and is defined as

$$\Phi \quad = \quad P - P_h$$
$$= \quad P - \rho\, g\, d$$
$$= \quad P - \rho\, d\, /\, 144 \qquad\qquad\qquad (\text{in field units})$$

With this consideration, the generalized differential form of Darcy's law becomes

$$q_s \quad = \quad -\, k_s\, \frac{A_s}{\mu}\, \frac{\partial \Phi}{\partial s} \quad = \quad -\, k_s\, \frac{A_s}{\mu}\, \frac{\partial (P - \rho g d)}{\partial s} \qquad\qquad (6.7)$$

It should be noted that if all points in the flow system are at the same depth, Equ. 6.7 reduces to Equ. 6.4.

6.3: Measurement of permeability

Permeability is almost always determined experimentally, and only if no laboratory data is available do we resort to empirical correlations. Such correlations will be discussed at the end of this section. Laboratory measurement is performed under steady-state conditions using a permeameter such as the one shown in Fig. 6.1. The clean and dry core sample is mounted in the core holder and then placed under a suitable confining pressure to simulate reservoir overburden conditions. The sample is then placed under vacuum for a sufficient period of time to remove all air from the sample. The fluid – usually brine, oil or air – is then flowed through the sample until steady-state flow is established; such state is characterized by equal fluid injection and production rates. The flow rate and the inlet pressure are then

recorded. Such data is sufficient to compute the permeability according to Equ. 6.2, however, the test is usually repeated at different sets of flow rate and inlet pressure and the data is plotted as shown in Fig. 6.2. The slope of the straight line is the core sample's permeability multiplied by A/ μL.
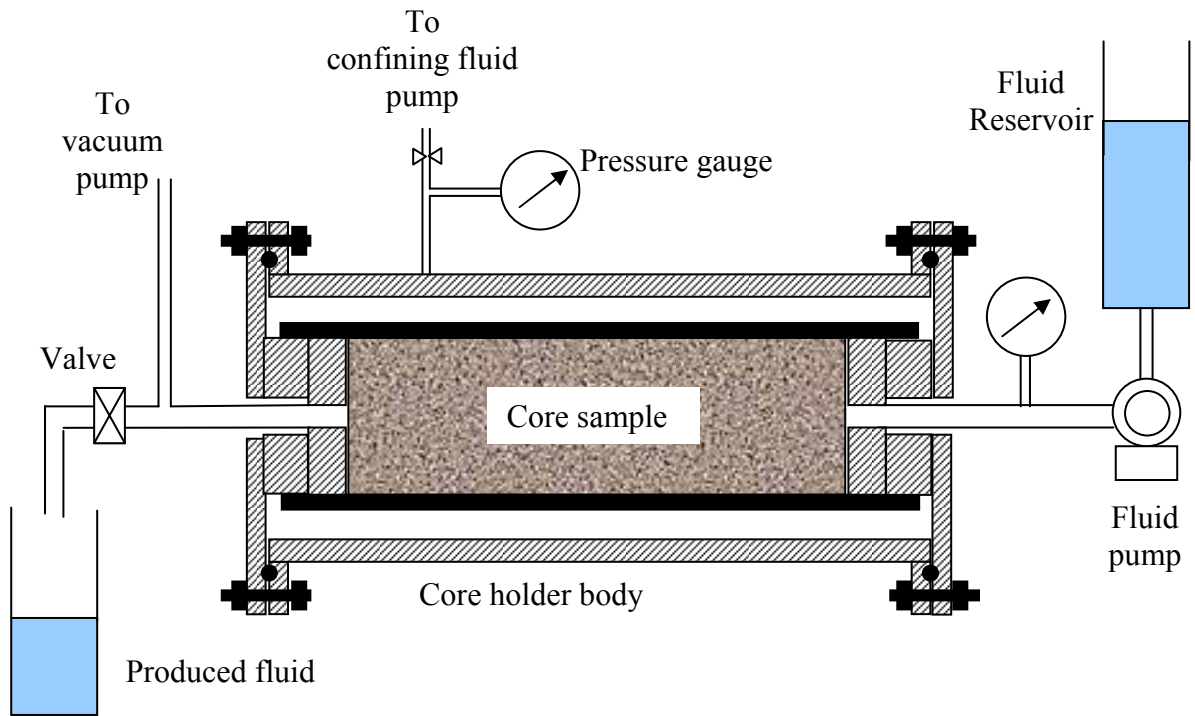

Fig. 6.1: Measurement of permeability
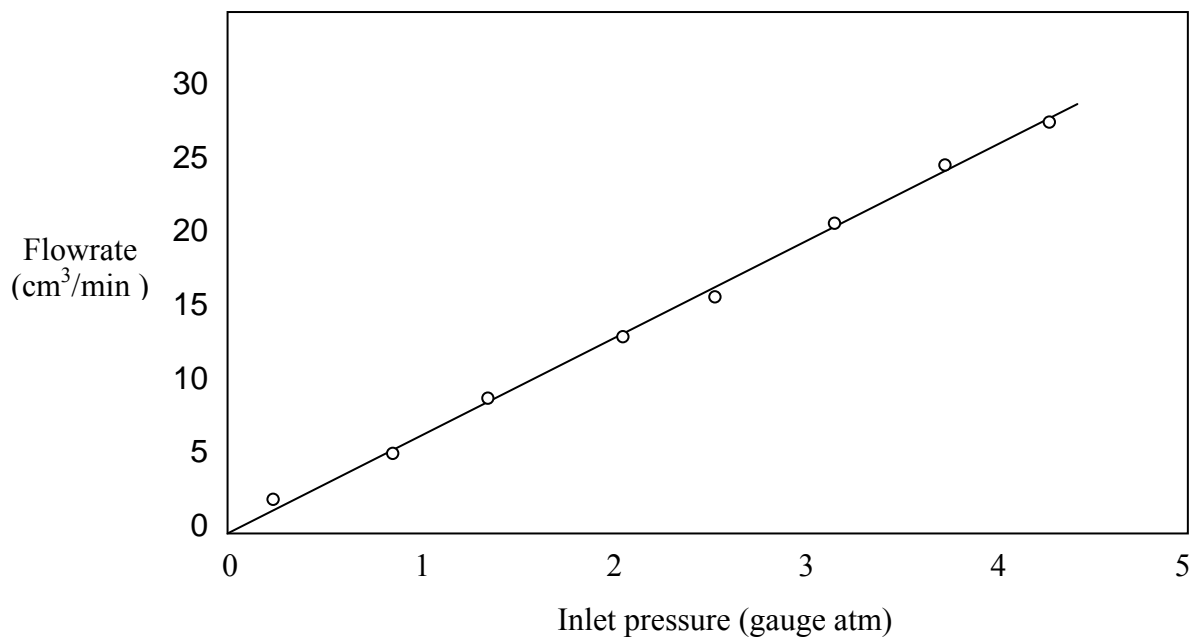
Fig. 6.2: Computation of permeability

Example 6.1

Compute the permeability of the core sample whose flow data is shown in Fig. 6.2 if the sample is 5 cm in diameter and 10 cm long. The fluid used in the experiment is an oil with a viscosity of 1.6 cp.

The cross-sectional area of the sample is

$$A \quad = \quad \frac{\pi}{4}(5)^2 \; = \; 19.63 \text{ cm}^2$$

The slope of the best-fit line, m, is 6.25 cm^3/min/atm, or 0.1 cm^3/s/atm. The core permeability is:

$$
\begin{aligned}
k \quad &= \quad m\,\mu\,L\,/\,A \\
&= \quad 0.1 \text{ x } 1.6 \text{ x } 10 \, / \, 19.63 \\
&= \quad 0.0815 \text{ d} \; = \; 81.5 \text{ md}
\end{aligned}
$$

Several precautions must be observed with this method. First, if the sample is sandstone that contains shale (clay particles), distilled water must not be used. Second, the flow rate must be reasonably low, as Darcy's law does not apply at excessive rates. Third, the inlet pressure should not be close to the confining pressure, as the fluid may bypass the sample and flow along the inner wall of the rubber sleeve. Finally, when gas is used, the mean gas pressure – average of inlet and outlet pressures – and the mean gas flow rate – rate measured at mean pressure – should be plotted instead.

Empirical correlations for estimation of permeability, sometimes called permeability transforms, are based on core data gathered for a given reservoir. Such data include permeability, porosity, bulk density and mineral composition. The basic assumption is that for a given type of reservoir rock, permeability varies with other rock properties according to a particular trend. Once a good number of core samples have been collected and tested, and a trend has been established, such trend would apply everywhere in the reservoir. Thereafter, additional core data becomes unnecessary and permeability can be estimated from log-derived data using the transform.

For clean sandstone rock, permeability has been found to correlate reasonably with porosity according to the following formula

$$k \quad = \quad a\,\varphi^{\,b} \tag{6.8}$$

where a and b are empirical constants that should be determined for a given reservoir. If the sandstone contains a significant amount of shale, a correction is added as follows

$$k \quad = \quad a\,\varphi^{\,b}\,(1\text{-}V_{sh})^{c} \tag{6.9}$$

where V_{sh} is the volumetric fraction of shale in the matrix and c is another empirical constant.

For carbonate rocks – limestone, dolomite, gypsum – a similar permeability transform is almost impossible to find. This is attributed to the effect of post-sedimentation processes on both porosity and permeability. Mineral deposition has a minor effect on porosity but reduces permeability drastically. On the other hand, minute fractures add little to porosity but improve permeability considerably. A typical example is the carbonate Khuff-C reservoir in the Uthmaniya area of Ghawwar field in eastern Saudi Arabia. As Fig. 6.3 shows, no correlation is evident in the data for this reservoir. In such cases, statistical analysis can sometimes provide meaningful trends. In general, permeability transforms involve variable margins of error, and they should be utilized mainly to provide a general estimate. Error margins could diminish as the transform's database expands.
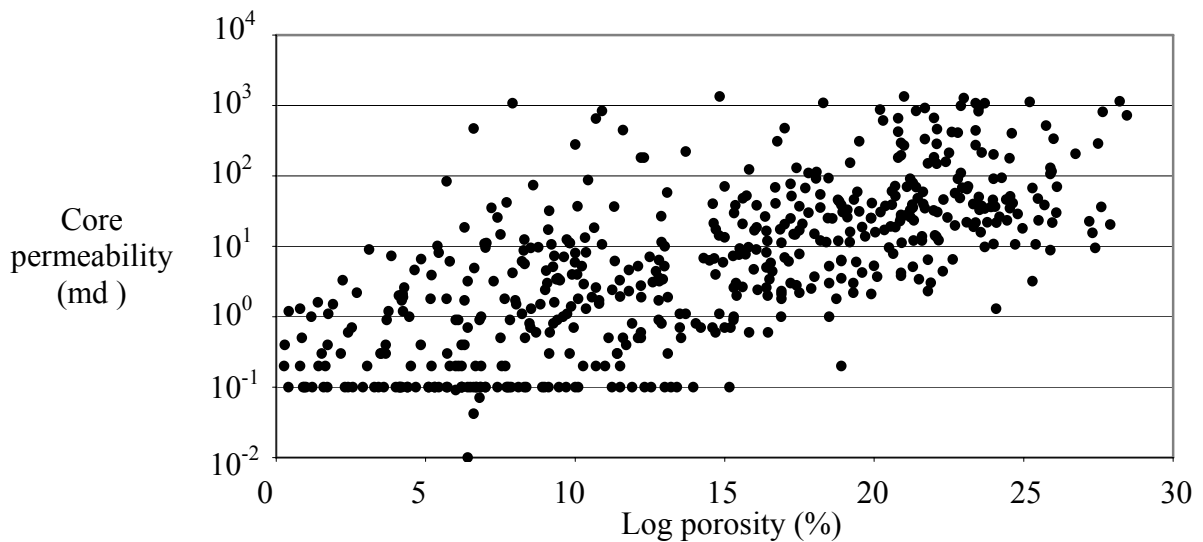
Fig. 6.3 : Core permeability versus log porosity for Khuff-C reservoir

6.4: Applications

In this section, the use of Darcy's law to establish a flow equation is presented for various common flow systems. The main objective is to derive an equation that enables us to compute the flow rate through a porous medium from data on the fluid's properties, the medium's properties and geometry, and the pressure drop across the medium. We shall begin with simple flow systems and then move on to more complex ones.

6.4.1: Linear flow

i. Horizontal, steady-state flow of an incompressible fluid

Assume that an incompressible fluid – a fluid whose density does not vary with pressure – is flowing through a rectangular porous medium, which is perfectly horizontal as shown in Fig. 6.4. We shall adopt a Cartesian coordinate system for this problem where the x-direction is along the length of the medium. Since the entire cross-sectional area of the medium is open for flow, the flow is linear and only in the x-direction. The flow potential gradient becomes

$$\frac{\partial \Phi}{\partial s} = \frac{\partial \Phi}{\partial x} = \frac{d\Phi}{dx}$$

Note that the partial derivative was replaced by the total derivative since the flow potential varies only in the x-direction. Expanding the derivative gives

$$\frac{d\Phi}{dx} = \frac{d}{dx}(P - \rho g d) = \frac{dP}{dx} - \rho g \frac{dd}{dx} \tag{6.10}$$
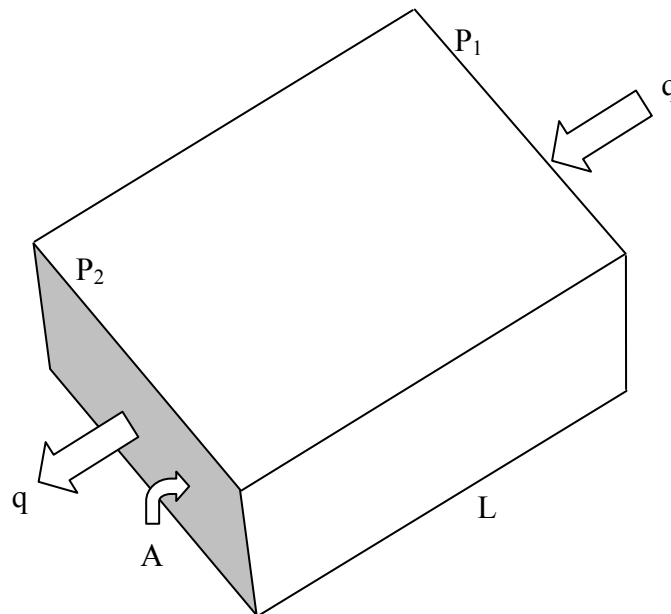
Fig. 6.4: Linear flow

As both ρ and g are constant with x, they are taken out of the differential in Equ. 6.10. Since the medium is horizontal, depth does not change with x, and the second term in Equ. 6.10 reduces to zero. The flow potential gradient then becomes equal to the pressure gradient of the fluid:

$$\frac{d\Phi}{dx} = \frac{dP}{dx} \tag{6.10}$$

and Darcy's law (Equ. 6.7) becomes

$$q = -k\frac{A}{\mu}\frac{dP}{dx} \tag{6.11}$$

Separating the variables in Equ. 6.11 and rearranging

$$\frac{q\mu}{kA}dx = -dP$$

Setting the integration limits at the two boundary conditions: $P = P_1$ at $x = 0$ and $P = P_2$ at $x = L$ gives

$$\int_0^L \frac{q\mu}{kA}dx = -\int_{P_1}^{P_2}dP \tag{6.12}$$

All the variables in the LHS integral are constant with x; therefore, they can be removed outside the integral. Upon integration, Equ. 6.12 becomes

$$\frac{q\mu}{kA}L = -(P_2 - P_1)$$

and after rearrangement

$$q = \frac{kA}{\mu}\frac{P_1 - P_2}{L} \tag{6.13}$$

Once again, Equ. 6.13 is written in the standard units. In field units, the conversion factor of 1.127 is multiplied by the right-hand side of the equation.

The pressure at any location x can be determined from Equ. 6.12 by setting the upper integration limits to P and x, which yields

$$P = P_1 - \frac{q\mu}{kA}x$$

A graph of the pressure profile is shown in Fig. 6.5, where the prominent feature is the constant pressure *gradient*, $\frac{dP}{dx}$, which is equal to $\frac{P_2 - P_1}{L}$. This true only for linear, steady-state flow. Note that the pressure gradient in this case is negative.

It is very pertinent, at this point, to explain the concept of steady-state flow, which tends to be confusing in some instances. The condition of steady state requires that all variables remain constant with *time* at any given point within the flow system. This does not necessarily mean that a variable cannot change between two locations. The pressure in the present case, for instance, drops from P_1 to P_2 between 0 and L, yet at any location x the

pressure is constant with time. On the other hand, the pressure gradient is the same everywhere in the system. In later cases, we will find that even the pressure gradient may vary across the flow system, yet the flow is still considered steady state. One variable that must be the same everywhere in the system is the mass flowrate, $\dot{m}$, which is dictated by a fundamental condition of steady state that no mass accumulation occurs within the system.
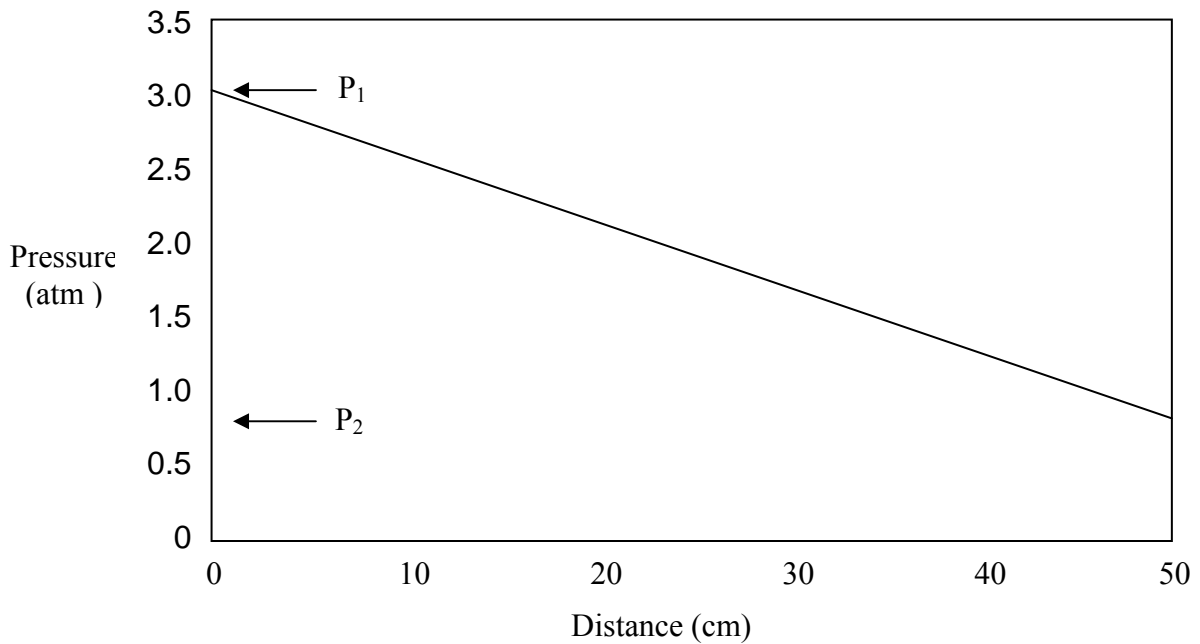
Fig. 6.5: Example pressure profile in linear flow

Example 6.2

Compute the steady-state flow of water in a core sample 4" long, 1" in diameter with permeability of 150 md if the inlet pressure is 50 psia and the outlet pressure is atmospheric. The viscosity of water at the conditions of the test is 0.95 cp.

The cross-sectional area of the sample is

$$A \quad = \quad \frac{\pi}{4}(1)^2 \; = \; 0.785 \text{ in}^2 \; = \; 5.45 \text{ x } 10^{-3} \text{ ft}^2$$

Substituting in Equ. 6.13 with other variables

$$q \quad = \quad 1.127\frac{(150/1000)\,5.45\text{x}10^{-3}}{0.95}\frac{50-14.7}{(4/12)}$$

$$= \quad 0.103 \text{ bbl/d}$$

$$= \quad 0.189 \text{ cm}^3/\text{s}$$

---

ii. Horizontal, steady-state flow of a slightly compressible fluid

This case is identical to the one presented in part (i) above except that the fluid's density, and consequently its viscosity, are weak functions of pressure. The conditions of the problem will lead us again to Equ. 6.12.

$$\int_0^L \frac{q\mu}{kA}\,dx = -\int_{P_1}^{P_2} dP \qquad (6.12)$$

Since pressure decreases from inlet to outlet, the fluid undergoes continuous expansion as it flows through the porous medium. This makes q vary with x and, hence, cannot be taken outside the integral. We can go around this obstacle by replacing the volumetric flowrate with the mass flowrate according to

$$\dot{m} = \rho q$$

Therefore,

$$\int_0^L \frac{\dot{m}}{kA}\,dx = -\int_{P_1}^{P_2} \frac{\rho}{\mu}\,dP \qquad (6.14)$$

All the variables in the LHS integral are now constant with x and, therefore, can be removed outside the integral. Since both density and viscosity vary slightly with pressure, we can approximate them by their mean values, $\bar{\rho}$ and $\bar{\mu}$, which are computed at the mean pressure of the system: $\bar{P} = (P_1 + P_2)/2$. Performing the integration in Equ. 6.14 yields

$$\dot{m} = \frac{kA}{\bar{\mu}}\,\bar{\rho}\,\frac{P_1 - P_2}{L} \qquad (6.15)$$

Equation 6.15 can be used to compute q at any location in the medium by the following steps:

1. Compute the pressure at the desired location. This is obtained from the linear pressure gradient.

2. Compute the fluid density at the computed pressure.

3. Compute the flowrate from $q = \dot{m}/\rho$

We should note that while $\dot{m}$ and all other parameters in Equ. 6.15 are constant, q varies with location. For such systems, the flowrate is commonly reported in two ways:

1. The mean flowrate:

$$\bar{q} = \frac{kA}{\bar{\mu}}\,\frac{P_1 - P_2}{L} \qquad (6.16)$$

which is the flowrate based on the mean density.

2. The base flowrate:

$$q_\circ = \frac{kA}{\bar{\mu}} \frac{\bar{\rho}}{\rho_\circ} \frac{P_1 - P_2}{L} \tag{6.17}$$

where the subscript (∘) refers to some base pressure, $P_\circ$, adopted for the system.

Example 6.3

Rework Example 6.2 but for a fluid whose density varies with pressure according to:

$$\rho = 0.86\, e^{P/2500}$$

where P is in psia and ρ is in g/cm^3. Compute the mean flowrate and the base flowrate (at $P_\circ = 14.7$ psia). Assume a mean viscosity of 0.6 cp.

The mean pressure is: $\bar{P} = (50 + 14.7)/2 = 32.35$ psia. The mean density is then

$$\bar{\rho} = 0.86\, e^{32.35/2500} = 0.871 \ \text{g/cm}^3$$

and the base density is

$$\rho_\circ = 0.86\, e^{14.7/2500} = 0.865 \ \text{g/cm}^3$$

Equation 6.16 yields

$$\bar{q} = 1.127 \frac{(150/1000)\, 5.45 \text{x} 10^{-3}}{0.6} \frac{50 - 14.7}{(4/12)}$$

$$= 0.163 \ \text{bbl/d}$$

Equation 6.17 yields

$$q_\circ = 1.127 \frac{(150/1000)\, 5.45 \text{x} 10^{-3}}{0.6} \frac{0.871}{0.865} \frac{50 - 14.7}{(4/12)}$$

$$= 0.164 \ \text{bbl/d}$$

---

iii. Horizontal, steady-state flow of an ideal gas

This case is identical to the one presented in part (ii) above except that gases are compressible, and their properties, especially density, vary appreciably with pressure. The conditions of the problem will lead us straight to Equ. 6.14.

$$\int_0^L \frac{\dot{m}}{kA} dx = - \int_{P_1}^{P_2} \frac{\rho}{\mu} dP \tag{6.14}$$

For ideal gases, the ideal gas law provides a precise relationship between density and pressure:

$$\rho \quad = \quad \frac{P\,M}{R\,T}$$

where M is the molecular mass of the gas, R is the universal gas constant and T is the absolute temperature of the gas. Substituting for ρ in the RHS integral of Equ. 6.14 yields

$$\int_0^L \frac{\dot m}{kA}\,dx = -\int_{P_1}^{P_2} \frac{M}{RT\mu}\,P\,dP \tag{6.18}$$

Assuming a mean viscosity and performing the integration in Equ. 6.18 yields

$$\frac{\dot m L}{kA} \quad = \quad \frac{M}{RT\bar\mu}\,\frac{(P_1^{\,2} - P_2^{\,2})}{2} \tag{6.19}$$

Substituting $(P_1 + P_2)(P_1 - P_2)$ for $(P_1^{\,2} - P_2^{\,2})$ in Equ. 6.19 yields

$$\frac{\dot m L}{kA} \quad = \quad \frac{M}{RT\bar\mu}\,\frac{(P_1 + P_2)(P_1 - P_2)}{2} \tag{6.20}$$

Substituting $\bar P$ for $(P_1 + P_2)/2$ and noting that $\bar\rho = \dfrac{\bar P\,M}{R\,T}$, Equ. 6.20 becomes

$$\frac{\dot m L}{kA} \quad = \quad \frac{\bar\rho}{\bar\mu}(P_1 - P_2) \tag{6.21}$$

Substituting $\bar q$ for $\dot m / \bar\rho$ and rearranging, we obtain the desired flow equation

$$\bar q \quad = \quad \frac{kA}{\bar\mu}\,\frac{P_1 - P_2}{L} \tag{6.22}$$

which is exactly the same as Equ. 6.16 for the slightly compressible fluid. We can also use Equ. 6.17 for the base flowrate case.

Example 6.4

Rework Example 6.2 but for an ideal gas whose molecular mass is 18. The system is at 150 ºF and the average gas viscosity is 0.015 cp. Compute the mean flowrate and the base flowrate at base conditions of $P_o = 15$ psia and $T_o = 60$ ºF.

Equation 6.22 yields

$$\bar q \quad = \quad 1.127 \frac{(150/1000)\,5.45\text{x}10^{-3}}{0.015}\,\frac{50 - 14.7}{(4/12)}$$

$$= \quad 6.50 \text{ bbl/d}$$

At a mean pressure of $\bar{P} = 32.35$ psia, the mean density is

$$\bar{\rho} \quad = \quad \frac{\bar{P} \, M}{R \, T} \quad = \quad \frac{32.35 \text{x} 18}{10.73(150+460)}$$

$$= \quad 0.0890 \text{ lb/ft}^3$$

Note that in the field system of units R $= 10.73 \; \dfrac{\text{psi ft}^3}{\text{lbmole } ^\circ \text{R}}$. Similarly, the base density is

$$\rho_\circ \quad = \quad \frac{15 \text{x} 18}{10.73(60+460)} \quad = \quad 0.0484 \text{ lb/ft}^3$$

The base flowrate is then computed:

$$q_\circ \quad = \quad 1.127 \frac{(150/1000) \, 5.45 \text{x} 10^{-3}}{0.015} \frac{0.0890}{0.0484} \frac{50-14.7}{(4/12)}$$

$$= \quad 11.96 \text{ bbl/d}$$

Note that by multiplying each flowrate by its corresponding density the same mass flowrate of 3.25 lb/d would be obtained.

Gas flowrate is not usually reported in bbl/d, rather the unit of ft^3/d is used. And since rate depends on the flow conditions, gas flowrate is normally expressed at the standard conditions of 14.7 psia and 60 °F. Thus, the unit SCF means one cubic foot of gas measured at the standard conditions, and SCF/D means one SCF per day. The prefix M indicates thousands and MM indicates millions.

iv. Inclined, steady-state flow of an incompressible fluid

Petroleum reservoirs are seldom perfectly horizontal; they are usually tilted in one direction, two opposite directions – the anticline – or in all directions like in the case of a dome. A reservoir's *angle of dip* is the angle between the horizontal plane and the plane of the reservoir's main flow path. Considering the case depicted in Fig. 6.6, the direction of flow, s, is taken to be along the reservoir's main flow path in the downward direction. The flow potential gradient then becomes:

$$\frac{d\Phi}{ds} = \frac{d}{ds}(P - \rho \, g \, d) = \frac{dP}{ds} - \rho \, g \, \frac{dd}{ds} \qquad\qquad (6.23)$$

Depth increases with s according to

$$\frac{dd}{ds} \quad = \quad \sin \theta$$
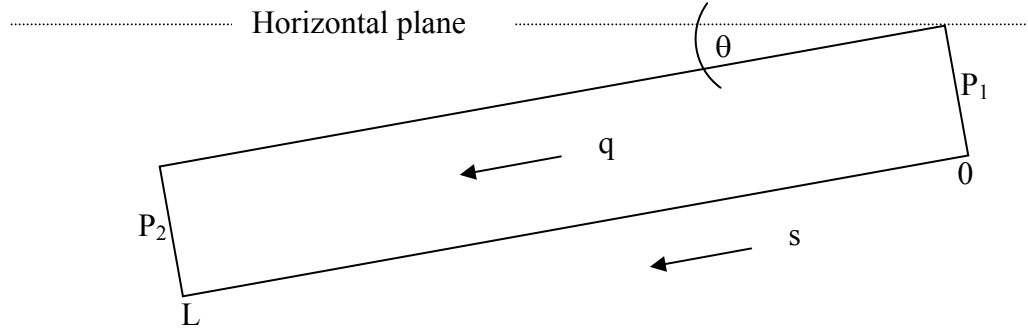
Fig. 6.6: Inclined flow

Therefore, Equ. 6.23 becomes

$$\frac{d\Phi}{ds} = \frac{dP}{ds} - \rho\, g \sin\theta \qquad (6.24)$$

which upon substitution in Darcy's law (Equ. 6.7) gives

$$q = -k\,\frac{A}{\mu}\left[\frac{dP}{ds} - \rho\, g \sin\theta\right] \qquad (6.25)$$

Separating the variables and setting the integration limits at $P = P_1$ at $s = 0$ and $P = P_2$ at $s = L$ yields

$$\int_0^L \left[\frac{q\mu}{kA} - \rho\, g \sin\theta\right] ds = -\int_{P_1}^{P_2} dP \qquad (6.26)$$

Since all parameters in the LHS integral are constant, integration would yield

$$\left[\frac{q\,\mu}{k\,A} - \rho\, g \sin\theta\right] L = P_1 - P_2 \qquad (6.27)$$

After rearrangement, the desired flow equation is obtained

$$q = \frac{k\,A}{\mu}\,\frac{(P_1 - P_2) + \rho\, g\, L \sin\theta}{L} \qquad (6.28)$$

and in field units, Equ. 6.28 is written

$$q = 1.127\frac{k\,A}{\mu}\,\frac{(P_1 - P_2) + \dfrac{\rho}{144}\,L\sin\theta}{L} \qquad (6.29)$$

It should be noted that for upward flow $\dfrac{dd}{ds} = -\sin\theta$ and Equs. 6.28 and 6.29 must be modified accordingly.

41

Example 6.5

A sandstone aquifer 8 miles long, 2 miles wide and 70 feet thick with a dip angle of 6 degrees and permeability of 80 md is conducting water from the ocean floor to a reservoir at the other end as shown in Fig. 6.7. The ocean floor is 600 feet deep, and sea water has a density of 68 lb/ft^3 and viscosity of 1.4 cp. If the reservoir pressure is 1600 psia, compute the steady-state rate at which the aquifer is charging water into the reservoir.

$$A \quad = \quad 2 \times 5280 \times 70 \; = \; 739200 \text{ ft}^2$$

The inlet pressure is the hydrostatic pressure at the ocean floor

$$P_1 \quad = \quad 68 \times 600 / 144 + 14.7 \; = \; 298 \text{ psia}$$

Since the aquifer's outlet pressure is equal to the reservoir pressure, water flowrate through the aquifer is computed by Equ.6.29 as

$$q \quad = \quad 1.127 \frac{0.08 \times 739200}{1.4} \; \frac{(298 - 1600) + \dfrac{68}{144} 8 \times 5280 \sin 6}{8 \times 5280}$$

$$= \quad 882.4 \text{ bbl/d}$$
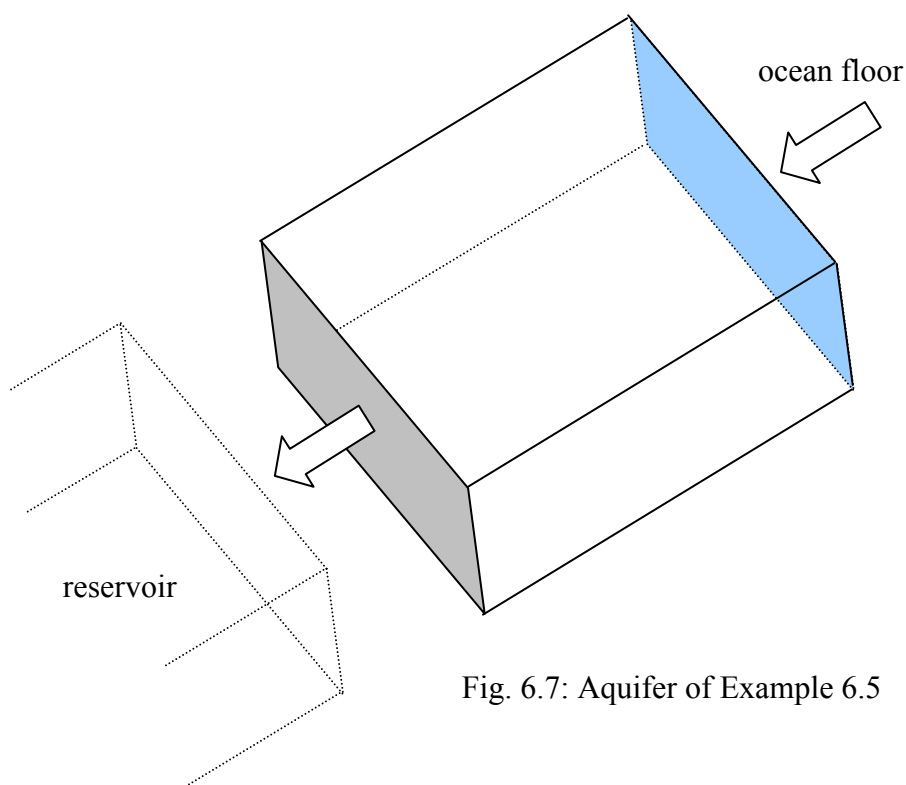
Fig. 6.7: Aquifer of Example 6.5

6.4.2: Radial flow

Fluids are produced from or injected into a petroleum reservoir via wells, which are cylindrical in shape and may penetrate the reservoir vertically, horizontally or at an angle. The well may penetrate the entire thickness of the reservoir or part of it. In any case, the whole circumference of the well is open for flow, which allows reservoir fluids to flow into the well from all directions and at all depths. This configuration makes the well act like a cylindrical sink into which fluids flow radially from nearby parts of the reservoir (Fig. 6.8).

Radial flow is assumed, therefore, to be the predominant mode of flow in petroleum reservoirs, and most analytical techniques of reservoir engineering are based on this assumption. The pressure in the wellbore is uniform while the pressure in the reservoir at any given distance from the well is essentially the same no matter in which direction we look. Because of the symmetry of the system, the flow equation is written in radial coordinates, which are: vertical direction, z, radial direction, r, and radial angle, φ.
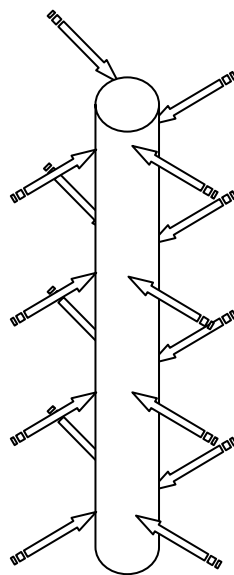
Fig. 6.8: Radial flow into a well

i. Horizontal, steady-state flow of an incompressible fluid

The flow system is depicted in Fig. 6.9 where a cylindrical porous medium with radius r_e and thickness h is penetrated along its axis by a well with radius r_w. The fluid flows from the outside boundary, where the pressure is P_e, towards the well where the pressure is P_w.
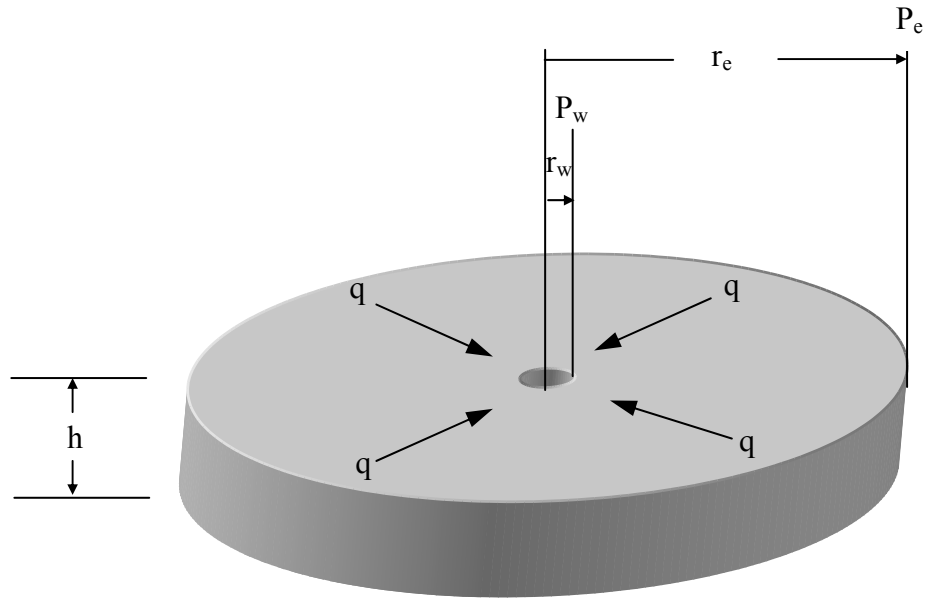
Fig. 6.9: Radial flow

Because the fluid flows in the radial direction only, the flow potential gradient exists only in the r-coordinate; and given that the medium is horizontal, the potential gradient reduces to the pressure gradient:

$$\frac{\partial \Phi}{\partial s} = \frac{dP}{dr}$$

Darcy's law for this case becomes:

$$q = k \frac{A}{\mu} \frac{dP}{dr} \tag{6.30}$$

The negative sign disappears from the RHS of Equ. 6.30 because pressure increases in the r-direction, which renders the radial pressure gradient (dP/dr) positive. Separating the variables and applying the integrals between the medium's boundary conditions gives

$$\int_{r_w}^{r_e} \frac{q\mu}{kA} \, dr = \int_{P_w}^{P_e} dP \tag{6.31}$$

All the variables in the LHS integral are independent of r except A. Remember that A is the cross-sectional area through which the flow passes. It is not the surface area of the medium, rather it is the circumferential area, which varies with radial distance according to

$$A = 2\pi r h$$

Substituting for A and performing the integration in Equ. 6.31 yields

$$\frac{q\mu}{2\pi kh} \ln \frac{r_e}{r_w} = P_e - P_w$$

Upon rearrangement, the desired flow equation is obtained

$$q = \frac{2\pi kh}{\mu} \frac{P_e - P_w}{\ln \dfrac{r_e}{r_w}} \tag{6.32}$$

In field units, Equ. 6.32 is written

$$q = 7.082 \frac{kh}{\mu} \frac{P_e - P_w}{\ln \dfrac{r_e}{r_w}} \tag{6.33}$$

The pressure profile can be established with Equ. 6.32 by substituting r for r_e and P for P_e. This profile, shown in Fig. 6.10, reveals a variable pressure gradient, which is largest near the well. This important observation indicates that most of the pressure drop occurs near the production end of the system, a feature of radial flow that calls for considerable care when drilling and completing petroleum wells.
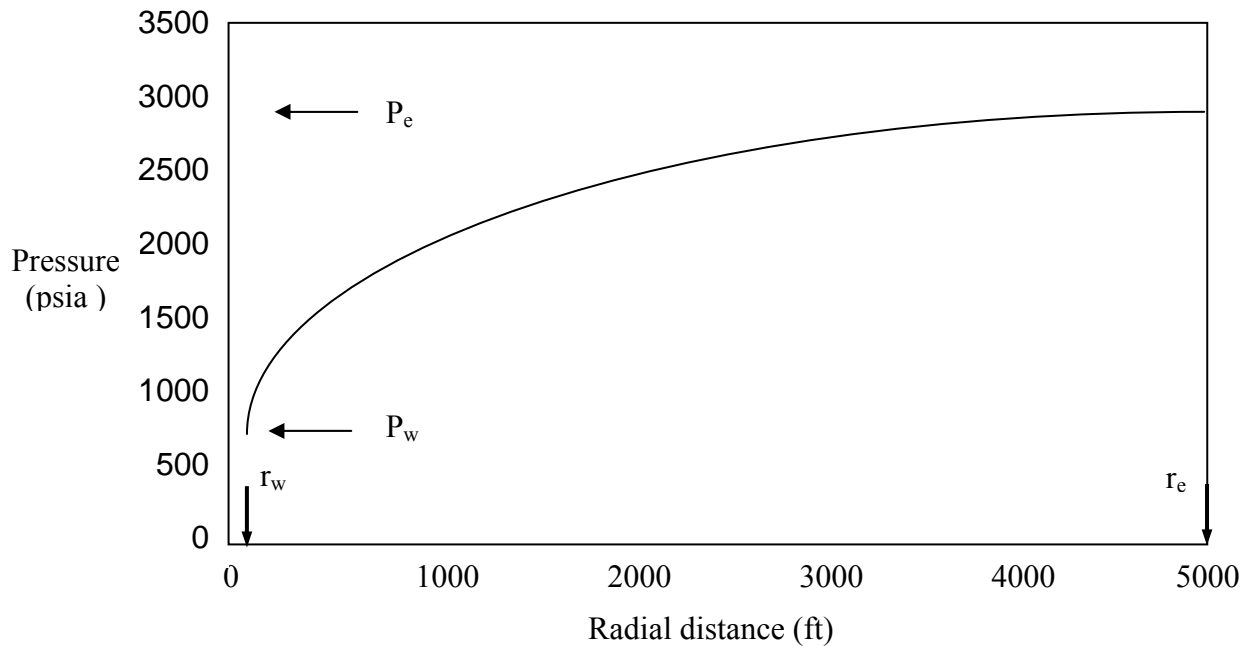
Fig. 6.10: Example pressure profile in radial flow

Example 6.6
A horizontal reservoir is nearly circular in shape with an area of 730 acres, thickness of 120 feet and permeability of 250 md. One well penetrates the reservoir at its approximate center

with a diameter of 9". If the pressure is 3200 psig at the periphery of the reservoir and 1500 psig at the wellbore; and if the reservoir oil is 2.5 cp in viscosity, compute the well's daily production rate assuming all pressures remain constant with time.

All parameters in Equ. 6.33 are provided except r_e. Since the reservoir is nearly radial, we can compute an equivalent radius by the following approximation:

$$r_e \;=\; \sqrt{\frac{A}{\pi}} \;=\; \sqrt{\frac{730 \times 43560}{\pi}}$$

$$= \; 3181.5 \text{ ft}$$

$$r_w \;=\; \frac{9}{12 \times 2} \;=\; 0.375 \text{ ft}$$

$$q \;=\; 7.082 \, \frac{0.25 \times 120}{2.5} \, \frac{3200 - 1500}{\ln \dfrac{3181.5}{0.375}}$$

$$= \; 15971 \text{ bbl/d}$$

---

ii. Horizontal, steady-state flow of an ideal gas

This case is identical to the one presented in section 6.4.1 part (iii) except for the radial geometry. Thus, we will begin with Equ. 6.18, but modified for radial coordinates.

$$\int_{r_w}^{r_e} \frac{\dot{m}}{2\pi rkh} \, dr = \int_{P_w}^{P_e} \frac{M}{RT\mu} \, P \, dP \tag{6.34}$$

Assuming an average viscosity, integrating Equ. 6.34 yields

$$\frac{\dot{m}}{2\pi kh} \ln \frac{r_e}{r_w} = \frac{M}{RT\bar{\mu}} \frac{P_e^{\,2} - P_w^{\,2}}{2} \tag{6.35}$$

Adopting base conditions of P_o and T_o at which $\rho_o = \dfrac{P_o M}{R\, T_o}$ and substituting $q_o \rho_o$ for $\dot{m}$, Equ. 6.35 becomes after rearrangement

$$q_o \;=\; \frac{\pi kh}{\bar{\mu}} \, \frac{T_o}{TP_o} \, \frac{P_e^{\,2} - P_w^{\,2}}{\ln \dfrac{r_e}{r_w}} \tag{6.36}$$

In oil field units, Equ. 6.36 is written

$$q_o = 19.88 \frac{kh}{\bar{\mu}} \frac{T_o}{TP_o} \frac{P_e^2 - P_w^2}{\ln \frac{r_e}{r_w}} \qquad (6.37)$$

where q_o is in ft^3/d measured at base conditions. Typical base conditions for gas wells are the standard conditions of 60 ºF (520 ºR) and 14.7 psia. For these conditions, Equ. 6.37 becomes

$$q_{sc} = 703.2 \frac{kh}{\bar{\mu}T} \frac{P_e^2 - P_w^2}{\ln \frac{r_e}{r_w}} \qquad (6.38)$$

where q_{sc} is in standard cubic feet per day or SCF/d.

Example 6.7

Rework Example 6.6 if the reservoir is at 180 ºF and contains gas of 0.055 cp viscosity. Report the flowrate in standard conditions.

$$q_{sc} = 703.2 \frac{0.25 \times 120}{0.055 \times 640} \frac{3214.7^2 - 1514.7^2}{\ln \frac{3181.5}{0.375}}$$

$$= 532.7 \times 10^6 \text{ SCF/d}$$

$$= 532.7 \text{ MMSCF/d}$$

6.5: Complex Flow Systems

In the previous section, only linear and radial flow systems were presented. While such types of flow can be encountered in real reservoirs, they are not usually seen across the entire reservoir, especially linear flow. The reason is that fluids are produced through wells, which force the flow to be radial at least in their vicinity.

A typical case is a well producing from an elongated reservoir as shown in Fig. 6.11. Far away from the well the flow is almost linear because the effect of the well is too small to be felt. As the fluid approaches the well, it is forced to converge upon the wellbore and, thus, shifts from linear to radial flow. To illustrate how a flow equation is derived for such a case let us first assume that the fluid is incompressible and is flowing at steady-state through this horizontal reservoir. Next, we must decide where in the reservoir we expect the flow to be linear or radial. Near the well, the flow is certainly radial; however, the question is: how far away from the well does radial flow start? We can safely assume that no linear flow exists

along the edge of the reservoir at the location of the well, and that only radial flow exists in this direction. This sets the width of the reservoir as the diameter of the radial flow region, which is depicted by a circle in Fig. 6.11. That is $r_e = W/2$, where W is the width of the reservoir.
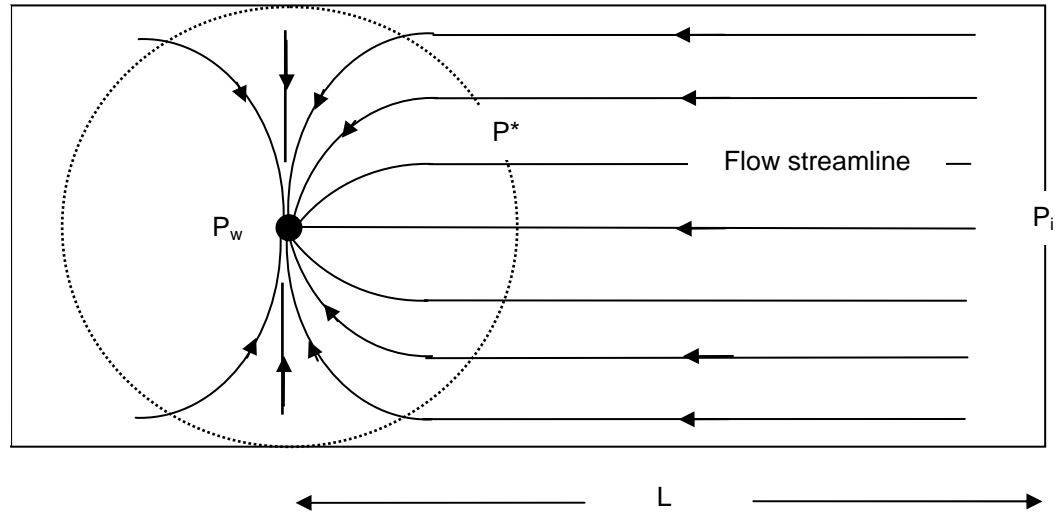
Fig. 6.11: Flow regimes near a well in a linear reservoir

Let the pressure at the reservoir inlet be P_i and at the well be P_w, and assume that P* - which is unknown - is the pressure at the boundary between the linear and radial flow regions. The production rate from the well is estimated by Equ. 6.32:

$$q_w = \frac{2\pi kh}{\mu} \frac{P^* - P_w}{\ln\dfrac{W/2}{r_w}} \tag{6.39}$$

To determine P^*, we must utilize the linear-flow region of the system. The length of this region can be approximated to be L - W/2. Therefore, the flowrate in this region is:

$$q_L = \frac{kWh}{\mu} \frac{Pi - P^*}{L - W/2} \tag{6.40}$$

Note that q_w is the total flow that arrives at the well from both right and left directions. Since the system is flowing at steady state, q_L must equal half of q_w ($q_w = 2\, q_L$). Combining both equations to solve for P^*, and substituting in Equ. 6.39 yields:

$$q_w = \frac{2\pi kh}{\mu} \frac{P_i - P_w}{\pi(\dfrac{L}{W} - \dfrac{1}{2}) + \ln\dfrac{W}{2r_w}} \tag{6.41}$$

Equation 6.41 provides the well production rate, q_w , and is written in terms of the known parameters of the system. In field units, the term 2π should be replaced by the conversion factor 7.082.

Another example of a complex-flow system is when the reservoir is not perfectly linear. Consider the case shown in Fig. 6.12 where the width of the reservoir is variable.
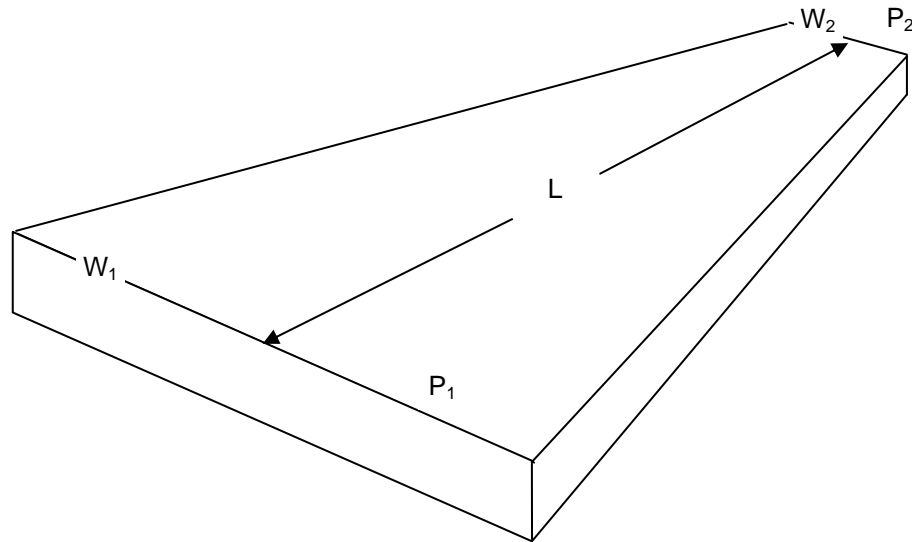
Fig. 6.12: Semi-linear reservoir with variable width

Horizontal, steady-state flow of an incompressible fluid is assumed once again for ease of analysis. Choosing the x-coordinate to be along the centerline of the reservoir, the flow equation is identical to Equ. 6.11:

$$q \quad = \quad -k \frac{A}{\mu} \frac{dP}{dx} \tag{6.11}$$

However, this equation cannot be readily integrated since the area, A, is not constant with x.

$$A \quad = \quad hW$$

where W is the width of the reservoir at any distance x from the inlet. From the geometry of the system,

$$W \quad = \quad W_1 - \frac{x}{L}(W_1 - W_2)$$

Substituting for W in Equ. 6.11, and integrating after rearrangement yields:

$$q \quad = \quad \frac{kh}{\mu} \frac{W_1 - W_2}{\ln \frac{W_1}{W_2}} \frac{P_1 - P_2}{L} \tag{6.42}$$

49

Comparing Equ. 6.42 with Equ. 6.13 shows that the quotient $\dfrac{W_1 - W_2}{\ln \dfrac{W_1}{W_2}}$ can be viewed as the

effective width of the reservoir. In mathematical terms, such parameter is called the log-mean width.

6.6: Averaging permeability

Petroleum reservoirs seldom show uniform permeability throughout, especially the larger ones. Seasonal and geographic variations in the sedimentation environment and post-sedimentation processes alter the nature of the sediments and the way they are packed together. This gives rise to a range of values for any rock property, with permeability being the most sensitive one. Core sample data provide a reasonable map of the distribution of permeability within a heterogeneous reservoir; and based on such data, an average permeability is usually estimated. An average permeability is a useful parameter, which allows application of the flow equation to the whole reservoir rather than to each segment at a time. In this section, various cases of reservoir heterogeneity will be treated.

6.6.1: Beds in parallel

The most common type of heterogeneity encountered in petroleum reservoirs is when the reservoir is made up of several stacked layers, or zones, each having a different permeability and thickness. Vertical communication between the zones is usually minimal and the predominant path of flow is along the plane of the reservoir. We shall consider both linear and radial flow configurations.

i. Linear flow

Assume that the porous medium is L feet long, W feet wide and h feet thick and is made up of n horizontal layers each with its own thickness, h_i , and permeability, k_i , as depicted in Fig. 6.13. All layers are exposed to the same inlet pressure, P_1 , and outlet pressure, P_2. To simplify the analysis, we shall assume steady-state flow of an incompressible fluid of viscosity μ for this case and all subsequent cases.

The flowrate through any layer, q_i , is computed by Equ. 6.13:

$$q_i = \frac{k_i A_i}{\mu} \frac{P_1 - P_2}{L}$$

The total flowrate through the medium is, then, simply the sum of all individual flowrates

$$q = \sum_{i=1}^{i=n} \frac{k_i A_i}{\mu} \frac{P_1 - P_2}{L}$$

Since $A_i = W\, h_i$, the sum reduces to:

$$q \quad = \quad \frac{P_1 - P_2}{\mu\, L}\, W \sum_{i=1}^{i=n} k_i\, h_i \tag{6.43}$$
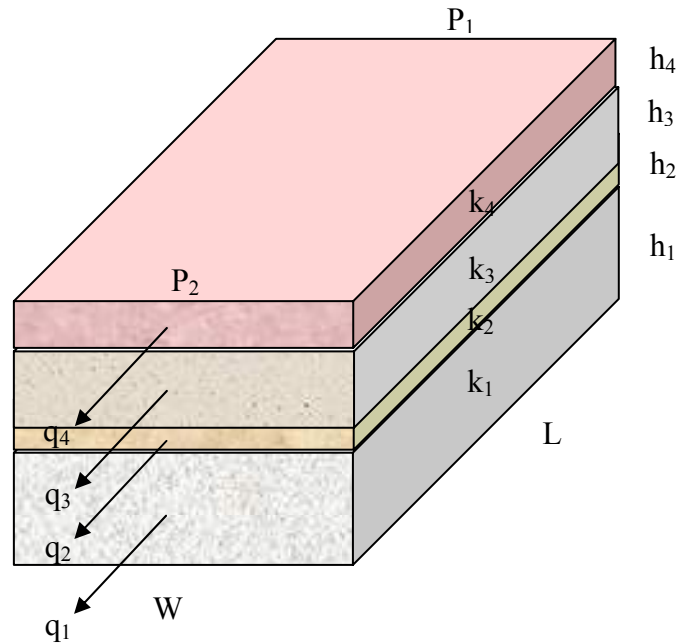
Fig. 6.13: Linear flow in parallel beds

If we are to consider the porous medium as one homogeneous unit with an average permeability, $\overline{k}$, Equ. 6.13 would be written for this medium as

$$q \quad = \quad \frac{\overline{k} A}{\mu} \frac{P_1 - P_2}{L}$$

$$\quad = \quad \frac{P_1 - P_2}{\mu\, L}\, \overline{k}\, W \sum_{i=1}^{i=n} h_i \tag{6.44}$$

Comparing Equ. 6.43 with Equ. 6.44, we can conclude that

$$\overline{k} \quad = \quad \frac{\displaystyle\sum_{i=1}^{i=n} k_i\, h_i}{\displaystyle\sum_{i=1}^{i=n} h_i} \quad = \quad \frac{\displaystyle\sum_{i=1}^{i=n} k_i\, h_i}{h} \tag{6.45}$$

ii. Radial flow

This case is similar to case (i) above except for the circular geometry of the porous medium. All layers have radius r_e and are penetrated by a well of radius r_w as depicted in Fig. 6.14.

The common inlet and outlet pressures are P_e and P_w, respectively. For each layer, Equ. 6.32 is written as:
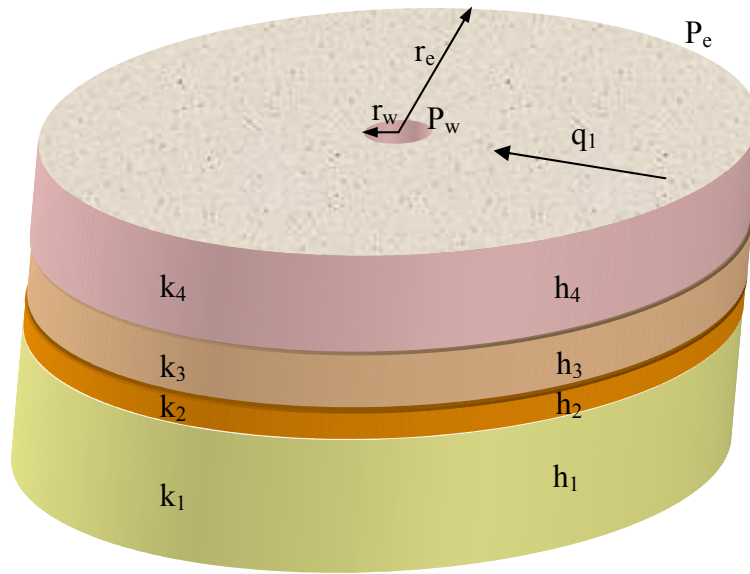
Fig. 6.14: Radial flow in parallel beds

$$q_i = \frac{2\pi k_i h_i}{\mu} \frac{P_e - P_w}{\ln \dfrac{r_e}{r_w}}$$

and the total flowrate is

$$q = \frac{2\pi}{\mu} \frac{P_e - P_w}{\ln \dfrac{r_e}{r_w}} \sum_{i=1}^{i=n} k_i h_i \tag{6.46}$$

Employing an average permeability, $\overline{k}$, Equ. 6.32 for the whole medium will be

$$q = \frac{2\pi \overline{k} h}{\mu} \frac{P_e - P_w}{\ln \dfrac{r_e}{r_w}}$$

$$= \frac{2\pi}{\mu} \frac{P_e - P_w}{\ln \dfrac{r_e}{r_w}} \overline{k} \sum_{i=1}^{i=n} h_i \tag{6.47}$$

Comparing Equ. 6.46 with Equ. 6.47 yields

$$\overline{k} = \frac{\displaystyle\sum_{i=1}^{i=n} k_i h_i}{\displaystyle\sum_{i=1}^{i=n} h_i} = \frac{\displaystyle\sum_{i=1}^{i=n} k_i h_i}{h} \tag{6.48}$$

6.6.2: Beds in series

Occasionally, heterogeneity in a petroleum reservoir is in the form of changing permeability along the path of flow, which allows representation of the reservoir as several sections in series. Such heterogeneity could be the result of natural causes as explained earlier, or it could be artificially introduced into the reservoir, primarily, in the vicinity of wellbores. A typical example of the latter case is damage to reservoir permeability caused by mud invasion during drilling operations. Clay and other foreign particles are carried into the rock by the drilling mud and get lodged between the grains causing severe pore-throat restriction. Well stimulation techniques, e.g., acidizing and fracturing, cause the opposite effect of improving reservoir permeability. We shall again consider both linear and radial flow configurations.

i. Linear flow

Assume that the porous medium is L feet long, W feet wide and h feet thick and is made up of n serial sections each with its own permeability, k_i, and length, L_i, as depicted in Fig. 6.15. The medium is exposed to inlet pressure P_1 and outlet pressure P_2.
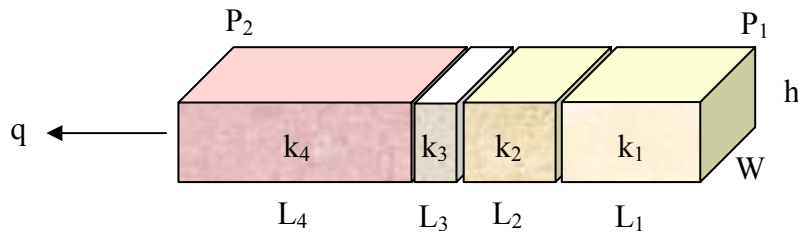
Fig. 6.15: Linear flow in serial beds

Steady-state conditions dictate no accumulation of mass within the system, which means that the flowrate is the same throughout the medium. We can, therefore, write Equ. 6.13 for each section (i) separately but in terms of its own inlet pressure, $P_{1,i}$, and outlet pressure, $P_{2,i}$.

$$q = \frac{k_i A}{\mu} \frac{P_{1,i} - P_{2,i}}{L_i} \qquad (6.49)$$

Rearranging Equ. 6.49 yields

$$P_{1,i} - P_{2,i} = \frac{q\mu}{A} \frac{L_i}{k_i} \qquad (6.50)$$

Remember that we can write n equations, all in the form of Equ. 6.50, for the n sections of the medium. Conditions of hydraulic continuity dictate that the outlet pressure of a given section (i) is equal to the inlet pressure of the adjacent section (i+1) downstream. That is

$$P_{2,i} = P_{1,i+1} \qquad (6.51)$$

Summing up all n equations and applying the condition of Equ. 6.51 yields

$$P_{1,1} - P_{2,n} = \frac{q\mu}{A} \sum_{i=1}^{i=n} \frac{L_i}{k_i} \qquad (6.52)$$

Note that $P_{1,1} = P_1$ and $P_{2,n} = P_2$. The general flow equation for the medium in terms of its average permeability is

$$P_1 - P_2 = \frac{q\mu}{A} \frac{L}{\bar{k}} \qquad (6.53)$$

Comparing Equ. 6.52 with Equ. 6.53 yields

$$\bar{k} = \frac{L}{\sum_{i=1}^{i=n} \frac{L_i}{k_i}} \qquad (6.54)$$

ii. Radial flow

In this case, the circular medium has radius r_e, is penetrated by a well of radius r_w, and is exposed to inlet and outlet pressures P_e and P_w, respectively, as depicted in Fig. 6.16.
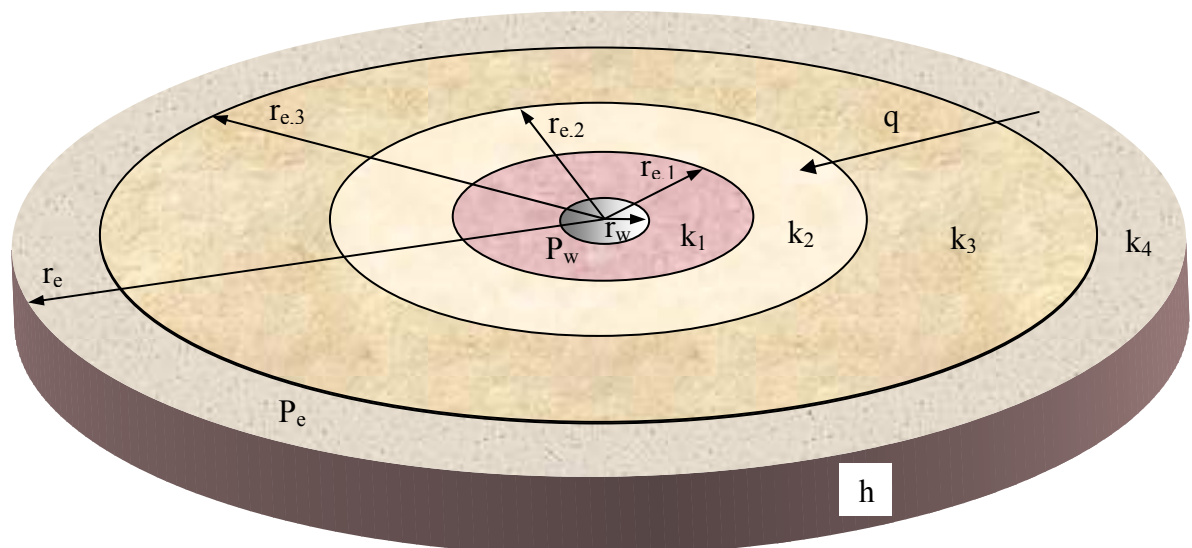
Fig. 6.16: Radial flow in serial beds

The medium is made up of n concentric sections each with its own permeability, k_i, inner radius, $r_{w,i}$, and outer radius, $r_{e,i}$. For each section, Equ. 6.32 is written, separately, in terms of its own inlet pressure, $P_{e,i}$, and outlet pressure, $P_{w,i}$.

$$q = \frac{2\pi k_i h}{\mu} \frac{P_{e,i} - P_{w,i}}{\ln\dfrac{r_{e,i}}{r_{w,i}}}$$

The general flow equation for the medium in terms of its average permeability is

$$q = \frac{2\pi \bar{k} h}{\mu} \frac{P_e - P_w}{\ln\dfrac{r_e}{r_w}}$$

Following the same procedure for the linear flow case yields the formula for the average permeability

$$\bar{k} = \frac{\ln\dfrac{r_e}{r_w}}{\displaystyle\sum_{i=1}^{i=n} \frac{\ln\dfrac{r_{e,i}}{r_{w,i}}}{k_i}} \tag{6.55}$$

Example 6.8

A 3000-ft diameter unit in a reservoir has a permeability of 320 md, and is produced by a 9" well. While drilling the well, the reservoir permeability is damaged down to 130 md in a zone 5 feet in diameter around the well. Acid stimulation of the well elevated the damage zone permeability up to 560 md. Compute the unit's average permeability before and after stimulation.

This is a case of radial flow in series. The effected zone has 4.5" (0.375 feet) inner radius and 2.5 feet outer radius, while the rest of the reservoir unit has 2.5 feet inner radius and 1500 feet outer radius. Equation 6.55 yields the following unit average permeabilities:

a. Before stimulation

$$\bar{k} = \frac{\ln\dfrac{1500}{0.375}}{\dfrac{\ln\dfrac{2.5}{0.375}}{130} + \dfrac{\ln\dfrac{1500}{2.5}}{320}}$$

$$= 239.8 \text{ md}$$

b. After stimulation

$$\bar{k} = \frac{\ln\dfrac{1500}{0.375}}{\dfrac{\ln\dfrac{2.5}{0.375}}{560} + \dfrac{\ln\dfrac{1500}{2.5}}{320}}$$

$$= \quad 354.8 \text{ md}$$

_____

Example 6.8 demonstrates the considerable loss of productivity caused by such a small damage zone, and the significant improvement gained by stimulation. Such a phenomenon is a direct consequence of the fact, presented in section 6.4.2-i, that most of the pressure drop in radial flow occurs near the wellbore.

6.7: Multi-fluid saturations

An implicit assumption in all flow equations derived in this chapter is that the porous medium is fully saturated with the fluid in question, which permitted use of the permeability as it is. But as indicated in chapter 4, the pore space of a petroleum reservoir is never fully saturated with one fluid. This raises the question of how to estimate the flowrate of a fluid in a reservoir where other fluids, either flowing or static, are present. One intuitive answer would be to divide the permeability among the fluids according to their saturations. Unfortunately, the problem is not that simple. Many forces come into play when two fluids come in contact with each other in the presence of a solid surface. It is true that such forces are very weak; however, within their microscopic domain they exert considerable influence on the fluids, which causes their flow behavior to change dramatically. A detailed look at fluid-rock interaction will be presented in the next chapter first before the permeability question is addressed in the final chapter.

Exercises
1. If 10^{-6} m is called a micrometer (μm) and 10^{-12} m^2 is called a micrometer squared (μm^2), convert 230 md to μm^2.

2. Water (μ = 1 cP) is flowing through a core sample (L = 10 cm, D = 2.5 cm) of 170 md permeability. Compute the flowrate if inlet and outlet pressures are 5 and 2 atm, respectively. Give your answer in cm^3/s and bbl/d.

3. Repeat Exercise 2 by converting all data to field units and applying Equ. 6.3.

4. Compute the absolute pressure at the bottom of the Arabian Gulf (depth = 820 ft) if sea water has an average density of 64 lb/ft^3 and atmospheric pressure is 14.7 psia.

5. Prove that the flow potential of water at sea level is the same as at the bottom of the sea.

6. The following core data were obtained from a sandstone reservoir.

Porosity	Permeability (md)
0.03	5
0.18	160
0.13	90
0.22	96
0.15	104
0.24	301
0.27	310
0.25	121
0.08	35
0.11	86
0.20	175
0.28	370

   a. Fit the data with an equation similar to Equ. 6.8.

   b. Explain why some points lie outside the general trend.

   c. Predict the permeability of a core sample from the reservoir if its porosity is 0.17.

7. Derive an equation for the linear, steady-state flowrate of an incompressible fluid **_upwards_** through a porous bed that is inclined with the horizontal at an angle θ.

8. A linear reservoir is 7 km long, 2 km wide and 20 m thick. It has a porosity of 22%, permeability of 350 md and it is inclined at 4° with the horizontal plain. If water (ρ = 1 g/cm^3, μ = 1 cP) enters the reservoir at a pressure of 150 atm, flows **_downwards_** through it, and exits the reservoir at 75 atm pressure. Compute the steady-state flowrate of water in m^3/d and in bbl/d.

9. Derive an equation for the linear, steady-state flow rate of an ideal gas **_downwards_** through a porous bed that is inclined with the horizontal at an angle θ.

10. A well with a diameter of $9\frac{3}{8}$ inches is drilled through an 80-ft thick reservoir with k = 220 md. If the bottom-hole pressure of the well is 2400 psig, and if the pressure 3000 feet away from the well (in all directions) is 5000 psig, what will the oil production rate be? Assume μ_o = 2.5 cP.

11. For Exercise 10, compute the pressure gradient (psi/ft) at 10, 1000 and 10,000 feet away from the well.

12. A well 4" in diameter penetrates a tight gas reservoir (h = 76 ft, k = 20 md). A recent test indicated that the reservoir pressure 2000 feet away from the well is 2750 psig. If the well pressure is maintained at 1450 psig, estimate the well production rate in standard

cubic feet per day (SCFD). The gas viscosity at the reservoir temperature of 180 °F and various pressures is given below.

Pressure (psia)	1450	2100	2750
Viscosity (cP)	0.016	0.019	0.021

13. A linear reservoir (k= 350 md, ϕ = 22%) is 23000 ft long, 3200 ft wide, 65 ft thick and is perfectly horizontal. Oil (ρ = 55 lb/ft^3, μ = 2.1 cP) enters the reservoir from one end at a pressure of 2940 psi, and it is produced from a well on the other end (see sketch below) at 880 psi pressure. If the well is 12 inches in diameter, compute the steady-state production rate of oil in bbl/d.
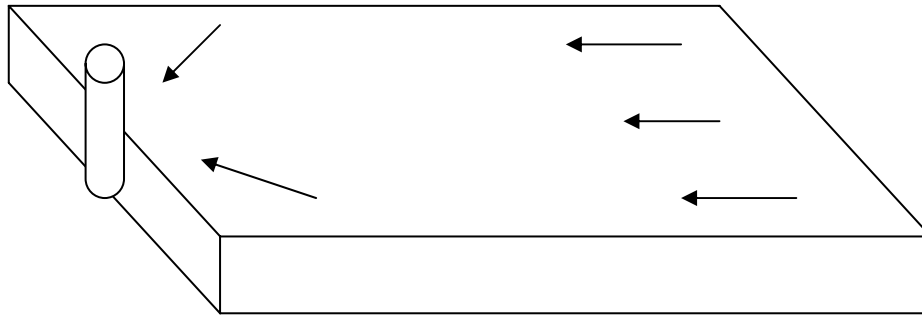
Hints:
a. *The flow is linear in the first 21400 ft then becomes radial in the last 1600 ft.*
b. *Only the right-hand **half** of the well is draining (producing) oil.*

14. A horizontal layer of rock has the shape and dimensions shown below.
    a. Derive an equation for the steady-state flow of an incompressible fluid through this layer if pressure P_1 is larger than pressure P_2 .
    b. For the data given below, compute the flowrate in barrels/day.

h = 30 ft	L_1 = 3 miles	L_2 = 1.2 miles	W = 0.8 miles
k = 150 md	μ = 2 cP	P_1 = 3400 psia	P_2 = 1200 psia
θ = 30°	r_w = 0.5 ft		
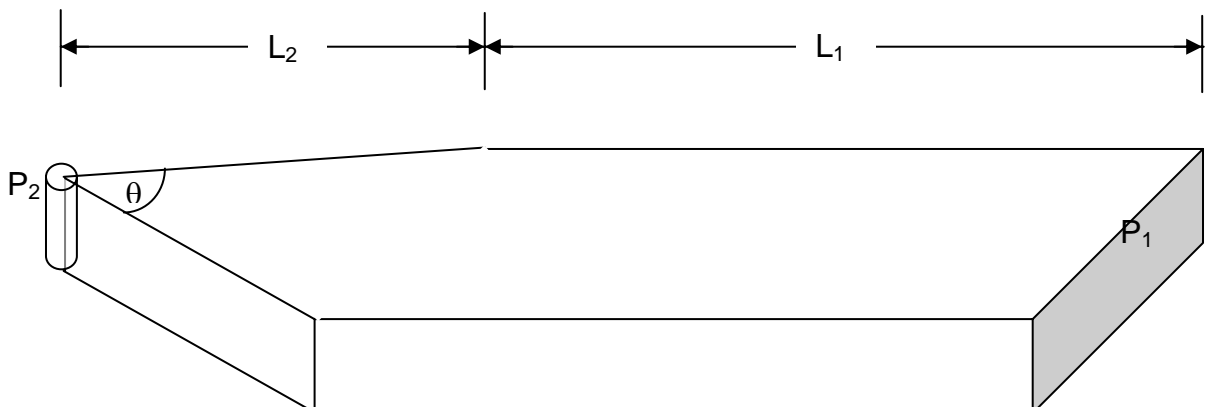
15. Derive an equation for the steady-state flowrate of an incompressible fluid in a spherical system. In such system, the flow converges from all directions on a hole of radius r_w.

16. A reservoir is 142 feet thick and consists of 7 horizontal zones with different permeabilities as listed below. Compute the average permeability of this reservoir.

Zone	Thickness (ft)	Permeability (md)
1	10	42
2	25	280
3	5	10
4	17	215
5	28	87
6	43	300
7	14	110

17. Because of low permeability, the well of Exercise 12 was acidized. This stimulation process increased the rock permeability to 95 md in a zone only 5 feet in diameter around the well.

   a. Estimate the reservoir's average permeability after acidizing.

   b. Estimate the well production rate after acidizing

   c. How much increase (or decrease) in the well's production do we gain with acidizing?

18. A 2-mile wide reservoir consists of several layers as shown below. An incompressible liquid with 1.5 cp viscosity flows through the reservoir at steady-state. Compute the flowrate (bbl/day) of the liquid through the layer with k = 200 md.

P = 750 psia	k = 140 md	k = 250 md h = 50 ft	P = 2300 psia
		k = 120 md h = 30 ft	
		k = 200 md h = 60 ft	
		k = 70 md h = 10 ft	
	L = 2.4 miles	L = 3.6 miles	
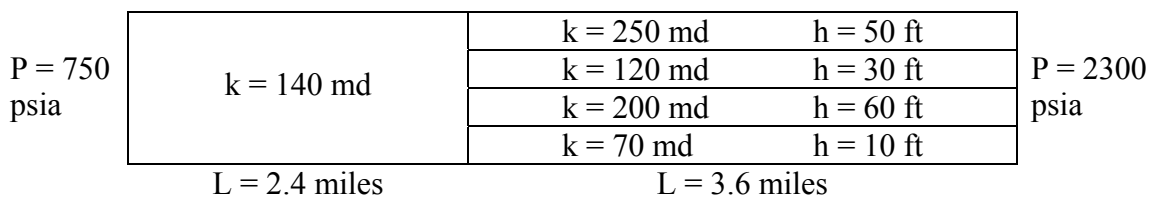
7. FLUID-ROCK INTERACTION

The study of fluid-rock interaction is of fundamental importance to reservoir engineering. Not only does such interaction influence fluid flow through the reservoir, it also plays a dominant role in the distribution of fluids within the reservoir's pore space and, more importantly, it dictates the maximum amount of a fluid that can be withdrawn from the reservoir. We shall start with the simplest form of such interaction and then move up to more complex ones.

7.1: Surface tension

The molecules of any substance are held together by inter-molecular forces whose magnitude depends on the molecular composition and structure of the substance. Different substances may display different levels of forces, and one way of illustrating such difference is to bring samples of two substances into contact. Since fluids are more noticeable in their interaction than rigid solids, we will conduct a simple experiment with water and air.

Fill a slim and clean glass cylinder with water, and observe the shape of the water surface. You will notice that it is concave as depicted in Fig. 7.1. The cause of surface concavity is that water molecules at the surface are pulled downward by other water molecules beneath them, while from above, they are pulled by air molecules with their much weaker inter-molecular forces. Since this force imbalance is equal everywhere on the surface, its effect cannot be readily detected. On the other hand, at the edge of the surface where water meets the wall of the cylinder, the opposite effect takes place. There, water molecules are attracted by glass molecules stronger than by air molecules. The result is that water creeps up the inner wall of the cylinder causing the surface to deform. This phenomenon is well known in surface science and is called *surface tension*.
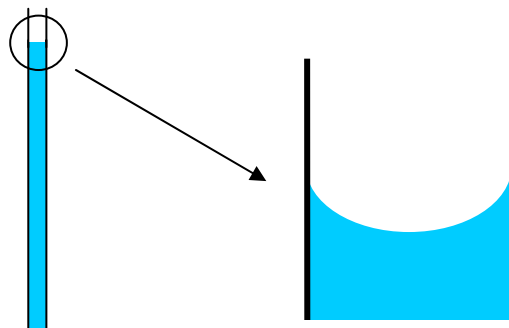
Fig. 7.1: Curvature of water meniscus

To quantify surface tension, we need to imagine another experiment. Suppose we have a container one side of which can be moved freely as shown in Fig. 7.2. Let us fill the container with a liquid, say water, and leave the container to stand in equilibrium. If we want
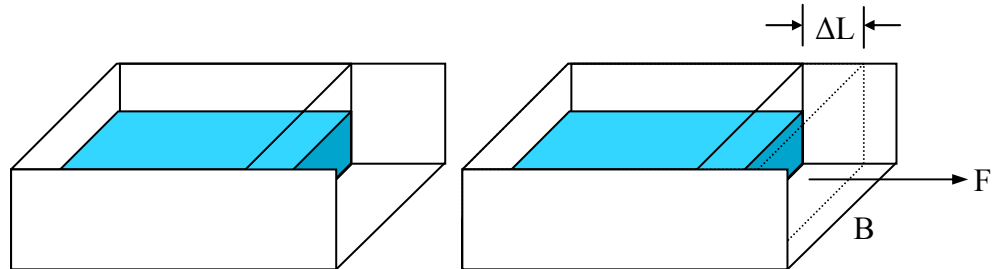
Fig. 7.2: Hypothetical measurement of surface tension

to enlarge the surface area of the water, we need to pull the movable side outwards. In doing so, we will find that a certain force, F, is required to overcome the resistance by the water, which doesnot want to expose more of its surface to air. To create new surface, water molecules have to be brought from within the body of the water, where they experience a zero net attraction force, to the surface where they are pulled by a net force downward. By creating a new surface, the whole body of water is raised to a higher level of internal energy, and work must be expended to supply the extra energy. This work is provided by the force F. Therefore, if the side is moved for a distance Δl, the work done is equal to

$$W = F \Delta l$$

Therefore, surface tension, σ, is defined as the amount of energy, E_s, needed to create a unit area of new surface. This energy is equal to

$$E_s = \frac{W}{\Delta A} = \frac{F \Delta l}{B \Delta l}$$

And,

$$\sigma = \frac{F}{B}$$

where B is the container width. The units of surface tension are thus Joules/cm^2; but since a Joule is equivalent to one dyne-cm, surface tension is commonly expressed in dyne/cm. Note that surface tension is a vector whose direction is parallel to the surface of the substance and opposite to the direction of area increase, i.e., opposite to F.

There are more accurate techniques to measure surface tension of a substance, and they all require, by definition, that the gas phase surrounding the substance be either air or the substance's own vapor. Surface tension decreases with temperature; for liquids it reaches zero at the boiling point. For pure distilled water, σ is 72 dyne/cm at 20 ºC while a typical value for a crude oil is 40 dyne/cm at room temperature.

7.2: Interfacial tension

Suppose the experiment of the glass cylinder is repeated with water covered by crude oil. Tension would still exist at the oil-water interface, which would still be concave but to a lesser degree as oil-water attractive force is stronger than air-water. Such tension is called *interfacial tension*; its units and direction are the same as surface tension and a useful formula to compute it is:

$$\sigma_{12} = \sigma_1 - \sigma_2$$

where

σ_{12} :   interfacial tension between substances 1 and 2, dyne/cm

σ_1 :   surface tension of substance 1, dyne/cm

σ_2 :   surface tension of substance 2, dyne/cm

A typical value of water-oil interfacial tension, σ_{wo}, at room temperature is 32 dyne/cm.

7.3: Wettability

All of us have observed how mercury drops tend to retain their spherical shape when they are placed over a glass surface while water drops tend to spread. We would normally say that water *wets* the glass, but mercury doesn't. In reservoir engineering terminology, we characterize water as a wetting phase to glass and mercury as a non-wetting phase. To understand the mechanics of wettability of a phase in relation to a particular solid, let us inspect closely a drop of water placed over a clean sheet of glass (Fig. 7.3-a). At point *a*, three
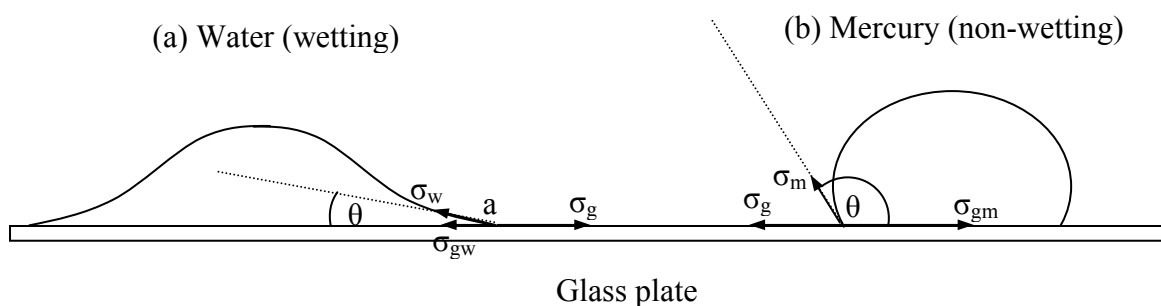
Fig. 7.3: Wettability and contact angle

forces are acting on the water surface: σ_{gw} (between glass and water), σ_g (between glass and air), and σ_w (between water and air); and each force is acting to decrease the area of interface

between the two substances concerned. Since the drop is at static equilibrium, the resultant force acting on the edge of the drop must be zero. Take one centimeter length of drop circumference and apply a force balance in the horizontal plane:

$$\sigma_g = \sigma_{gw} + \sigma_w \cos \theta_w \tag{7.1}$$

where θ_w is called the *contact angle* in water-air-glass system. Define the adhesion tension as:

$$A_t = \sigma_g - \sigma_{gw}$$

Thus,

$$A_t = \sigma_w \cos \theta_w \tag{7.2}$$

If the contact angle is less than 90, as in the case of θ_w, A_t will be positive, which makes glass pull the water drop to spread over. In other words, the glass prefers to be in contact with water rather than with air, which makes water the wetting phase to glass in the presence of air. If the contact angle is greater than 90, as in the case of mercury (Fig. 7.3-b), A_t will be negative, causing the glass to repel the mercury drop forcing it to contract. This makes air the wetting phase to glass in the presence of mercury. If the contact angle is close to 90, neither fluid will be the wetting phase and both will have neutral wettability. Note that the contact angle is always measured within the denser fluid.

Wettability in an oil reservoir can be determined by a similar experiment with reservoir water, crude oil and a crystal of the predominant mineral in the reservoir rock. In general, water is the wetting phase to quartz in the presence of oil, while oil is the wetting phase to carbonate minerals in the presence of water. Natural gas is always the non-wetting phase in the presence of other liquids except mercury.

Classification of wettability based on contact angle alone is not always correct. Other criteria have been proposed based on other manifestations of fluid-rock interaction. These will be presented in due course. For the time being, we shall look at the contact angle as a simple rule-of-thumb to characterize wettability.

7.4: Capillary pressure

Capillary pressure is another manifestation of fluid-solid interaction. To explain this phenomenon, we have to recall a familiar experiment in which one end of a glass capillary tube is immersed in a beaker full of water, which causes water to rise in the tube up to a particular height. The force that pulls water into the tube against gravity has to do with the adhesion tension. To investigate this force, let us look closely at the water meniscus illustrated in Fig. 7.4-a. At the periphery of the meniscus, the adhesion tension is given by Equ. 7.2 and it acts vertically upwards along the inner wall of the tube. Since this tension is a force per unit length of periphery, the adhesion force, F_t, is then computed by:

(a) Water   (b) Mercury
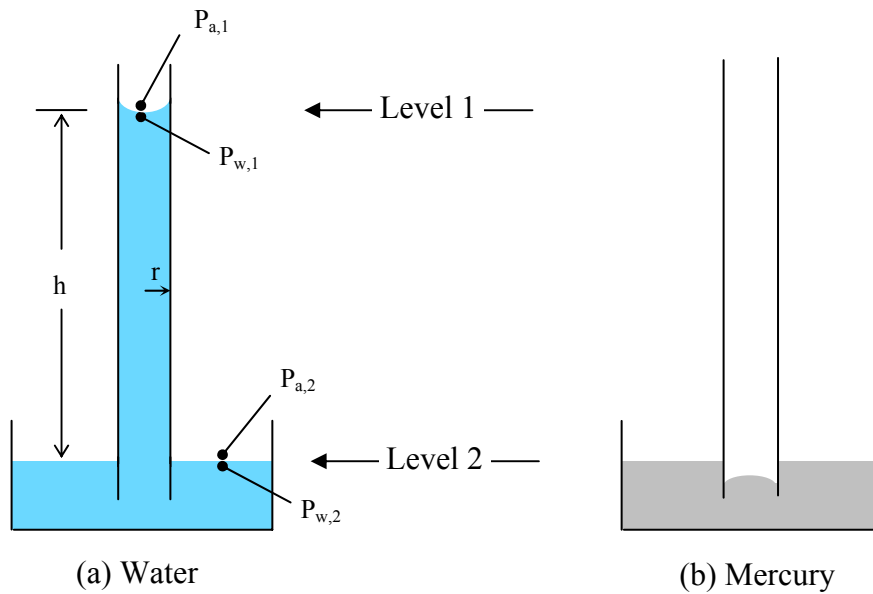
Fig. 7.4: Liquid rise in a capillary tube

$$F_t = A_t (2\pi r) = 2\pi r \, \sigma_w \cos \theta_w \tag{7.3}$$

where r is the radius of the capillary tube. At equilibrium, the adhesion force must be equal to the weight of the water column in the tube, F_g, given by:

$$F_g = \pi r^2 h \, \rho_w \, g \tag{7.4}$$

where h is the height, in cm, of the water column above the free water surface.

Equating the two forces yields:

$$h = \frac{2\sigma_w \cos \theta_w}{\rho_w g r} \tag{7.5}$$

It is informative to consider the effect of modifying some the experimental parameters. Using a larger tube would result in a shorter water column; so would replacing water with oil. However, using mercury would cause a depression in the mercury level (Fig. 7.4-b) because $\cos \theta_m$ is negative.

Example 7.1

One end of a glass tube, 1 mm in diameter, is dipped in a beaker full of distilled water at 20 ºC. Compute the rise of water in the tube if water-air-glass contact angle is 30º and water density is 1 g/cm³.

Applying Equ. 7.5

$$h = \frac{2 \times 72 \cos 30}{1 \times 980 \times 0.05}$$

$$= \quad 2.55 \text{ cm}$$

To understand the concept of capillary pressure, let us examine Fig. 7.4-a from the prospective of pressure. The pressure at the free water surface (level 2) outside the tube is atmospheric in both the air and water phases:

$$P_{w,2} = \quad P_{a,2} = P_{atm}$$

Because of hydrostatic equilibrium, the water pressure inside the tube at level 2 should be atmospheric too. Due to the negligible density of air, the pressure in the air phase just above the water meniscus (level 1), $P_{a,1}$, is also atmospheric. We are ready now to calculate the pressure in the water phase just below the meniscus, $P_{w,1}$. Due to the weight of the water column, this pressure is:

$$P_{w,1} = \quad P_{w,2} - \rho_w g h \quad = \quad P_{atm} - \rho_w g h \qquad (7.6)$$

which is less than atmospheric. In other words, there is a drop in pressure as we move across the meniscus from the air phase into the water phase. Such a drop in pressure is termed the *capillary pressure*, P_c, and it arises as a result of the preferential wettability of a solid (glass) towards one phase (water) over another phase (air) when both phases are in contact with the same solid. We can look at it as a difference in pressure which is created between the non-wetting and wetting phases as soon as these two phases come in contact with the solid. In terms of interfacial parameters, the capillary pressure in our example can be computed by combining Equs. 7.5 and 7.6 as

$$P_c \quad = \quad P_{a,1} - P_{w,1}$$

$$= \quad \frac{2\sigma_w \cos\theta_w}{r} \qquad (7.7)$$

It should be emphasized that, due to surface phenomena, the pressure in the wetting phase is always smaller than the pressure in the non-wetting phase by the magnitude of the capillary pressure.

Suppose we repeat the capillary tube experiment but with oil overlaying the water as shown in Fig. 7.5. Following the same analysis above we conclude that:

$$P_{w,2} = \quad P_{o,2}$$

and

$$P_{w,1} = \quad P_{w,2} - \rho_w g h$$

However, the hydrostatic pressure drop in the oil phase cannot be ignored in this case because oil density, ρ_o, is appreciable, and $P_{o,1}$ is computed to be:

$$P_{o,1} = P_{o,2} - \rho_o \, g \, h$$
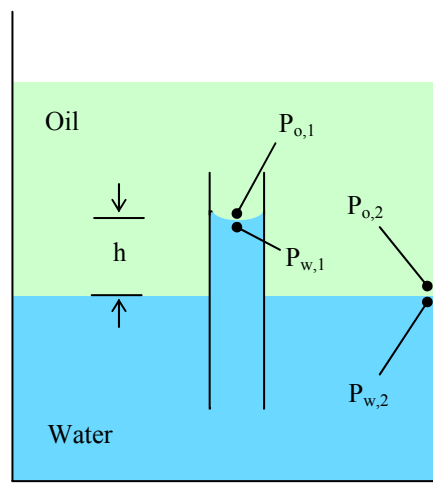
Fig. 7.5: Liquid rise in oil-water system

The capillary pressure would then be given by:

$$P_c = P_{o,1} - P_{w,1}$$
$$= (\rho_w - \rho_o) \, g \, h \tag{7.8}$$

Performing a force balance as previously, the adhesion force is given by:

$$F_t = A_t \, (2\pi r) = 2\pi r \, \sigma_{wo} \cos \theta_{wo} \tag{7.9}$$

where σ_{wo} is the water-oil interfacial tension and θ_{wo} is the water-oil contact angle. When computing the weight of the water column, the effect of buoyancy has to be included this time. The buoyancy force, F_b, acting on the water column is equal to the weight of displaced oil, which is:

$$F_b = \pi \, r^2 h \, \rho_o \, g$$

Therefore, the net weight of the water column is:

$$F_g = \pi \, r^2 h \, g \, (\rho_w - \rho_o) \tag{7.10}$$

Equating Equs. 7.9 and 7.10 yields:

$$h = \frac{2\sigma_{wo} \cos \theta_{wo}}{(\rho_w - \rho_o) g \, r} \tag{7.11}$$

By substituting Equ. 7.11 into Equ. 7.8, the capillary pressure can also be expressed by:

$$P_c = \frac{2\sigma_{wo} \cos \theta_{wo}}{r} \tag{7.12}$$

Example 7.2

Rework Example 7.1 but with oil (0.85 g/cm^3 density and 42 dyne/cm surface tension) overlaying water, and water-oil-glass contact angle is 50º. Also compute the capillary pressure in the tube.

Applying Equ. 7.11:

$$h = \frac{2 \, x \, (72-42) \cos 50}{(1-0.85)980 \, x \, 0.05}$$

$$= 5.25 \text{ cm}$$

The capillary pressure is computed by Equ. 7.12

$$P_c = \frac{2 \, x \, (72-42) \cos 50}{0.05}$$

$$= 771 \text{ dyne/cm}^2$$

$$= 0.011 \text{ psi}$$

7.5: Capillary pressure in porous rock

The pore space within reservoir rock is comprised of a large number of pores of different sizes and shapes, which are interconnected into a complex network of channels and pathways. A pore may be accessible through one or several entrances, or may be completely isolated. Due to the nature of inter-granular pore space, pore entrances – or throats – are usually smaller in diameter than the pore itself. This fact plays a crucial role in the distribution of fluids within the pore space as will be illustrated shortly.

When two or more fluids share the pore space of a rock, the wetting fluid will readily coat the walls of the pores whenever possible, and a capillary pressure will exist at the interface between the wetting fluid and the non-wetting fluid(s). The magnitude of the capillary pressure will vary from pore to pore according to pore geometry. To illustrate this phenomenon, we shall follow the developments of a simple experiment. Assume that a sandstone core sample is fully saturated with water, the wetting phase, and is loaded in the setup shown in Fig. 7.6. Oil, the non-wetting phase, can be injected at one end and water can be produced from the other.

A magnified picture of the core's inlet, Fig. 7.7-a, shows water filling all the pores and oil is just coating the inlet face of the core. Since the system is at hydrostatic equilibrium, we expect that an infinitesimal increase in the oil pressure would cause the oil to enter the core displacing water inwards. However, this is not the case as every pore acts like a minute

capillary tube that develops capillary pressure at the two-phase interface. To start the displacement, we would have to increase the oil pressure until the pore(s) with the smallest P_c give way first, at which instant the oil-water pressure difference, ΔP, would be just above the required P_c. Intuitively, such pores would be the largest ones. This minimum P_c is called the *threshold pressure*, $P_{c,th}$, and is thus given by:

$$P_{c,th} = \frac{2\sigma_{wo}\cos\theta_{wo}}{r_{max}} \tag{7.13}$$
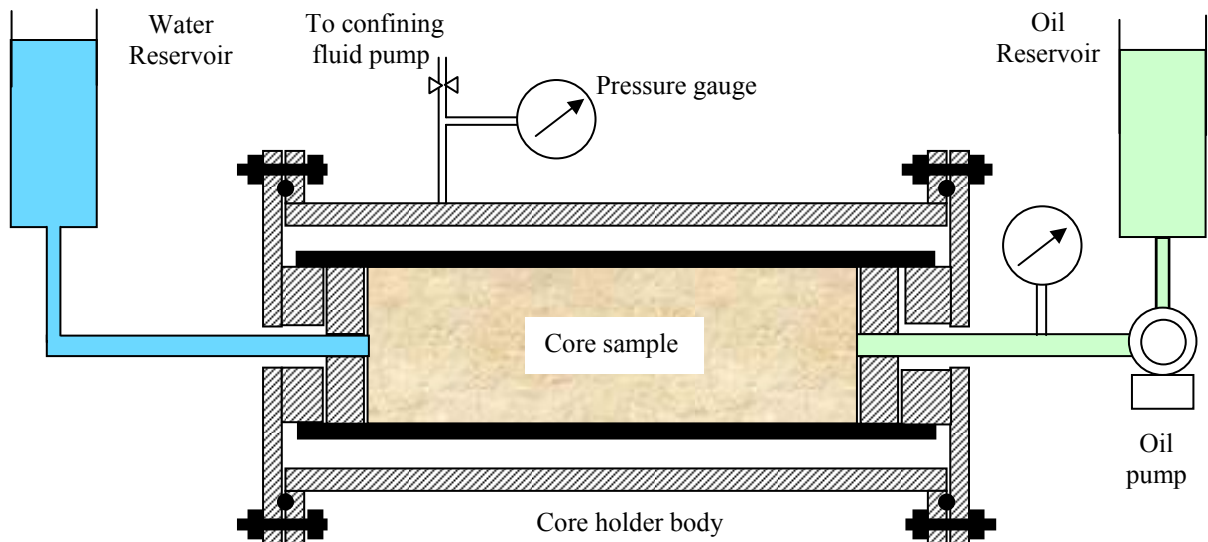
Fig. 7.6: Capillary displacement in a core sample

Once oil enters the core through the largest pores, it will continue displacing water until it reaches a pore whose diameter requires a larger ΔP to push through (Fig. 7.7-b). At this stage, raising the oil pressure would carry water displacement forward in these pores as well as invading the next smaller pores at the inlet. Successive increases in oil pressure, hence, P_c, would cause more water to be displaced out of the core and reduce the water saturation progressively (Figs. 7.7-c and d). Therefore, a relationship between P_c and S_w can be deduced where a larger P_c leads to a smaller S_w. Such a relationship can actually be obtained by plotting the P_c versus S_w values computed from the experiment producing what is termed the capillary pressure curve for the water-oil-rock system.

(a) $P_c = 0$

(b) $P_c = P_{c,th}$

(c) $P_c > P_{c,th}$

(d) $P_c \gg P_{c,th}$

Fig. 7.7: Microscopic views of water displacement by oil (drainage)

A typical capillary pressure curve is shown in Fig. 7.8-a. One can readily identify the $P_{c,th}$, the minimum P_c value required to invade the rock, thus reducing S_w below 100%. One can also see how P_c increases steadily with decrease in S_w as smaller and smaller pores are invaded. A typical and interesting feature of the P_c curve is observed at the lower range of S_w where it seems that the curve approaches a certain saturation in an asymptotic mode. In other words, it appears that there exists a saturation value, which can never be achieved no matter how large a capillary pressure is exerted. Such a saturation is called the *irreducible water saturation*, S_{wi}, and it results from isolated droplets of water surrounded and trapped in some pores by oil (refer to Fig. 7.7).

The process described above in which the wetting phase is displaced out of a porous medium by a non-wetting phase is called a *drainage process*, and the P_c curve that results is called a drainage curve. A question may be raised as to what would happen if at the end of the

drainage process, water were reintroduced into the core sample. Such a process is called *imbibition*, and the resulting capillary pressure curve would look like curve 2 in Fig. 7.8-b.

(a) Drainage capillary pressure curve

(b) Effect of direction of displacement on capillary pressure
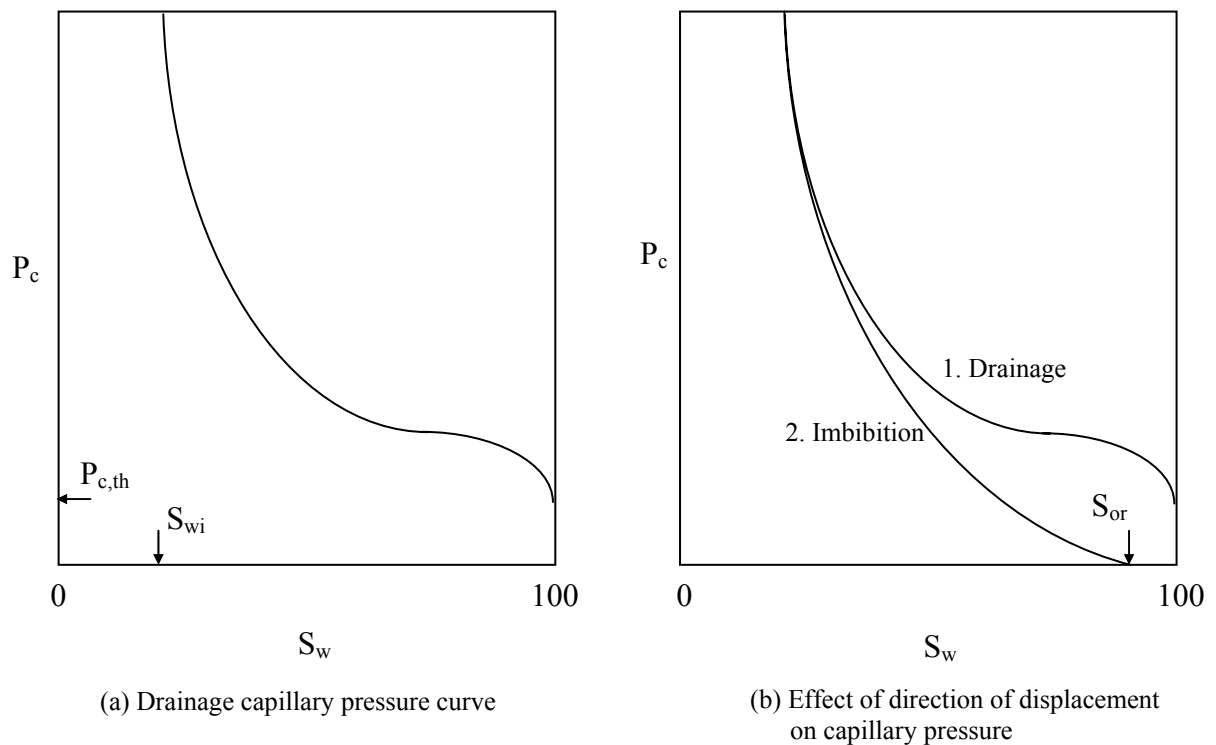
Fig. 7.8: Typical capillary pressure curves for water-wet rock

A striking feature of Fig. 7.8-b is the difference between the two curves. Specifically, the drainage P_c is greater than the imbibition P_c at every S_w. This phenomenon is attributed to three effects. First, it has been shown that the contact angle when the wetting phase is receding is smaller than when it is advancing, which reduces the P_c for any given S_w. Second, because of complex pore geometry, some pores may have two inlets with different diameters. It may well happen that one such pore could not be invaded by oil from one side during drainage because of its small pore throat (Fig. 7.9-a). The P_c at the prevailing S_w would be high. Yet, during imbibition, this same pore would be invaded by water through the other larger inlet, at a lower P_c, causing complete oil displacement and restoring S_w to its former value (Fig. 7.9-b). Therefore, for the same S_w, a smaller P_c is required during imbibition. The third effect has to do with *hysterisis*, which is, basically, a gradual shift in the wettability preference of a solid towards a fluid that it has been coated with for a prolonged time. Therefore, originally water-wet grains that were coated with oil during drainage become less water wet with time, causing them to display a somewhat larger contact angle.

(a) High capillary pressure   (b) Low capillary pressure

Fig. 7.9: Effect of displacement direction on capillary pressure

Another feature of the imbibition P_c curve is an apparent maximum S_w, or an apparent minimum S_o. This *residual oil saturation*, S_{or}, is caused by a similar entrapment process where oil globules become isolated within large pores. The negative P_c associated with S_{or} is a consequence of the definition of P_c. Remember that P_c is defined as the difference between non-wetting and wetting phase pressures regardless of which phase is being displaced.

A reservoir engineer should apply the capillary pressure curve that is appropriate to the process taking place in the reservoir. Usually, all reservoir rock becomes saturated with water during sedimentation or shortly thereafter. Migrating hydrocarbons that accumulate in the rock gradually displace water out of the pores in a drainage process. When the reservoir is discovered, capillary forces would have distributed water in such a way that S_w is close to S_{wi} within the oil column, then comes an interval over which S_w increases gradually from S_{wi} to 100%, and finally the water aquifer lies beneath. The depth interval over which S_w changes from S_{wi} to 100% changes is called the *transition zone*, and its characteristics must be analyzed according to the drainage P_c curve. Later in the life of the reservoir when water is injected to boost the pressure or displace the oil, the imbibition P_c curve must be applied.

7.6: Measurement of capillary pressure

Many methods, both direct and indirect, have been devised to measure the capillary pressure for rock samples. In this section, the centrifuge method, which is the most widely used direct technique, will be presented.

The centrifuge is a devise with a rotating shaft to which several core holders, usually eight, are held by radial arms. Figure 7.10 illustrates design of the core holder. One core

sample saturated with water or another wetting fluid is placed in each holder and the shaft is rotated at a constant speed for a sufficient time. The centrifugal force causes the pressure within the core sample to drop below atmospheric. Such pressure drop allows air to drive the water out of the core sample where it accumulates in a receiving tube at the end of the core holder. The difference between the atmospheric pressure of air and the new pressure of water, which can be computed by a simple formula, simulates a capillary pressure exerted on the water by air. Raising the rotation speed, which simulates a higher capillary pressure, drains more water from the core providing another reading.
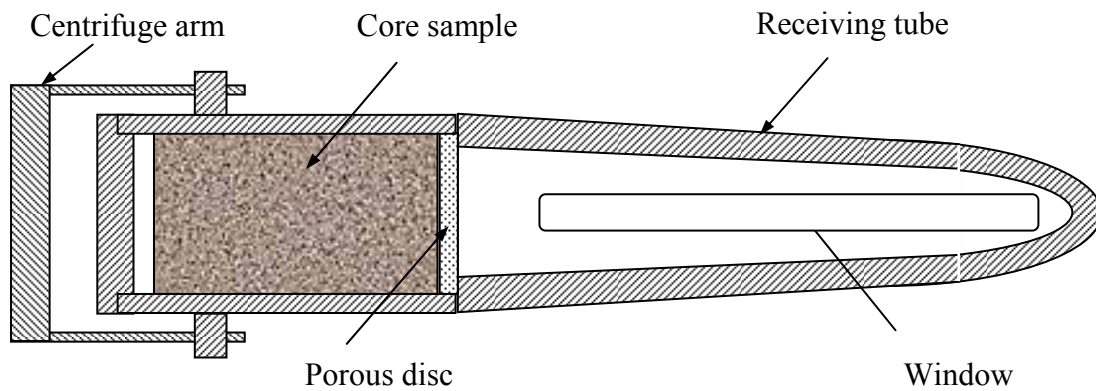

Fig. 7.10: Centrifuge core holder assembly

The air-water drainage capillary pressure curve is then graphed from the pressure drop values versus the water saturation remaining in the core sample at the end of each rotation step.

The reservoir P_c curve is generated from the laboratory data by a simple conversion technique employing Equ. 7.12. For any pore within the core sample,

$$P_{c,L} = \frac{2\sigma_w \cos\theta_w}{r}$$

and

$$P_{c,R} = \frac{2\sigma_{wo} \cos\theta_{wo}}{r}$$

where subscripts "L" and "R" refer to laboratory and reservoir conditions, respectively. Note that for the lab data, air-water contact angle is applied, while for the reservoir oil-water angle is applied. Combining the two equations above yields:

$$P_{c,R} = \frac{\sigma_{wo} \cos\theta_{wo}}{\sigma_w \cos\theta_w} P_{c,L} \tag{7.14}$$

Note that the pore radius has disappeared from Equ. 7.14, which means that this equation applies to any pore within the rock. Therefore, for any S_w compute $P_{c,R}$ from the corresponding value of $P_{c,L}$ using Equ. 7.14.

Example 7.3

The following capillary pressure data was generated in the lab using air and water. For each water saturation, compute the corresponding reservoir capillary pressure for the same rock but saturated with oil and water. $\sigma_w = 72$ dyne/cm, $\sigma_o = 32$ dyne/cm, $\theta_w = 20°$, $\theta_{wo} = 40°$.

S_w (%)	20	30	40	50	60	70	80
$P_{c,L}$ (psi)	4.91	4.52	4.26	4.11	4.04	3.95	3.77

$\sigma_{wo} = 72 - 32 = 40$ dyne/cm

From Equ. 7.14, the conversion factor is:

$$\frac{\sigma_{wo} \cos\theta_{wo}}{\sigma_w \cos\theta_w} = \frac{40 \times \cos 40}{72 \times \cos 20} = 0.46$$

The reservoir capillary pressure is then computed as below.

S_w (%)	20	30	40	50	60	70	80
$P_{c,R}$ (psi)	2.26	2.08	1.96	1.89	1.86	1.82	1.73

7.7: Applications of capillary pressure

The capillary pressure curve provides valuable insight into the fluid-rock system under study. Much information can be inferred from a simple inspection of the curve. This includes:

a. Largest pore diameter within the rock: The higher the threshold pressure, the smaller the largest pore is.

b. Pore-size distribution: The slope of the P_c curve follows the gradual change in pore-diameters. A steep curve indicates a wide distribution.

c. S_{wi} and S_{or} from the limits of the curve.

The threshold pressure can also indicate the wettability preference of the rock. A positive $P_{c,th}$ in an oil-displacing-water process indicates preferential wettability to water, and the relative magnitude of $P_{c,th}$ reflects the strength of such wettability. In fact, the concept of the contact angle as an indicator of wettability is refined by the incorporation of $P_{c,th}$ through the *wettability number*, N_{wet}, which is defined as:

$$N_{wet} = \frac{\sigma_o \cos\theta_{wo} \, P_{th,wo}}{\sigma_{wo} \cos\theta_{oa} \, P_{th,oa}} \qquad (7.15)$$

where subscripts "wo" and "oa" refer to water-oil and oil-air systems, respectively. A wettability number of one indicates complete wettability to oil, while a value larger than 1 indicates more wettability to water. Based on the definition of the wettability number, we can define an *apparent* contact angle, θ_{app}, as:

$$\cos\theta_{app} = \frac{\sigma_o \, P_{th,wo}}{\sigma_{wo} \, P_{th,oa}} \qquad (7.16)$$

If available, the apparent contact angle is a better indicator of wettability preference than the ordinary contact angle.

The most important application of capillary pressure data is, probably, the construction of the S_w profile within the transition zone. First, we have to define the *free water table*, which is the uppermost horizon (depth) within the reservoir where the capillary pressure is zero. The free water table is actually the upper limit of the water aquifer where S_w is naturally 100%. Above the free water table, p_c increases with height according to Equ. 7.8 rewritten as follows:

$$h = \frac{P_c}{(\rho_w - \rho_o)g}$$

and in field units:

$$h = \frac{144 \, P_c}{\rho_w - \rho_o} \qquad (7.17)$$

Equation 7.17, thus, provides the P_c profile within the transition zone. Recall that every P_c corresponds to a water saturation. Hence, Equ. 7.17 establishes the S_w profile in the transition zone too. An example profile is shown in Fig. 7.11. Note that this profile is generated in nature from top to bottom, not the other way around. This is because when oil migrates into the reservoir it is kept at the top portion by buoyancy forces, which causes water displacement downwards. In this drainage process, capillary forces, however, prevent complete displacement of water and some water is retained in the oil zone as irreducible water. Moreover, water is not drained out equally everywhere in the reservoir; there will be a gradual increase in water saturation as we move closer to the aquifer. With more accumulation of oil, the transition zone grows thicker as a result of continued shift in equilibrium between capillary and buoyancy forces.
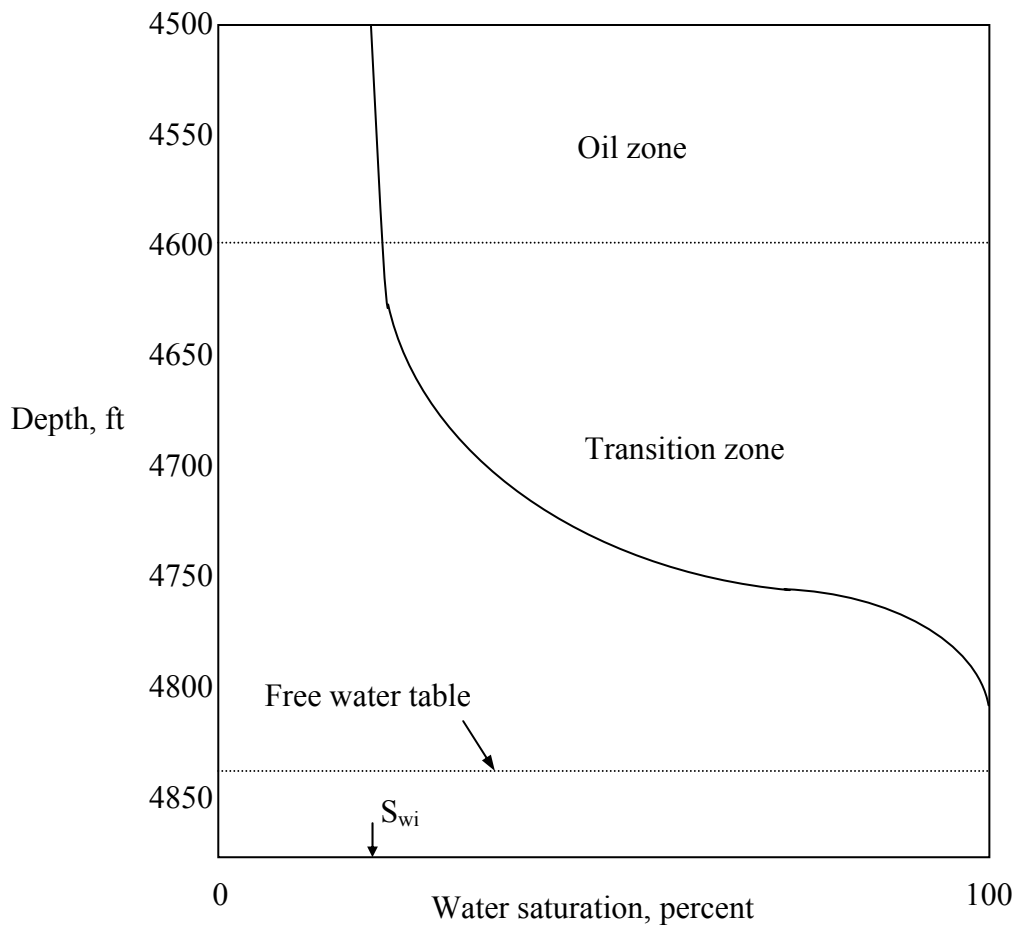
Fig. 7.11: Water saturation profile in the transition zone

It is interesting to note that 100% water saturation extends even above the free water table in Fig. 7.11. This, seemingly, contradictory situation is explained by the threshold pressure. Recall that at and below the free water table the capillary pressure is zero, and it starts increasing as we move into the transition zone. Since the smallest capillary pressure, $P_{c,th}$, corresponds to $S_w = 100$, this necessitates that this saturation should also exist in the transition zone up to a height dictated by the threshold pressure.

If a well penetrates the transition zone, well logs could provide the water saturation profile within this zone. Coupled with Equ. 7.17, this profile provides an indirect means of establishing the capillary pressure curve for the reservoir.

Example 7.4

The capillary pressure curves for a sandstone reservoir are shown in Fig. 7.12. Estimate the height, in feet above the free water table, where S_w drops below 100% and where it is equal to 45%. Oil and water densities are 55 and 64 lb/ft^3, respectively.

The drainage P_c curve is used. S_w drops below 100% when P_c exceeds $P_{c,th}$, which is 1.2 psi. From Equ. 7.17,

$$h_{(S_w=100)} = \frac{144 \times 1.2}{64-55}$$

$$= 9.2 \text{ ft}$$

For S_w of 45%, P_c is 3.0 psi. Therefore,

$$h_{(S_w=45)} = \frac{144 \times 3.0}{64-55}$$

$$= 48.0 \text{ ft}$$

Consulting saturation logs, the two heights can help estimate the depth of the free water table.
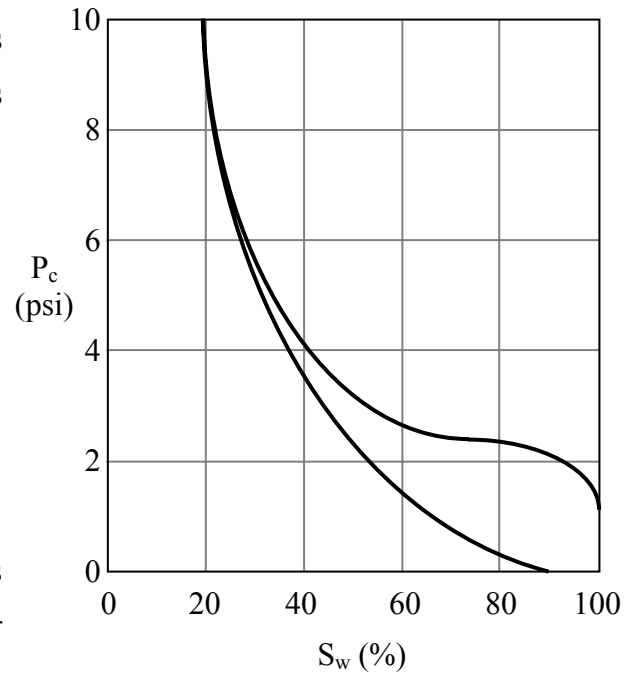

Fig. 7.12: Capillary pressure curves for Example 7.4

7.8: Correlating capillary pressure data

It is evident from discussions presented in the previous section that the pore-size distribution within the core sample under study greatly influences the magnitude of the sample's P_c curve. Since this distribution has a strong influence on the porosity and permeability of the sample, it is, therefore, expected that different core samples from the same reservoir would display different P_c curves. The range in Pc curves would become wider as the reservoir rock displays greater porosity and permeability variation. Having to deal with a multitude of capillary pressure data would render many reservoir calculations more cumbersome. If all such data were reduced to one "master" curve, in a fashion similar to a permeability-porosity transform, the capillary pressure curve for a given section of the reservoir would be derived from the master curve utilizing local properties only. Leverett[3] was able to derive the correlating function, called the Leverett J-function, which he defined as:

$$J = \frac{P_c}{\sigma_{wo} \cos\theta_{wo}} \sqrt{\frac{k}{\varphi}} \qquad (7.18)$$

For a given core sample, the J-function is dimensionless and varies with S_w only since all parameters in the right-hand side of Equ. 7.18 are independent of saturation except P_c.

Note that for Equ. 7.18 to be consistent, P_c must be in dynes/cm^2, k in cm^2, and φ in fractions. Figure 7.13 shows how capillary pressure data for six core samples from a dolomite reservoir collapsed into one narrow band once it was converted according to Equ. 7.18. An equation describing the smooth curve drawn through the data can be obtained by any curve-fitting technique. For any location within the reservoir, the capillary pressure at any S_w can now be approximated by reading the J-function value at that S_w and combining it with relevant core data in the form:

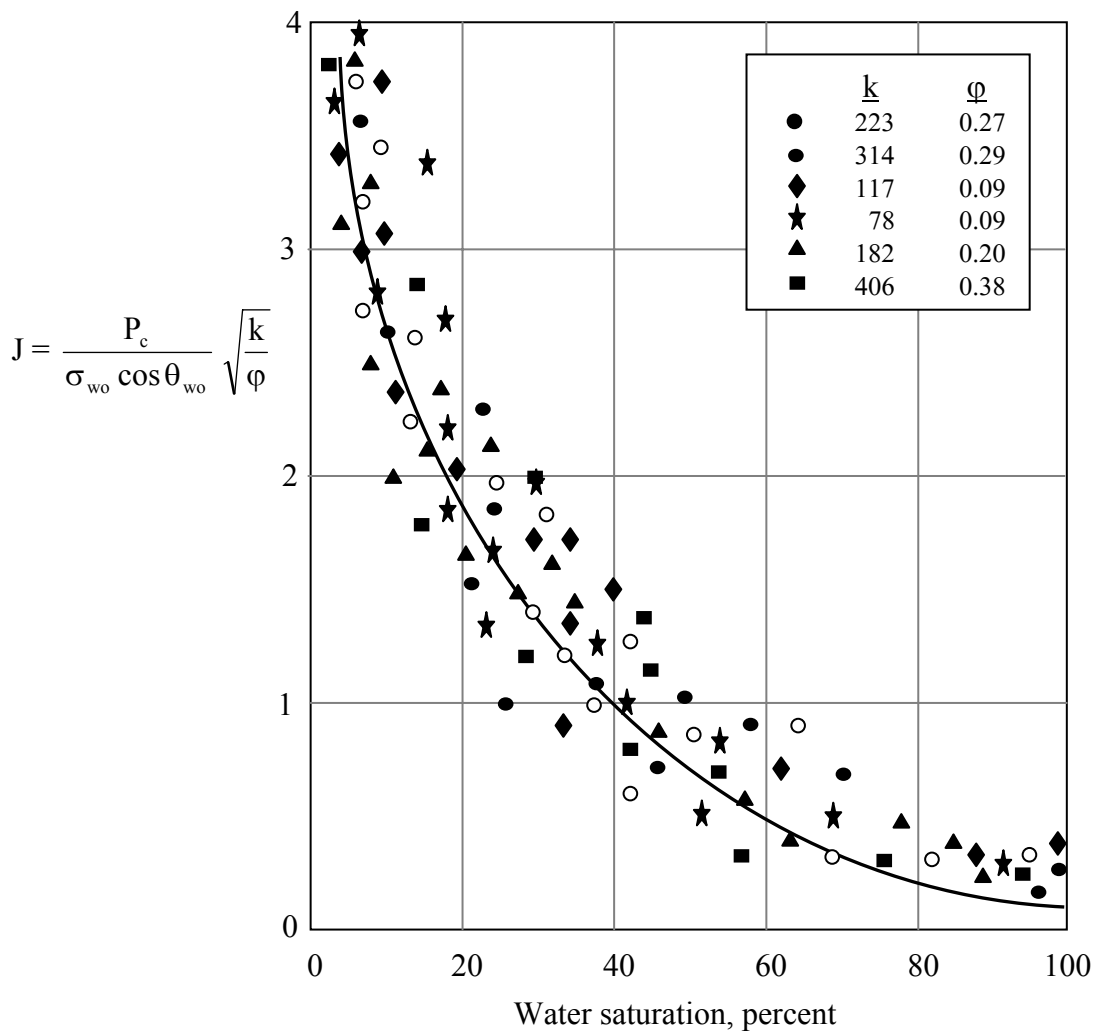$$P_c \quad = \quad J\,\sigma_{wo}\,\cos\theta_{wo}\sqrt{\frac{\varphi}{k}} \tag{7.19}$$

Fig. 7.13: Capillary pressure data for a dolomite reservoir

Example 7.5
A sandstone core sample with 240 md permeability and 27% porosity was used to determine the drainage water-air capillary pressure curve in the laboratory (T = 75 °F). For S_w of 35%,

P_c was measured at 1.65 psi. Estimate the P_c for S_w of 35% (S_o = 65%) in a location within the reservoir (T = 180 °F) where k = 160 md and φ = 15%. Relevant fluid and rock data are given below.

Air-water-quartz contact angle @ 75 °F: 24°

Oil-water-quartz contact angle @ 180 °F: 40°

Water surface tension @ 75 °F: 73 dyne/cm

@ 180 °F: 21 dyne/cm

Oil surface tension @ 75 °F: 39 dyne/cm

@ 180 °F: 10 dyne/cm

The core sample's equivalent reservoir P_c for S_w of 35% is computed first by Equ. 7.14:

$$P_{c,R} = \frac{\sigma_{wo} \cos \theta_{wo}}{\sigma_w \cos \theta_w} P_{c,L}$$

$$= \frac{(21-10)\cos 40}{73 \cos 24} 1.65$$

$$= 0.21 \text{ psi}$$

$$= 14{,}470 \text{ dynes/cm}^2$$

Note that data at reservoir temperature are used. At reservoir conditions, Leverett's J-function for the core sample at S_w of 35% would be:

$$J = \frac{14470}{(21-10)\cos 40} \sqrt{\frac{0.240 \times 9.87 \times 10^{-9}}{0.27}}$$

$$= 0.1608$$

At any other location within the reservoir, the J-function at S_w of 35% would always be approximately 160.8. Therefore, for the second location:

$$P_c = J \sigma_{wo} \cos \theta_{wo} \sqrt{\frac{\varphi}{k}}$$

$$= 0.1608 \times (21-10) \cos 40 \sqrt{\frac{0.15}{0.160 \times 9.87 \times 10^{-9}}}$$

$$= 13{,}206 \text{ dynes/cm}^2$$

$$= 0.19 \text{ psi}$$

Note that non-consistent units could have been employed in the computation of J since the same units would be used again in estimating the final P_c.

Exercises

1. Compute the depression of mercury in a glass tube (D = 0.5 mm) immersed in a beaker of mercury.

   σ_{HG} = 470 dyne/cm θ_{HG} = 150° ρ_{HG} = 13.4 g/cm^3.

2. If water overlays mercury in Exercise 1, what will the depression be? (θ_{wHG} = 150°)

3. What is the capillary pressure in Exercise 2?

4. For a capillary glass tube of 1 mm diameter, compute the rise of water above the water surface if the water is overlain by oil. Also compute the capillary pressure in the tube.

   σ_w = 72 dyne/cm σ_o = 35 dyne/cm

   ρ_w = 1 g/ml ρ_o = 0.82 g/ml

   θ (water/oil/glass) = 47° θ (oil/air/glass) = 65°

5. The grains of a sandstone core sample are 10 microns in diameter and are packed in the cubic arrangement. The core is saturated with water at atmospheric pressure (14.7 psia). If we want to displace the water from the core completely by using the oil of Exercise 4, what is the minimum oil pressure required? Water/oil/quartz contact angle is 45°.

   Hint: To estimate the radius of a pore, assume it to be a circle of the same area as the pore.

6. Consider Example 7.4. Suppose a drainage experiment was conducted on the same sandstone but with oil and air, and the threshold pressure was 0.6 psia. Compute the wettability number for this rock assuming the same fluid data as Exercise 4.

7. A resistivity log in the transition zone of a reservoir produced the water saturation data given below. Construct the capillary pressure curve for this reservoir if ρ_w = 1 g/ml and ρ_o = 0.8 g/ml.

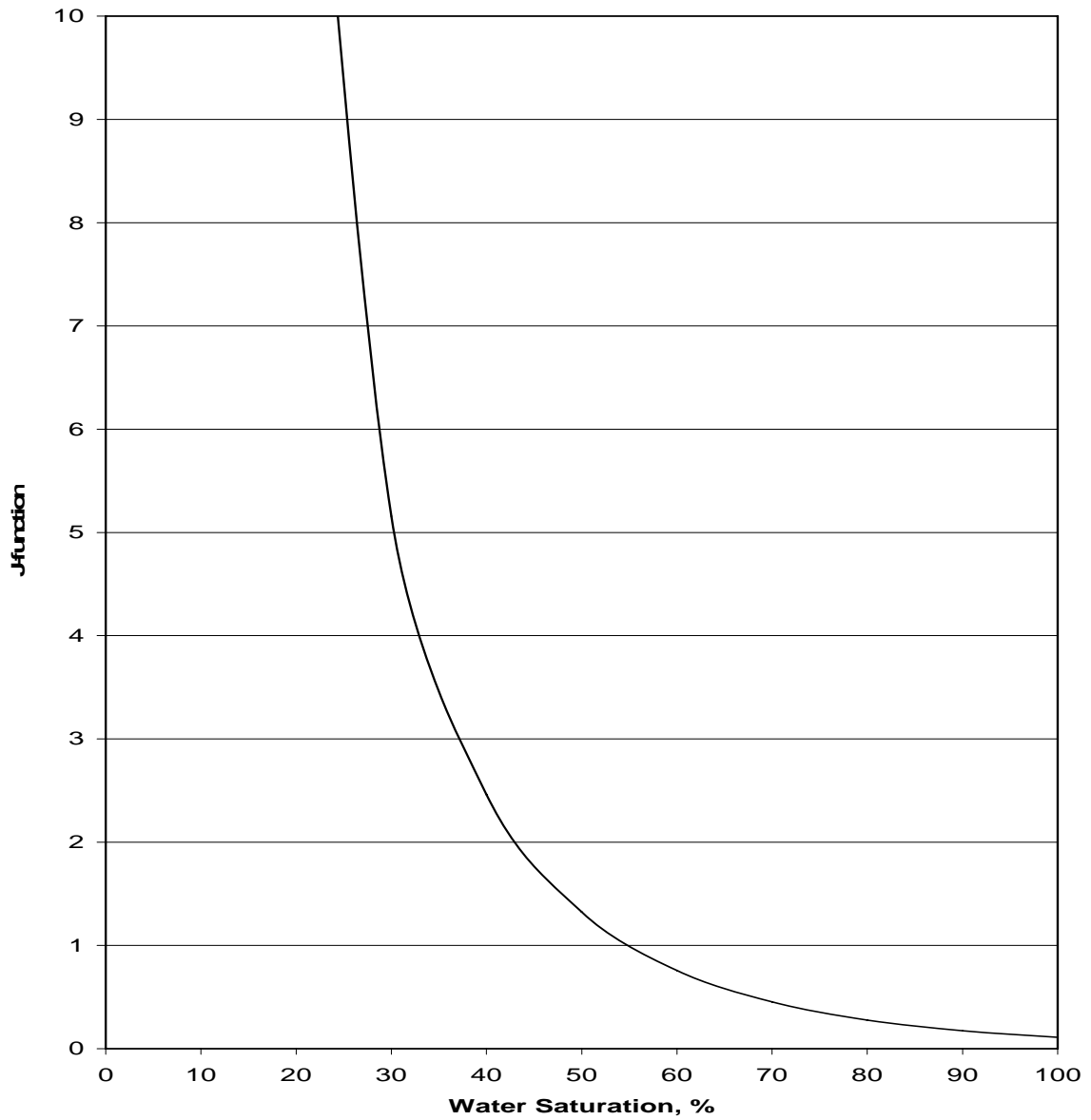| Depth, ft	4000	4100	4200	4300	4400	4500	4600	4700	4800	4900	5000
S_w, %	25.6	25.6	25.7	26.0	27.0	29.0	31.0	34.2	37.8	41.5	46.2

Depth, ft	5100	5200	5300	5370	5430	5550	5700	5800	5900	6000*
S_w, %	52.0	59.4	70.8	82.0	93.0	98.0	100.0	100.0	100.0	100.0

   * Free water table

8. The Leverett capillary pressure function for a reservoir is shown in the figure on the next page. For a core sample from this reservoir whose properties are given below, compute the irreducible (interstitial) water saturation and the threshold pressure.

   k = 520 md ϕ = 18%
   σ_o = 38 dyne/cm σ_w = 73 dyne/cm θ_{wo} = 27°

Y-axis label: Jfunction

X-axis label: Water Saturation, %

9. In a certain part of the reservoir of Prob. #8, k = 315 md and ϕ = 21%. The free water
    table is at 5300 feet subsea. Compute the water saturation at a depth of 5265 feet.

    $\rho_o = 53.0 \ lb/ft^3$ $\rho_w = 62.6 \ lb/ft^3$

8. EFFECTIVE AND RELATIVE PERMEABILITY

In the last section of chapter 6, a question was posed as to how to estimate the flowrate of a fluid in a reservoir where other fluids, either flowing or static, were present. It should have become obvious by now that for every fluid within the pore space of a porous medium there exists a critical saturation, irreducible or residual, that cannot be reduced unless excessively large pressure gradients are applied. Under normal reservoir conditions, such gradients cannot be attained, which makes a fluid near or at its critical saturation virtually immobile. This provides a partial answer to the question above; that is a fluid can flow only when its saturation is greater than the critical value. This condition is dictated by capillary forces. The magnitude of a fluid's mobility (ability to flow) is, intuitively, proportional to the fluid's saturation as long as such saturation is above the critical value. If we are to distribute the permeability of the medium among the fluids, we must take this fact into consideration.

8.1: Effective permeability

When several fluids are flowing through a porous medium, the flowrate of each fluid will be governed by Darcy's law. Basically, such flowrate is dictated by the fluid's viscosity and flow potential gradient, the portion of the total cross-sectional area of the medium that is available to the fluid's flow, and the permeability of the medium. In equation form, Darcy's law is written:

$$q_i \quad = \quad - k \, \frac{A_i}{\mu_i} \, \frac{\partial \Phi_i}{\partial s} \tag{8.1}$$

where subscript "i" refers to fluid i. Since A_i is difficult and impractical to determine, the total cross-sectional area of the medium is preferred instead. This necessitates replacing k with k_i, which is termed the *effective permeability* to fluid i. Equation 8.1 is, therefore, rewritten:

$$q_i \quad = \quad - k_i \, \frac{A}{\mu_i} \, \frac{\partial \Phi_i}{\partial s} \tag{8.2}$$

The effective permeability to a fluid is, thus, defined as the ability of a porous medium to conduct that fluid when the fluid's saturation in the porous medium is less than 100%.

The units of effective permeability are obviously the same as permeability. Besides the permeability of the medium, the effective permeability to a fluid depends also on the fluid's saturation, the types and saturations of other fluids present in the medium, the wettability preference of the medium, and its pore characteristics and size distribution. In essence, the effective permeability is affected closely by the capillary characteristics of the fluid-rock system.

A set of typical water and oil effective permeability curves for a strongly water-wet rock is shown in Fig. 8.1. Several features of those curves deserve close examination.
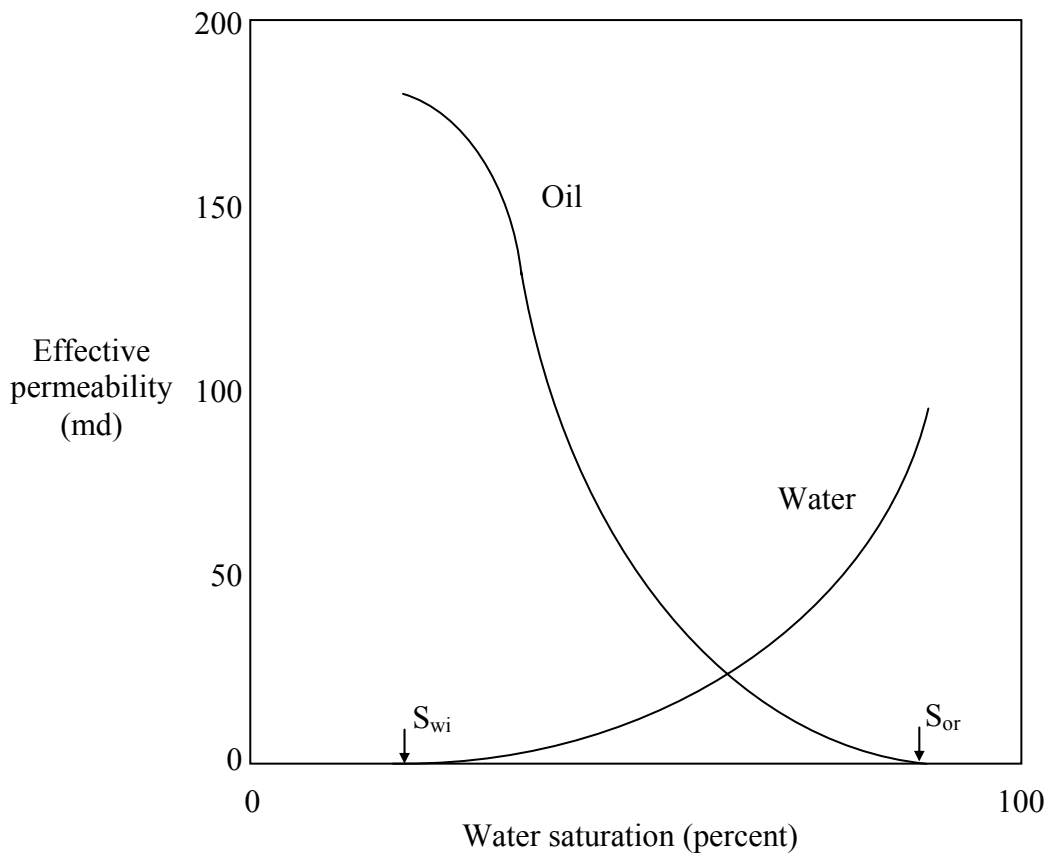

Fig. 8.1: Typical effective permeability curves

a. The most prominent feature occurs at the critical saturations where both effective permeabilities drop to zero. In other words, water becomes immobile ($k_w = 0$) at $S_w = S_{wi}$ and oil becomes immobile ($k_o = 0$) at $S_o = S_{or}$ or $S_w = 1 - S_{or}$.

b. At their maxima, neither k_w nor k_o equals k. This feature is expected since at either point, the pore space is partially occupied by the other fluid, which deprives the flowing fluid of conductive pore space.

c. S_{wi} is larger than S_{or}. Due to wettability preference, water ceases to flow at a larger saturation because adhesion binds water to the grain surfaces with a stronger force.

d. Even though S_{wi} is larger than S_{or}, which means that the pore space available to oil at S_{wi} is smaller than that available to water at S_{or}, the maximum k_w is less than the maximum k_o. To explain this feature, we have to look closely at the distribution of each fluid at its critical saturation as depicted in Fig. 8.2. Being the wetting phase, water at S_{wi} is reduced to rings lodged at the smallest pore throats and/or droplets

filling the smallest pores. Since these locations contribute little to the permeability of the medium, compared with their contribution to the pore volume, oil enjoys the most conductive part of the pore space. Compare this situation with that of oil at S_{or}, where oil is reduced to globules isolated at the largest pores posing a significant restriction to water flow.
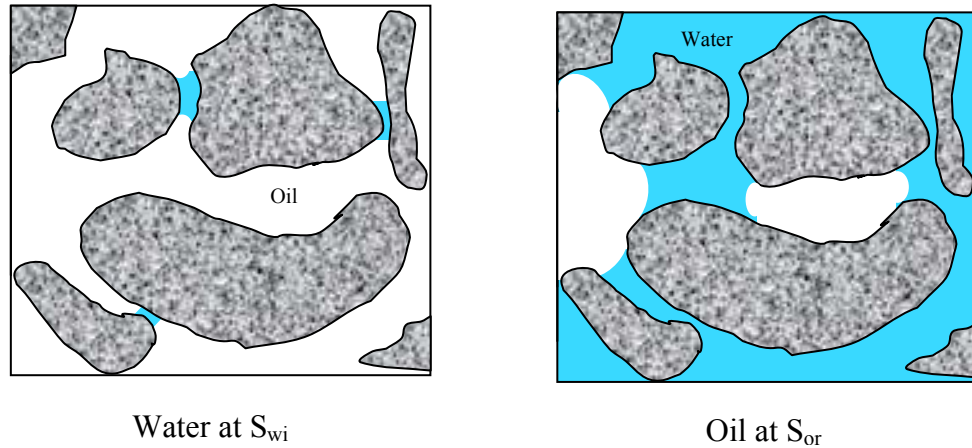

Water at S_{wi} Oil at S_{or}

Fig. 8.2: Distribution of oil and water at critical saturations

e. At any S_w, the sum of k_w and k_o does not add up to k. Once again, capillary forces hinder the movement of water through the medium in the presence of oil, which reduces the overall conductivity of the medium.

8.2: Measurement of effective permeability

Effective permeability is measured by several methods classified according to the nature of the flow experiment. The steady-state method is simple and accurate, though very time consuming. In this method, a permeameter similar to the one shown in Fig. 6.1 is used with minor modifications. First, both water and oil are simultaneously injected into the core sample at different flowrates, and, second, the production rates of oil and water are measured individually.

A test begins with mounting the core sample, whose pore volume is known and is fully saturated with water, into the core holder. Once the confining pressure is applied, some water would squeeze out of the sample, which requires recalculation of its initial pore volume. Then both oil and water are injected into the sample at constant, but different, rates. Normally, the q_o /q_w ratio is set initially at a small value. Injection is continued until steady state is achieved where the production rate of each fluid is equal to its injection rate. At this point, the saturation of each fluid in the sample is computed by material balance, and the effective

permeability to each fluid is computed by Equ. 8.2. Note that the flow potential gradient for each fluid is approximately equal to the total pressure gradient applied to the core sample. This step provides one value each for k_w and k_o at the corresponding S_w in the sample. The procedure is repeated for progressively larger q_o/q_w ratios and the steady-state effective permeabilities are computed at each new S_w. In the last step of this sequence, only oil is injected into the sample. Steady state is achieved when water production ceases signaling the complete removal of all mobile water from the sample. This step provides both S_{wi} and k_o at S_{wi}

The procedure described above involves a drainage process. Accordingly, the effective permeability curves that result are drainage curves. For the imbibition curves, the procedure has to be repeated starting with the core sample fully saturated with oil, and the oil saturation is reduced stepwise. Note that in the last step of this procedure, only water is injected until oil ceases to flow out of the sample. This step provides S_{or} and k_w at S_{or}.

It is interesting to note that the drainage and imbibition k_o curves usually differ, while the k_w curves are virtually the same. A typical example of effective permeability curves is shown in Fig. 8.3. It is customary to plot those curves versus the wetting-phase saturation.
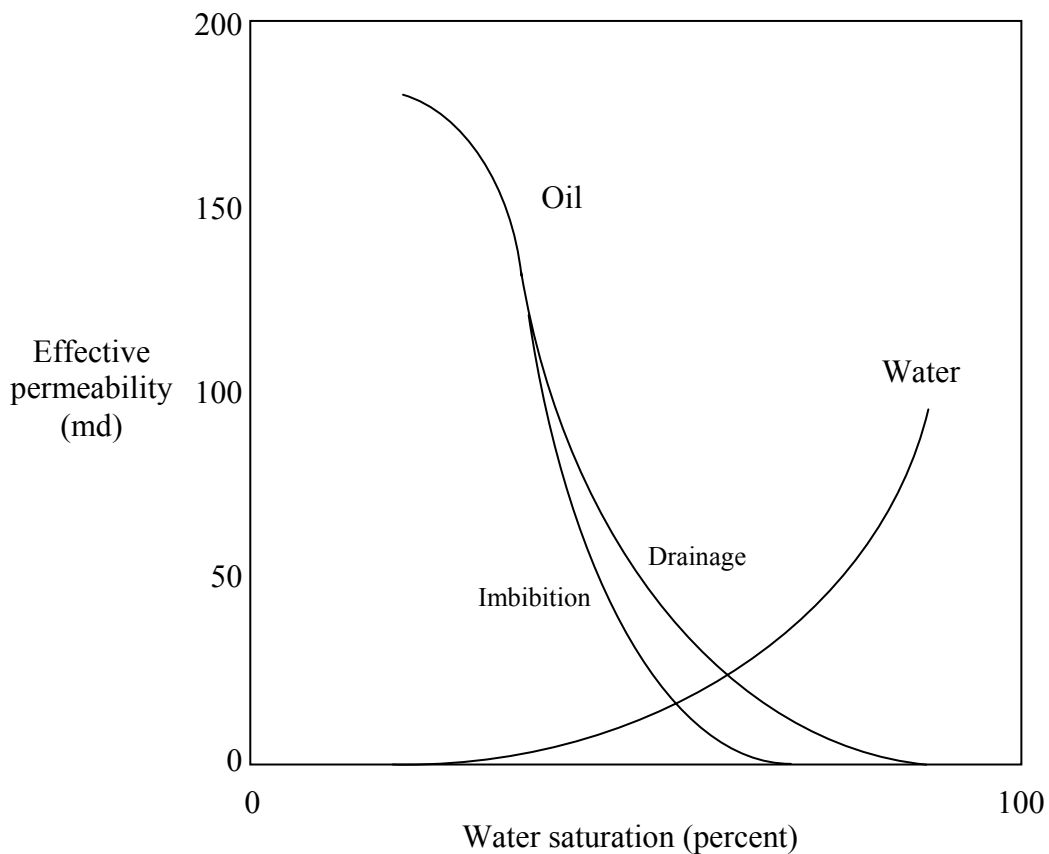

Fig. 8.3: Drainage and imbibition effective permeability curves

Example 8.1

A steady-state flow test was conducted on a core sample 1" in diameter and 2" long. The table below lists the total pressure drop, fluid flowrates and saturation data for each step of the test. Compute and plot the effective permeability curves for this core and estimate S_{wi} and S_{or}. Oil and water viscosities are 2.5 and 1.1 cp, respectively.

ΔP (psi)	3.9	5.2	4.9	3.7	3.5	3.2	3.8	3.7
q_o (cm^3/min)	0.000	0.000	0.023	0.089	0.573	1.680	3.570	4.570
q_w (cm^3/min)	12.300	7.890	5.050	3.560	1.170	0.207	0.004	0.000
S_w (%)	100.0	79.5	73.9	70.0	60.0	50.1	40.2	36.3

From the test data, we observe:

$q_o = 0$ @ $S_w = 79.5$ Therefore, $S_{or} = 100 - 79.5 = 20.5\%$

$q_w = 0$ @ $S_w = 36.3$ Therefore, $S_{wi} = 36.3\%$

Oil flowrate is given by Equ. 8.2:

$$q_o = -k_o \frac{A}{\mu_o} \frac{\partial \Phi_o}{\partial s} = k_o \frac{A}{\mu_o} \frac{\Delta P}{L}$$

Rearrangement of the above equation yields:

$$k_o = \frac{q_o \mu_o L}{A \Delta P}$$

Applying this equation, with consistent units, to every step yields the effective permeability to oil. For example, at $S_w = 70\%$,

$$k_o = \frac{(0.089/60)(2.5)(2 \times 2.54)}{(\frac{\pi}{4}1^2 \times 2.54^2)(3.7/14.7)}$$
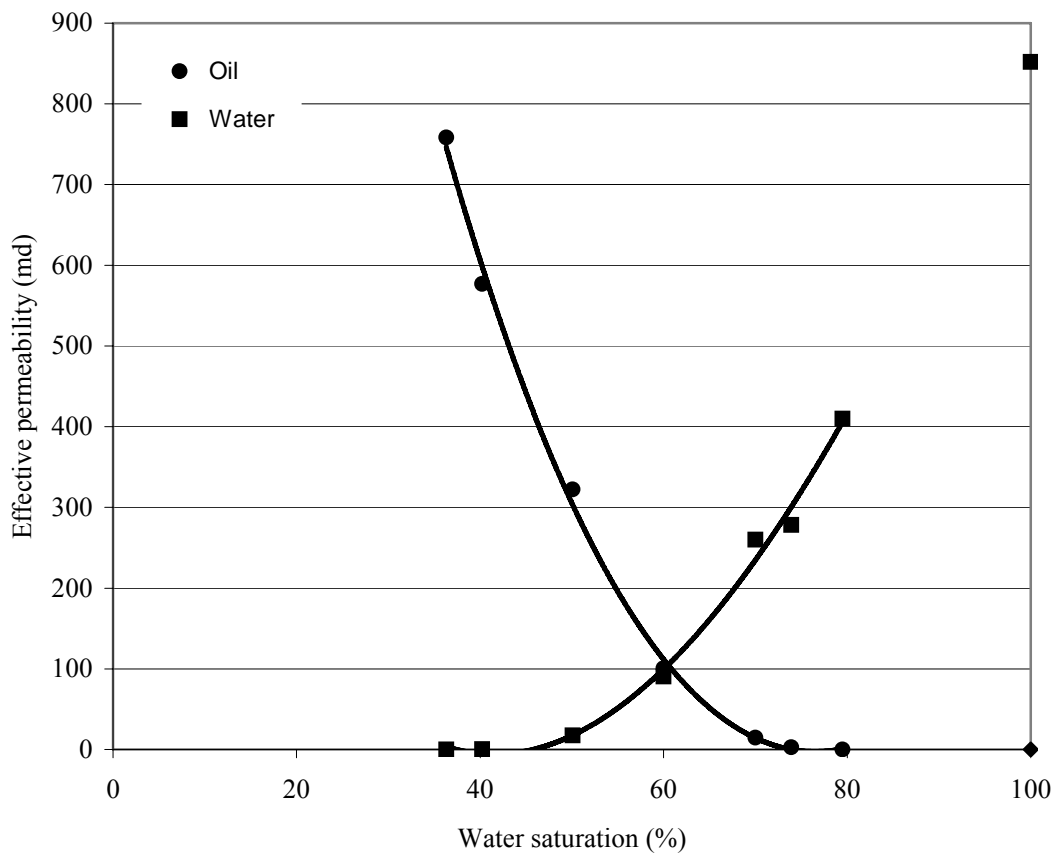
$$= 0.0148 \ darcy = 14.8 \ md$$

Similarly, the effective permeability to water is computed by:

$$k_w = \frac{q_w \mu_w L}{A \Delta P}$$

At $S_w = 70\%$,

$$k_w = \frac{(3.560/60)(1.1)(2 \times 2.54)}{(\frac{\pi}{4}1^2 \times 2.54^2)(3.7/14.7)}$$

$$= 0.2599 \ darcy = 260 \ md$$

The effective permeability values are plotted in the figure below with smooth curves drawn through the data points. Note that at $S_w = 100$, k_w is the permeability of the core sample.

A faster method for determining effective permeability employs unsteady-state displacement of oil by water. The procedure is similar to that of the steady-state method except that only water is injected into the core and at one constant rate. During displacement, both oil and water are produced from the core sample at variable rates and the pressure drop across the sample varies as well. A mathematical technique to analyze the data had been developed by Johnson *et al.*[4] in 1959 and was later modified by Jones and Rozelle[5] in 1978. The technique provides the relative permeabilities, defined in the following section, rather than the effective permeabilities.

Effective permeabilities can also be obtained from field production data. An oil well would produce both oil and water if the saturations of the two fluids within the well's production area were above their respective critical values. The production rate of each fluid would be controlled by Equ. 8.2. Assuming that the flow potential gradients for both fluids are equal, the ratio of production rates would be given by:

$$\frac{q_o}{q_w} = \frac{k_o}{k_w} \frac{\mu_w}{\mu_o} \qquad\qquad (8.3)$$

The effective permeabilities would correspond to the average water saturation within the well's area of the reservoir, which could be estimated from well logs. Other wells producing from the same reservoir could supply additional data points to complete the curves. Note that only the ratio of effective permeabilities is provided by Equ. 8.3.

This technique is not wholly reliable for several reasons. Daily fluctuations in the production rates compel the engineer to resort to average rates, which introduces inaccuracies in the analysis. Also, both fluids are not uniformly distributed around the well making average water saturation a difficult parameter to assess. Lastly, assuming the computed effective permeability ratio to correspond to the average water saturation is not technically correct.

8.3: Correlating effective permeability

Similar to the problem of the capillary pressure curves, heterogeneous reservoirs display a range of effective permeabilities as wide as permeability variation. To overcome this problem, reservoir engineers have adopted the concept of the *relative permeability*, which is simply the ratio of the effective permeability to some base permeability, k_b. Therefore,

$$k_{ri} = \frac{k_i}{k_b} \qquad\qquad (8.4)$$

where k_{ri} is the relative permeability to fluid i at the saturation of k_i. Relative permeability is dimensionless and varies with the wetting-phase saturation in a form identical to that of effective permeability. Plotting all sets of relative permeability curves for a reservoir, each set based on its own base permeability, usually collapses all such curves into one set.

There are no criteria for the choice of base permeability; however, convention has settled on the effective permeability to oil at irreducible water saturation (k_o at S_{wi}). The relative permeability curves corresponding to the example of Fig. 8.3 are shown in Fig. 8.4.

8.4: Smoothing relative permeability data

Effective permeability and, consequently, relative permeability data usually show scatter caused by experimental errors. Smoothing relative permeability data is achieved by two techniques.

a. Relative permeability ratio

The ratio of non-wetting to wetting-phase relative permeability, e.g., k_{ro}/k_{rw} or k_{rg}/k_{ro}, has been found to fall on a semi-logarithmic straight line over most saturations as illustrated in

Fig. 8.5. Once plotted and fitted by the best straight line, the smoothed data could be used instead of the original one.
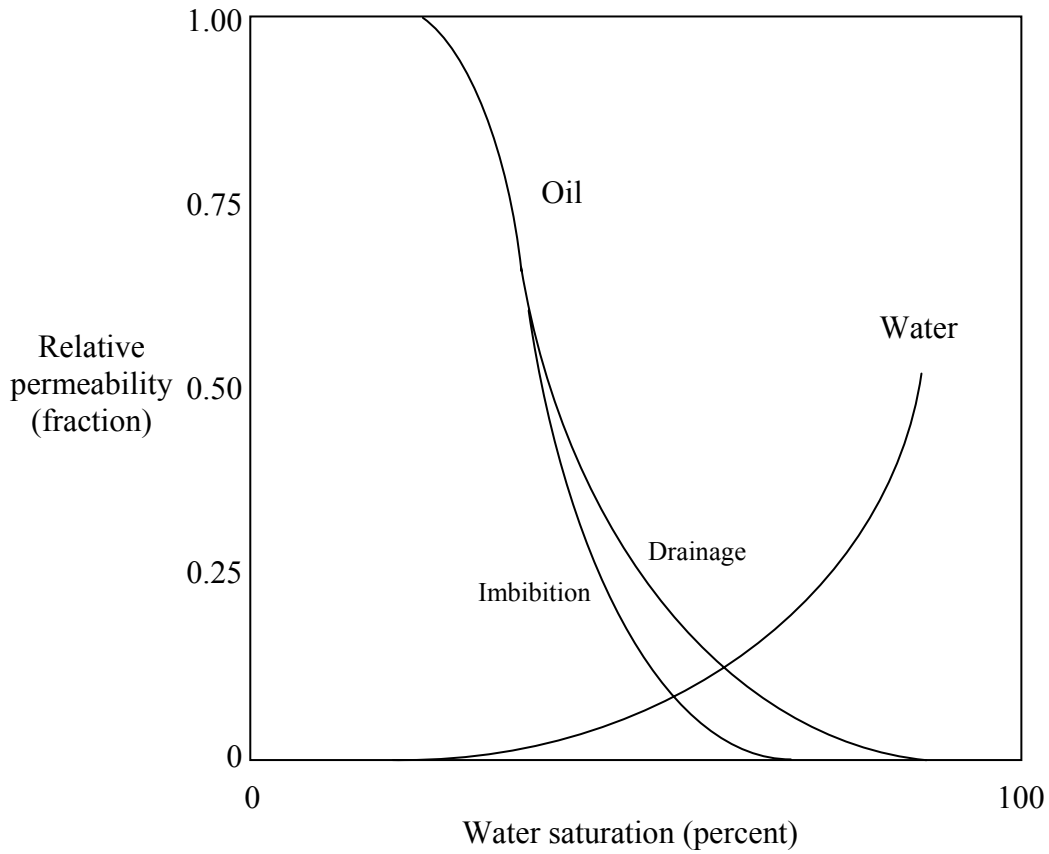

Fig. 8.4: Drainage and imbition relative permeability curves

b. Dimensionless saturation

For water-wet rock, dimensionless water saturation is defined as:

$$S_{wD} = \frac{S_w - S_{wi}}{1 - S_{wi} - S_{or}} \tag{8.5}$$

Employing this definition, the following correlations have been found to fit most relative permeability data:

$$k_{ro} = (1 - S_{wD})^b \tag{8.6}$$

$$k_{rw} = a\, S_{wD}{}^c \tag{8.7}$$

where a, b and c are empirical constants to be determined by regression on the data. Once the data is fitted, Equs. 8.6 and 8.7 can be employed for generating relative permeability data.
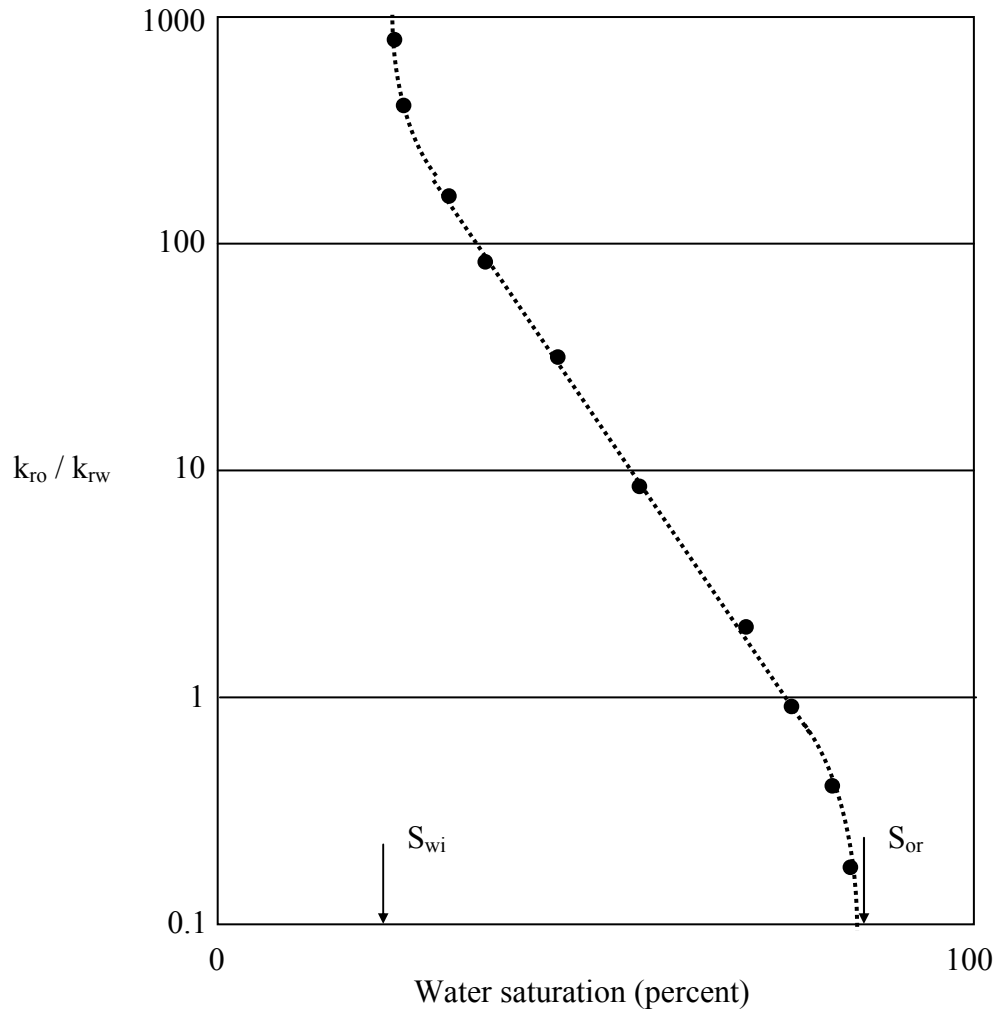
Fig. 8.5: Variation of relative permeability ratio with water saturation

---

Example 8.2

Compute the relative permeability data for Example 8.1 and smooth it using Equs. 8.5, 8.6 and 8.7.

In Example 8.1, the effective permeability to oil at S_{wi} was found to be 758.4 md. This shall be employed as the base permeability. Converting normal water saturation to dimensionless water saturation is done according to Equ. 8.5:

$$S_{wD} = \frac{S_w - 0.363}{1 - 0.363 - 0.205} = \frac{S_w - 0.363}{0.432}$$

All effective permeability values are converted to relative permeabilities using the base permeability. For example, at $S_w = 70\%$:

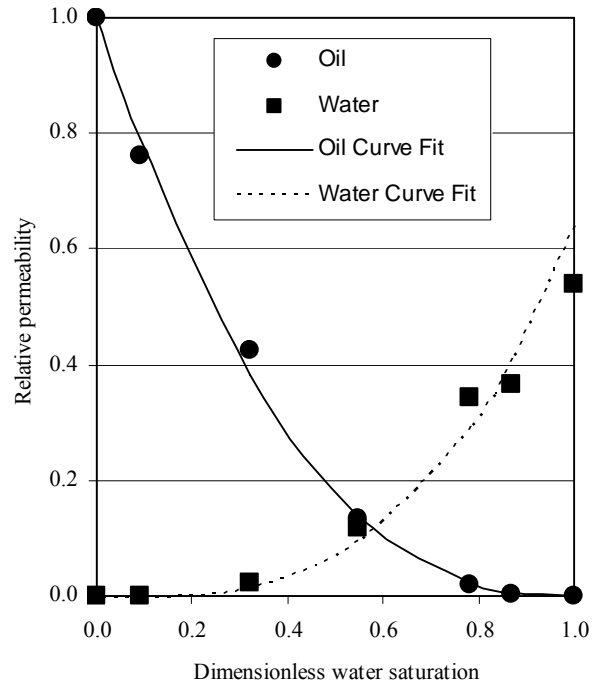$$S_{wD} = \frac{0.7 - 0.363}{0.432} = 0.78$$

$$k_{rw} = \frac{260}{758.4} = 0.343 \qquad\qquad k_{ro} = \frac{14.8}{758.4} = 0.02$$

The relative permeability data is plotted in the figure shown to the right. Best-fitting curves of the form given by Equs. 8.6 and 8.7 are determined by plotting log k_{rw} vs. log S_{wD} to find a and c, and log k_{ro} vs. Log $(1 - S_{wD})$ to find b. The two curves are also shown in the figure, and their equations are:

$$k_{ro} = (1 - S_{wD})^{2.5}$$

$$k_{rw} = 0.64\, S_{wD}^{3.15}$$

8.5: Estimation of relative permeability

Because of difficulties associated with displacement experiments, a number of techniques have been proposed for the estimation of relative permeability from other sources of fluid-rock data. One such technique was outlined by Purcell[6] in 1949 utilizing capillary pressure data. For a water-wet system, Purcell derived equations which have been modified as follows:

$$k_{rw} = \frac{\displaystyle\int_{S_{wi}}^{S_w} \frac{dS_w}{p_c^{\,2}}}{\displaystyle\int_{S_{wi}}^{1-S_{or}} \frac{dS_w}{p_c^{\,2}}} \tag{8.8}$$

$$k_{ro} = \frac{\displaystyle\int_{S_w}^{1-S_{or}} \frac{dS_w}{p_c^{\,2}}}{\displaystyle\int_{S_{wi}}^{1-S_{or}} \frac{dS_w}{p_c^{\,2}}} \tag{8.9}$$

The integrals in Equs. 8.8 and 8.9 are evaluated by graphical means as shown in Fig. 8.6.
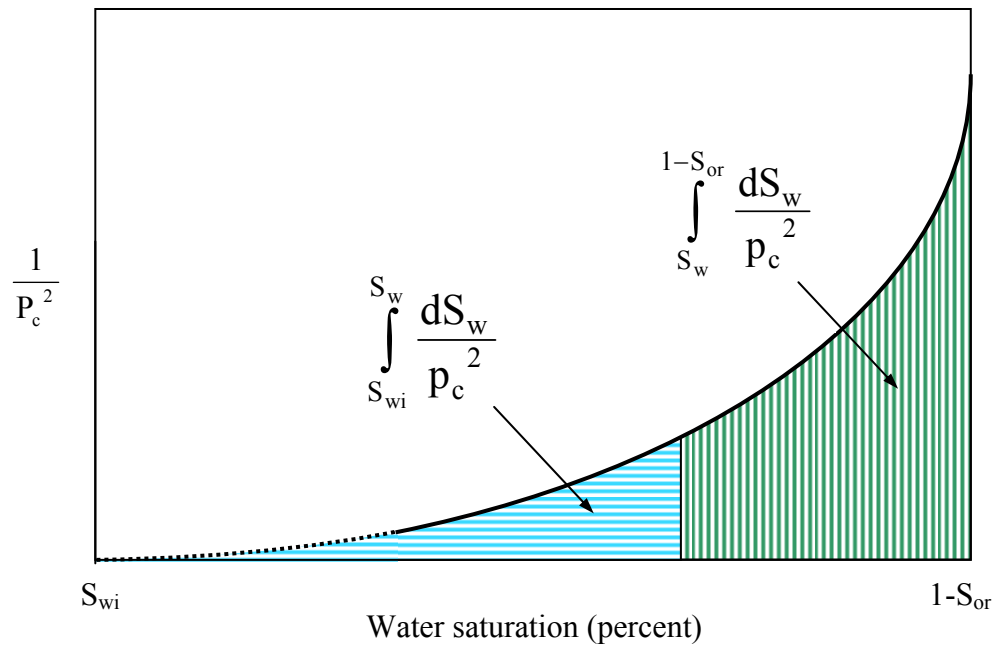
Fig. 8.6: Estimating relative permeability by Purcell's method

The relative permeabilities computed by Purcell's method are based on the permeability of the porous medium. One limitation exists with this method, namely, the sum of k_{rw} and k_{ro} is equal to one for any given S_w, which is not correct. Another limitation relates to the value of P_c at S_{or}, which is usually zero for the imbibition curve. We can work around this problem by using the closest data to S_{or} and then setting k_{ro} at S_{or} to zero.

Example 8.3
Estimate the imbibition relative permeability data for the reservoir of Example 7.4.

Imbibition P_c values are read from Fig. 7.12 at various water saturations, then $1/P_c^2$ is computed:

S_w	0.20	0.30	0.40	0.50	0.60	0.70	0.80	0.85	0.90
P_c (psi)	10.0	5.0	3.5	2.5	1.4	0.8	0.3	0.2	0
$1/P_c^2$ (psi^{-2})	0.010	.040	.082	0.160	0.510	1.56	11.1	25.0	-

$1/P_c^2$ is then plotted vs. S_w, as shown below, and the integrals in Equs. 8.8 and 8.9 are determined graphically at various saturations. The relative permeability curves that result are also shown below.
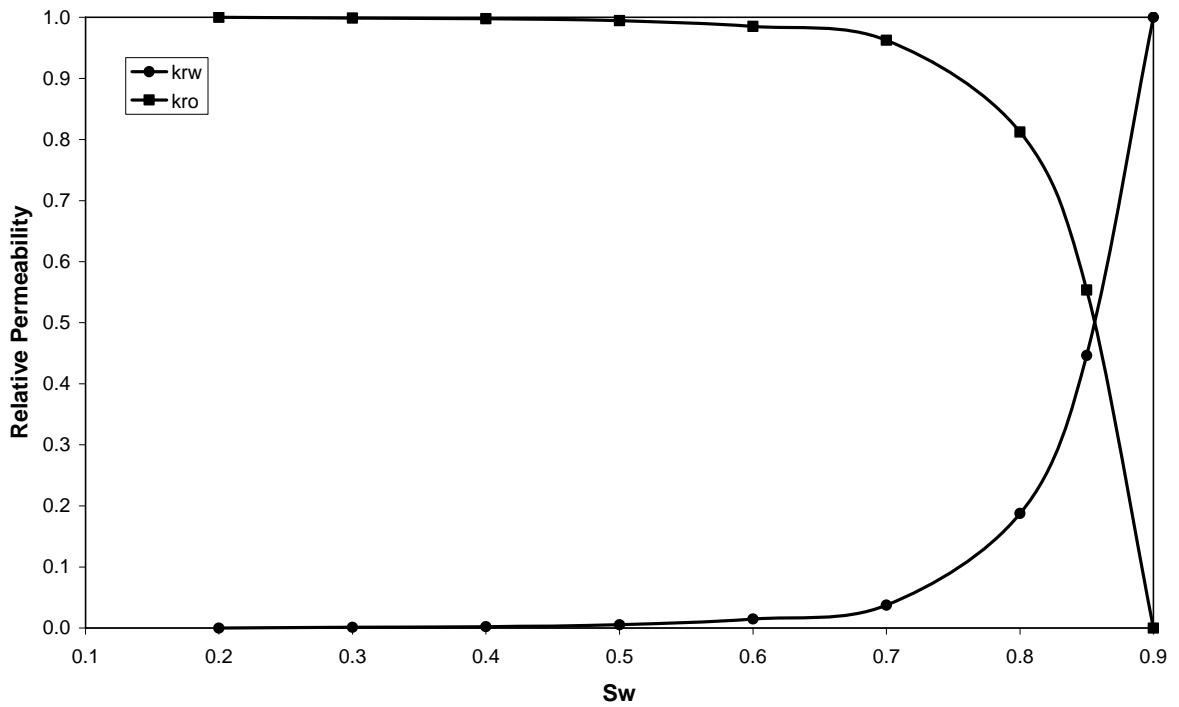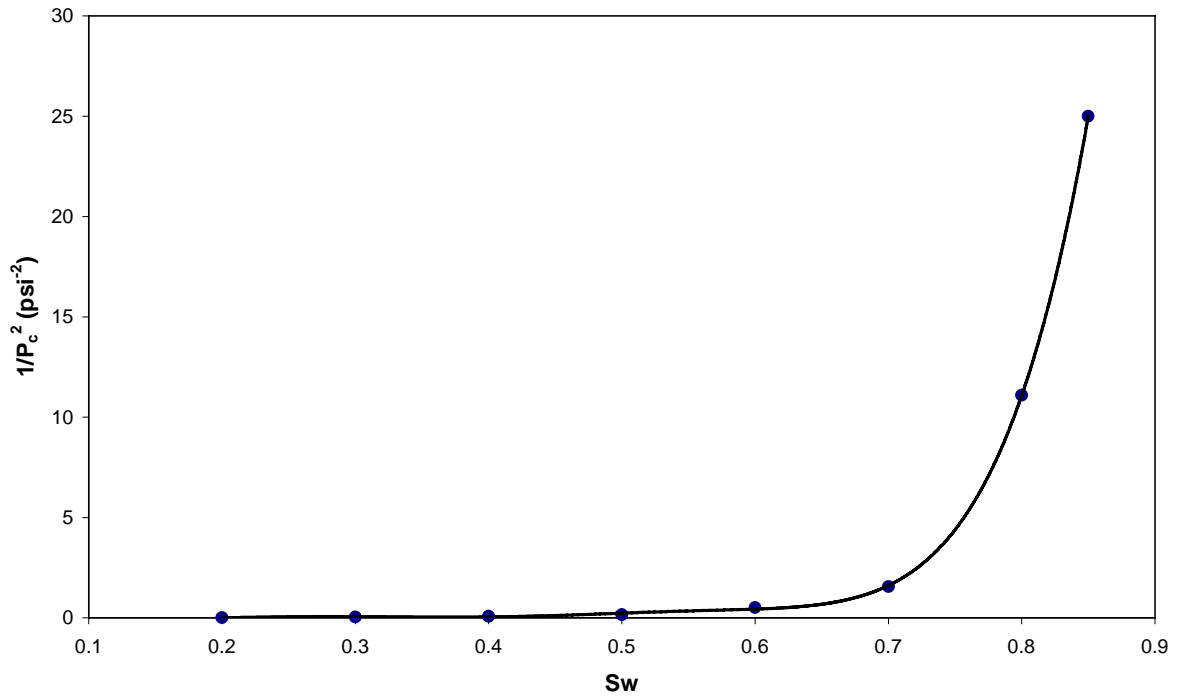
Note that k_{rw} at S_{or} ($S_w = 90\%$) is equal to 1, which is not always true especially for water-wet rock. This is another artifact of the Purcell method.

8.6: Three-phase relative permeability

Petroleum reservoirs often contain three phases: water, oil and gas. The gas phase could be present initially or may evolve out of the oil phase during the life of the reservoir. It may also be introduced into the reservoir to assist displacement of oil. In any case, the flowrate of any phase is controlled by its own effective permeability as stated by Equ. 8.2.

Measurement of 3-phase effective, or relative, permeabilities is carried out by experiments similar to those involving two phases; the amount of work is much larger, though. The difficulty lies, however, in the presentation of such data. While a tabular form is simple, it would render interpolation between data points rather inaccurate. A graphical form is more practical.

For a given rock, studies have shown that the relative permeability to the wetting phase varies with its saturation only. In a water-wet system, for example, k_{rw} appears to be dependant on S_w only regardless of S_o or S_g. This observation is explained by the fact that water tends to occupy the smallest pores and it considers all other fluids as non-wetting phases. Therefore, water behaves as though it is flowing in a 2-phase system. On the other hand, relative permeability to gas, the least wetting of all three fluids, varies mainly with gas saturation. Gas considers both oil and water as wetting phases and thus occupies the largest pores. In a close fashion to water, gas behaves as though it is flowing in a 2-phase system with it being the non-wetting phase. This leaves oil whose relative permeability has been observed to depend on both S_w and S_g. Having intermediate wettability, oil is limited to intermediate-size pores where its flow is hindered by both water and gas.

Leverett and Lewis[7] presented 3-phase relative permeability data on a water-wet, unconsolidated sand pack. Figure 8.7 shows the k_{rw} curve for this medium. Notice that for some water saturations more than one value of k_{rw} are plotted. These were measured at the same S_w but at different combinations of S_o and S_g. Nevertheless, all k_{rw} data fall on a narrow band and can be smoothed by a single curve.

The k_{ro} data is presented in ternary-diagram form as shown in Fig. 8.8. In a ternary diagram, each corner of the triangle represents complete saturation by one phase and the base opposite to a corner represents zero saturation of that same phase. Phase saturations between 0 and 100% are represented by lines parallel to the base. For example, point α in Fig. 8.8 represents 50% S_w, 30% S_o, and 20% S_g, while point β represents 10% S_w, 30% S_o, 60% S_g. Points of constant k_{ro} are connected by a curve with the k_{ro} value denoted next to the curve. For points α and β, k_{ro} equals 5% and 2%, respectively. S_{or} is estimated at 20%. The k_{rg} data for the sand pack is shown in the ternary diagram of Fig. 8.9. The critical gas saturation, S_{gc},

is estimated at about 10%. The base permeability in Leverett and Lewis's data is the permeability of the sand pack as can be deduced from Fig. 8.7.
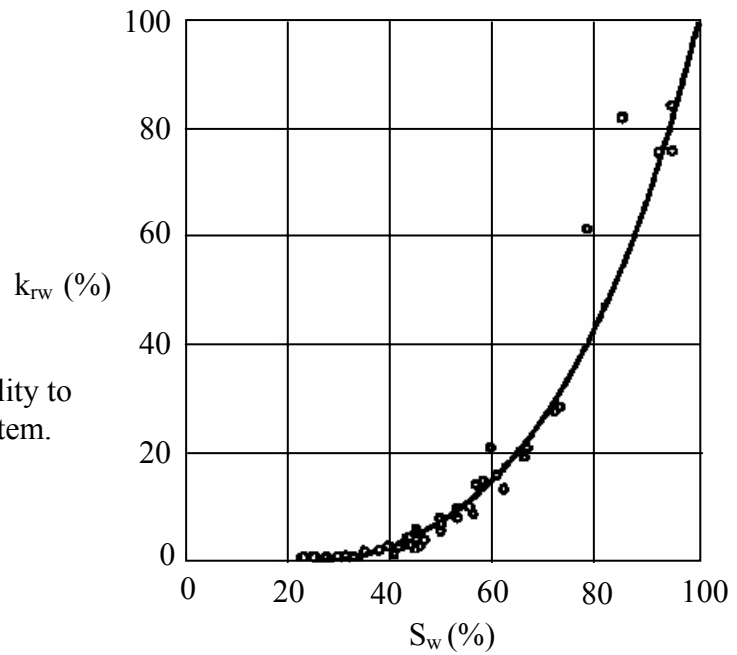

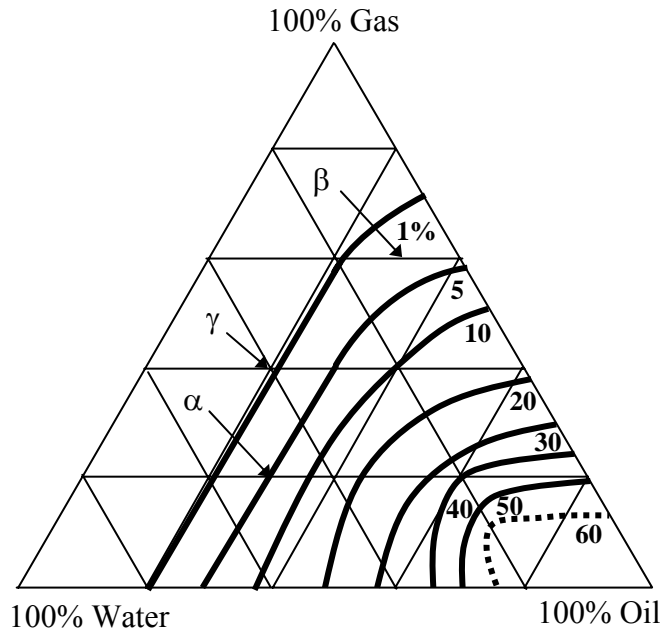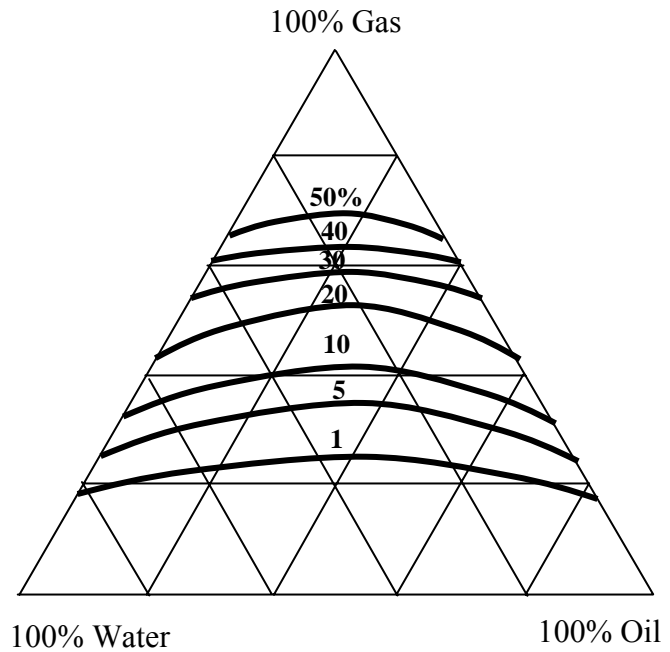Fig. 8.7: Realtive permeability to water in a 3-phase flow system.

Fig. 8.8: Realtive permeability to oil in a 3-phase flow system.

Fig. 8.9: Realtive permeability to gas in a 3-phase flow system.

100% Gas

100% Water   100% Oil

Liquid flow is severely curtailed when gas is present at appreciable saturations. Consider point γ in Fig. 8.8 where S_o = 20% and S_w = S_g = 40%. The relative permeabilities in this case are k_{rw} = 3%, k_{ro} < 1% and k_{rg} = 10%. With a viscosity two orders of magnitude smaller than those of oil and water, gas flowrate could be hundred of times larger than oil. Such domination by gas affects oil production adversely and drains the energy out of the reservoir. For this reason, reservoir engineers plan exploitation of an oil reservoir in a way that obviates build up of significant gas saturation in the oil zone.

8.7: Applications of relative permeability

Any reservoir analysis that involves estimation of multi-phase flow requires relative permeability. Examples of such analyses are too many to present in this introductory course. We will select one application to illustrate the utility of relative permeability.

At a certain stage in the life of an oil reservoir, water is injected into the reservoir to displace the oil and, consequently, enhance the recovery. This process is called *waterflooding*. In areas swept by water, complete oil displacement is not possible due to capillary effects; rather, both oil and water would flow simultaneously. The ratio of oil to water flowrates within the swept area would be given by Equ. 8.3, which indicates that such ratio varies with water saturation. If we are to maximize the q_o/q_w ratio, we must keep the effective permeability ratio at a maximum. This is achieved by either maintaining S_w within the swept area to a minimum, which is rather difficult since buildup of water in this area is inevitable, or modifying the relative permeability characteristics of the reservoir. The second option is not too difficult for we only need to adjust the properties of injected water - which is within our control - in such a way that reduces the capillary pressure. Equation 7.12 provides the clue:

$$P_c = \frac{2\sigma_{wo}\cos\theta_{wo}}{r} \tag{7.12}$$

If we reduce the water-oil interfacial tension, the capillary pressure for any pore radius would drop. The relative permeability curves would, then, shift towards the left, i.e., smaller S_w, and the q_o/q_w ratio would increase for all S_w values. Reducing σ_{wo} is achieved by dissolving special chemicals, called *surfactants*, in the water at pre-determined concentrations, and the water flood becomes a *surfactant flood*. Note that we can also increase the ratio by dissolving polymers in the water to raise μ_w, and the water flood becomes a *surfactant/polymer flood*.

Exercises

1. The table below gives the flow rate and saturation data for a steady-state test to estimate effective permeability. The pressure drop across the core sample was constant throughout the test.

S_w (%)	q_o (cc/min)	q_w (cc/min)
100.0	0.000	12.300
79.5	0.000	7.890
73.9	0.023	5.050
70.0	0.089	3.560
60.0	0.573	1.170
50.1	1.680	0.207
40.2	3.570	0.004
36.3	4.570	0.000

$\mu_o = 2.5$ cP
$\mu_w = 1.0$ cP

  a. Estimate S_{wi} and S_{or} .

  b. Compute and plot the *relative* permeability curves for this core. The base permeability is k_o @ S_{wi}

  Note: you don't need to compute k_o and k_w individually

2. Prepare a semi-logarithmic graph of the relative permeability ratio (k_{ro}/k_{rw}) vs. S_w for Exercise 1 and determine the range over which the trend is linear.

3. Suppose the data of Exercise 1 applies to the reservoir of Exercise 6.10. If k_o @ S_{wi} is 170 md, compute oil and water flowrates at locations in the reservoir where the saturations are as follows:

  a. $S_w = 45\%$ b. $S_w = 55\%$ c. $S_w = 65\%$

4. If the well of Exercise 3 produces 900 bbls/d and 230 bbls/d of oil and water, respectively, what and where in the reservoir is the corresponding water saturation?

5. Smooth the data of Exercise 1 by applying Equs. 8.6 and 8.7.

6. Using Figs. 8.7, 8.8 and 8.9, estimate k_{rw}, k_{ro} and k_{rg} at the following conditions:

   a) $S_w = 32\%$ $S_o = 50\%$

   b) $S_w = 20\%$ $S_o = 35\%$

   c) $S_w = 10\%$ $S_o = 72\%$

7. A well 6" in diameter penetrates a reservoir, which is 80 feet thick and has an absolute permeability of 120 md. The reservoir pressure 4000 feet away from the well is 3750 psig and the well pressure is maintained at 1650 psig. If the relative permeabilities are the same as Exercise 6, and oil and water saturations are the same as Exercise 6(b), compute the well's oil, water and gas (at reservoir conditions: $P = 1650$ psig, $T = 180$ °F) production rates.

   $\mu_o = 2.5$ cP $\mu_w = 1.0$ cP $\mu_g = 0.015$ cP

   Note : Assume the absolute permeability to be the base permeability.

8. If you have the relative permeability curves for a rock sample, is it possible to extract the capillary pressure curve from them using Purcell's method (Equs. 8.8 and 8.9)?

References

1. Fatt, I.: "Pore Volume Compressibilities of Sandstone Reservoir Rocks," *J. Pet. Tech.*, March 1958.

2. Archie, G.E.: "The Electrical Resistivity Log as an Aid in Determining Some Reservoir Characteristics," *Pet. Tech.*, Vol. 5 (1), January 1952.

3. Leverett, M.C.: "Capillary Behavior in Porous Solids," *Trans. AIME* (1941).

4. Johnson, E.F., Bossler, D.P., and Naumann, V.O.: "Calculation of Relative Permeability from Displacement Experiments," Trans. AIME (1959), V. 216, 370-372.

5. Jones, S.C. and Rozelle, W.O.: "Graphical Techniques for Determining Relative Permeability from Displacement Experiments," *J. Pet. Tech.*, May 1978.

6. Purcell, W.R.: "Capillary Pressures – Their Measurement Using Mercury and the Calculation of Permeability Therefrom," *Trans. AIME* (1949).

7. Leverett, M.C. and Lewis, W.B.: "Steady Flow of Gas-Oil-Water Mixtures through Unconsolidated Sands," *Trans. AIME* (1941).

8. Collins, R.E.: "Flow of Fluids Through Porous Media," The Petroleum Publishing Co., Tulsa, OK, USA (1976).

9. Calhoun, J.C., Jr.: "Fundamentals of Reservoir Engineering, " University of Oklahoma Press, Norman, OK, USA (1951).

10. Amyx, J.W., Bass, D.M., Jr., and Whiting, R.L.: "Petroleum Reservoir Engineering," McGraw-Hill Book Co., New York, NY, USA (1960).

Appendix A. CONVERSION FACTORS

1 darcy	=	9.87×10^{-9}	cm^2
	=	0.987	μm^2
1 atm	=	1.013	bar
	=	101,300	Pascal
	=	1,013,000	$dyne/cm^2$
	=	14.7	psi
1 barrel (bbl)	=	5.615	ft^3
	=	42	gallons
	=	159	liters
	=	159,000	cm^3
	=	0.159	m^3
1 pound (lb)	=	454	grams
1 short ton	=	2,000	lb
1 metric ton	=	1,000	kg
	=	2,203	lb
1 foot (ft)	=	12	inches
	=	30.5	cm
1 mile	=	5,280	ft
	=	1,609	m
1 acre	=	43,560	ft^2
	=	4,047	m^2
1 sq. mile	=	2,560,000	m^2
	=	640	acres
1 centipoise (cP)	=	1	mPa.s
	=	0.01	g/cm.s
	=	0.000672	lb/ft.s
°K	=	°C + 273.1	
°R	=	°F + 460	